Molecular mechanisms regulating G protein signaling in brain and heart: Role of R7 RGS proteins and their binding partners

A DISSERTATION
SUBMITTED TO THE FACULTY OF THE GRADUATE SCHOOL
OF THE UNIVERSITY OF MINNESOTA
BY

Ekaterina N. Posokhova

IN PARTIAL FULFILLMENT OF THE REQUIREMENTS
FOR THE DEGREE OF
DOCTOR OF PHYLOSOPHY

Advisor Kirill A. Martemyanov

September, 2012

Acknowledgements

First and foremost I would like to thank my advisor, Dr. Kirill Martemyanov. It is his contributions of time, expertise, and funding that made my PhD experience not only possible, but also enjoyable and productive. It is his outstanding mentorship that advanced my professional development far beyond just learning experimental techniques, scientific presentation, and writing skills. And most importantly, it is his scientific creativity and enthusiasm that inspired me throughout my PhD pursuit.

It was a great pleasure to work with an amazing team of talented scientists from the Martemyanov lab, including Dr. Garret Anderson, Dr. Yan Cao, Dr. Keqiang Xie, Dr. Ikuo Masuho, Dr. Cesare Orlandi, Dr. Ignacio Sarria, Dr. Olga Ostrovskaya, Hideko Masuho, and Natalia Martemyanova. I was privileged to collaborate with many of them, and it was their advice, expertise, and scientific discussion that have been instrumental in this project.

I am deeply indebted to Drs. LeeAnn Higgins and Matthew Stone from the University of Minnesota Mass Spectrometry core. They taught me literally everything I know about the technique, as well as acquired mass spectrometry data and provided help with iTRAQ data analysis.

Several other groups contributed immensely to this thesis, thus helping us achieve our scientific goals effectively and in a timely manner. This proved to be especially invaluable for the RGS6 project, which turned into a fierce race against rough competition. Specifically I want to mention Dr. Vladimir Uversky from Indiana University School of Medicine for his work on predictive modeling of RGS9-2 intrinsic disorder domain; Dr. William Simonds from NIH for the generous gift of anti-R7BP and anti-Gβ5 antibodies; Dr. Cam Patterson from the University of North Carolina School of Medicine for providing HSC70 construct; Dr. Ching-Kang Chen from the Virginia Commonwealth University for supplying us with RGS9-2 and Gβ5 knockout mice; Dr. Kevin Wickman, Kevin L. Allen, and Nicole Wydeven from the University of Minnesota

for electrophysiology recordings and assistance in the development of SAN cells isolation techniques.

I gratefully acknowledge the sources of funding that made my PhD work possible. Dr. Martemyanov is supported by the NIH grants R01 DA021743, R01 EY018139 and R01 HL105559. I have also received travel awards from the American Society for Biochemistry and Molecular Biology and the Federation of European Biochemical Societies. This financial support gave me an opportunity to attend Experimental Biology 2010 meeting in Anaheim, CA and a workshop on transient molecular interactions in Seville, Spain, which were very stimulating scientifically and without any doubt aided in my professional growth.

Finally, I would like to thank my past and present graduate committee members Dr. Kevin Wickman (chair), Dr. Jonathan Marchant, Dr. Timothy Griffin, and Dr. Brock Grill for their time, comments, and insightful questions.

Ekaterina N. Posokhova
University of Minnesota
September, 2012

Abstract

G Protein Coupled Receptor (GPCR) signaling pathways convert signals from the extracellular environment into cellular responses, which is critically important for neurotransmitter action both in central and peripheral nervous systems. The ability to promptly respond to rapidly changing stimulation requires timely inactivation of G proteins, a process controlled by a family of specialized proteins known as Regulators of G protein Signaling (RGS). The R7 group of RGS proteins (R7 RGS) has received special attention due to pivotal roles in the regulation of a range of crucial neuronal processes such as vision, motor control, reward behavior, and nociception in mammals.

One member of R7 RGS family, RGS9-2 has been previously implicated as a key regulator of dopamine and opioid signaling pathways in the basal ganglia of the brain, where it mediates motor control and reward behavior. Dynamic association of RGS9-2 with R7BP (R7 family Binding Protein) is critically important for the regulation of RGS9-2 expression level by proteolytic mechanisms. Changes in RGS9-2 expression are observed in response to a number of signaling events and are thought to contribute to the plasticity of the neurotransmitter action. To unravel the molecular mechanisms regulating levels of RGS9-2 upon its dissociation from R7BP we developed a novel application of the quantitative proteomics approach to monitor interactome dynamics of RGS9-2 in mice. We show that a molecular chaperone HSC70 (Heat Shock Cognate protein 70) identified by this approach is a critical regulator of RGS9-2 expression. HSC70 binds the intrinsically disordered C-terminal domain of RGS9-2 upon the dissociation of R7BP•RGS9-2 complex, and targets the complex to degradation.

In addition to their critical role in shaping neurotransmitter response in the brain, RGS proteins can regulate function of peripheral organs by modulating their responses to the influences of autonomic nervous system. The role of RGS proteins in the regulation of cardiac function and heart rate has received significant attention in the recent years. With over 30 RGS proteins identified, their specific roles in heart physiology remain to be established. Parasympathetic autonomic influence plays an important role in shaping cardiac output acting to decrease heart rate and counteract the pro-arrhythmic effects of

sympathetic activation. Acetylcholine (ACh) released from post-ganglionic parasympathetic neurons activates M2 muscarinic receptor (M2R) and its downstream effector, potassium channel I_{KACh}, in pacemaker cells and atrial myocytes. This leads to cell hyperpolarization and ultimately, decreased heart rate (HR). The second part of the dissertation demonstrates cardiac expression of RGS6 member of R7 RGS family, which has been previously thought to be a neuron-specific regulator. Elimination of RGS6 in mice results in potentiated M2R-I_{KACh} signaling, as evidenced by prolonged deactivation kinetics of I_{KACh} in cardiomyocytes, mild resting bradycardia, and augmented HR deceleration in response to M2R activation. Furthermore, RGS6 specifically co-precipitates with one of the two subunits of I_{KACh}, GIRK4 in transfected HEK293 cells. Direct binding to the effector channel might serve to facilitate RGS6-mediated modulation of parasympathetic influence on atrial myocytes and in mice.

Altogether, the findings comprising this dissertation demonstrate a novel role of RGS6 in regulation of cardiac function, as well as two novel protein-protein interactions of R7 RGS proteins. Identified protein complexes influence G protein signaling by either (i) altering the availability of the regulator (RGS9-2•HSC70), or (ii) by serving to co-localize the major pathway components (RGS6•GIRK4).

Table of Contents

List of Tables

List of Figures

List of Abbreviations

AA – amino acid(s)

ACh – acetylcholine

ACN – acetonitrile

AngII – angiotensin II

ANOVA – analysis of variance

ATP – adenosine triphosphate

BSA – bovine serum albumin

Bpm – beats per minute

cAMP – cyclic adenosine monophosphate

CaMK – calcium/calmodulin-dependent protein kinase

CCh – carbachol (carbamylcholine)

cGMP – cyclic guanosine monophosphate

CHIP – C terminus of HSC70-interacting protein

CI – confidence interval

CID – collision-induced dissociation

CNS – central nervous system

CT – C terminus

DEP – Disheveled, EGL-10, Pleckstrin

DHEX – DEP helical extension

DMAP – DNMT-associated protein

DMEM – Dulbecco's modified Eagle's media

DNA – deoxynucleic acid

DNMT – DNA methyltransferase

ECG – electrocardiogram

EF – error factor

EGTA – ethylene glycol tetraacetic acid

ERK – extracellular signal-regulated kinase

FBS – fetal bovine serum

FL – full length

GABAB – γ-aminobutyric acid receptor B

GAP – GTPase activating protein

GDP – guanosine diphosphate

GFP – green fluorescent protein

GGL – G-protein gamma like

GIRK – G protein gated inwardly rectifying potassium channel

GPCR – G protein-coupled receptor

GRK – G protein-coupled receptor kinase

GTP – guanosine triphosphate

Gβ5 – G protein beta subunit 5

HEK – human embryonic kidney

HR – heart rate

HRV – heart rate variability

HSC – heat shock cognate protein

HSP – heat shock protein

ID – identification

IP – immunoprecipitation

iTRAQ – isobaric tag for relative and absolute quantitation

L-DOPA – L-3,4,-dihydroxyphenylalanine

LAMP – lysosomal-associated membrane protein

LC – liquid chromatography

M_2R – M_2 muscarinic acetylcholine receptor

MALDI – matrix-assisted laser desorption/ionization

MCX – mixed cation exchange

mGluR – metabotropic glutamate receptor

MMTS - methyl methanethiosulfonate

mRNA – messenger ribonucleic acid

MS – mass spectrometry

MS/MS – tandem mass spectrometry

NCBI – national center for biotechnology information

NMDA – N-methyl-D-aspartic acid

NT – N terminus

PAGE – polyacrylamide gel electrophoresis

PBS – phosphate buffered saline

PCR – polymerase chain reaction

PD – pull-down

PDE – phosphodiesterase

PI3K – phosphoinositide 3-kinase

PLC – phospholipase C

PONDR - predictor of natural disordered regions

PSD – postsynaptic density

PVDF – polyvinylidene fluoride

R7BP – R7 RGS binding protein

R9AP – RGS9 anchor protein

RGS – regulator of G protein signaling

RNA - ribonucleic acid

ROS – rod outer segment

S/N – signal to noise ratio

SAN – sinoatrial node

SCG – superior cervical ganglia

SDS – sodium dodecyl sulfate

SIMPL – signaling molecule that associates with the mouse pelle-like kinase

siRNA – small interfering ribonucleic acid

SNARE – SNAP (soluble N-ethylmaleimide-sensitive factor attachment protein) receptors

SNP – single nucleotide polymorphism

TFA – trifluoroacetic acid

TNF – tumor necrosis factor

TOF – time of flight

UV – ultraviolet

VSMC – vascular smooth muscle cells

WT – wild type

Y2H – yeast two-hybrid screening

List of Published Manuscripts

1. Anderson G.R., **Posokhova E.N.**, Martemyanov K.A. The R7 RGS protein family: multi-subunit regulators of neuronal G protein signaling. *Cell Biochemistry and Biophysics,* 2009. 54(1-3):33-46.
2. **Posokhova E.**, Uversky V., Martemyanov K.A. Proteomic identification of HSC70 as a mediator of RGS9-2 degradation by *in vivo* interactome analysis. *Journal of Proteome Research,* 2010. 9(3):1510-1521.
3. **Posokhova E.**, Wydeven N., Allen K.L., Wickman K., Martemyanov K.A. RGS6•Gβ5 complex accelerates I_{KACh} gating kinetics in atrial myocytes and modulates parasympathetic regulation of heart rate. *Circulation Research,* 2010. 107(11):1350-1354.

Chapter 1 – Introduction of the R7 RGS protein family: multi-subunit regulators of G protein signaling

Garret R. Anderson, Ekaterina N. Posokhova, and Kirill A. Martemyanov

From the Department of Pharmacology, University of Minnesota, MN, 55455, USA

Content taken from published manuscript:

Anderson G.R., **Posokhova E.N.**, Martemyanov K.A. The R7 RGS protein family: multi-subunit regulators of neuronal G protein signaling. *Cell Biochemistry and Biophysics,* 2009. 54(1-3):33-46.

G protein-coupled receptor (GPCR) signaling pathways mediate the transmission of signals from the extracellular environment to the generation of cellular responses, a process that is critically important for neurons and neurotransmitter action. The ability to promptly respond to rapidly changing stimulation requires timely inactivation of G proteins, a process controlled by a family of specialized proteins known as Regulators of G protein Signaling (RGS). The R7 group of RGS proteins (R7 RGS) has received special attention due to their pivotal roles in the regulation of a range of crucial neuronal processes such as vision, motor control, reward behavior and nociception in mammals. Four proteins in this group: RGS6, RGS7, RGS9 and RGS11 share a common molecular organization of three modules: (i) the catalytic RGS domain, (ii) a GGL domain that recruits Gβ5, an outlying member of the G protein beta subunit family, and (iii) a DEP/DHEX domain that mediates interactions with the membrane anchor proteins R7BP and R9AP. As heterotrimeric complexes, R7 RGS proteins not only associate with and regulate a number of G protein signaling pathway components, but have also been found to form complexes with proteins that are not traditionally associated with G protein signaling. This review summarizes our current understanding of the biology of the R7 RGS complexes including their structure/functional organization, protein-protein interactions and physiological roles.

- ***The role of RGS proteins in setting the timing of G protein signaling***

G protein signaling pathways are ubiquitous systems that mediate the transmission of signals from the extracellular environment to generate cellular responses. In these pathways, propagation of a signal from plasma membrane receptors to effectors is mediated by molecular switches known as heterotrimeric G proteins [1, 2]. In the prototypical sequence of events, G Protein-Coupled Receptors (GPCRs) are activated by ligand binding, which catalyzes GDP/GTP exchange on many Gα protein molecules. Upon GTP binding, Gα-GTP and Gβγ subunits dissociate from one another, and both proceed to activate or inhibit a variety of downstream signaling molecules (ranging from enzymes that regulate second messenger homeostasis to ion channels and protein kinases) that are collectively referred to as effectors (reviewed in [3, 4]). Thus, a cellular response is elicited by modulation of the activity of an effector molecule by G protein subunits. The extent of effector activity regulation, and consequently the magnitude and duration of the response, depends on how long the G proteins stay in the activated state. Processes that inactivate G proteins therefore play critical roles in shaping the kinetics of the response. The first recognized molecular events that contribute to the inactivation of G protein signaling were those that lead to GPCR desensitization, including phosphorylation by receptor kinases, binding of arrestin molecules and internalization via endocytosis (reviewed in [5]). Currently well accepted, these reactions represent powerful mechanisms for limiting G protein activation during sustained stimulation of GPCRs. Controlling G protein activation can be further modulated by controlling the inactivation of G protein subunits, which occurs when the Gα subunit hydrolyzes GTP and its inactive GDP-bound state re-associates with Gβγ subunits [6]. Although Gα subunits can hydrolyze GTP and self-inactivate, this process is rather slow and does not account for the fast deactivation kinetics observed under physiological conditions (discussed in [7]). Timely inactivation of G proteins is controlled by a specialized family of proteins classified as Regulators of G protein Signaling (RGSs). Comprising more than 30 members, RGS proteins act to accelerate the rate of GTP hydrolysis of G protein a subunits [8-10]. This activity makes RGS proteins key elements that determine the

lifetime of the activated G proteins in the cell, thus determining the overall duration of the response to GPCR activation. The importance of RGS proteins in regulating the magnitude of cellular reactions within an organism is underscored by a number of studies with genetic mouse models either deficient in genes encoding individual RGS proteins [11-18] or carrying G proteins insensitive to RGS action [19]. These mouse models often suffer from a range of dysfunctions that severely affect most systems in the organism. Furthermore, recent evidence suggests that the activity of RGS proteins may in fact be a rate-limiting step in the termination of G protein-mediated responses in a similar way to that of the visual signal transduction pathway in retinal photoreceptors [20]. In this context, understanding the mechanisms that regulate RGS protein function will provide critical insight into how the timing of G protein-mediated cellular reactions is achieved.

- ***Regulation of G protein signaling in the nervous system and the R7 group of the RGS family***

Perhaps one of the most impressive features of G protein signaling in neuronal cells is the exquisite timing of signaling events. Neurons heavily rely on GPCR pathways for mediating neurotransmitter action, requiring simultaneous processing of multiple incoming signals in a rapid timeframe and in a constantly changing environment (reviewed in [21]). In many cases, changes in the precise timing of these signaling events lead to a range of grave dysfunctions of the nervous systems [22, 23]. Thus, it is perhaps not surprising that regulation of neuronal G protein signal termination mediated by RGS proteins has raised considerable interest. Neuronal RGS proteins have been implicated in many neurological conditions such as anxiety, schizophrenia, drug dependence and visual problems (See [23-25] for reviews).

Although the expression of several RGS proteins has been detected in the nervous system, the R7 group of RGS proteins has received special attention due to their pivotal roles in the regulation of a range of crucial neuronal processes such as vision, motor control, reward behavior and nociception in animals from *C. elegans* to humans [10, 26]. Additionally, R7 RGS proteins are key modulators of the pharmacological effects of drugs involved in the development of tolerance and addiction [12, 27-29]. In mammals,

the R7 subfamily consists of four highly homologous proteins, RGS6, RGS7, RGS9 and RGS11, all of which are expressed predominantly in the nervous system [30]. Despite the important role that R7 RGS proteins play in controlling neuronal G protein signaling, relatively little was known about their operational principles. Over the last few years, significant progress has been achieved in elucidating many exciting principles underlying the function of R7 RGS proteins, essentially making them one of the best-understood subfamilies of the RGS family. The purpose of this review is to summarize our understanding of this important protein family and its role in regulating neuronal processes. We hope that the lessons learned from the studies on R7 RGS proteins may lead to better understanding of the general principles underlying G protein signaling in neurons and help spur the progress in studying other members of the RGS protein family with less understood roles.

- ***R7 RGS proteins are multi-domain protein complexes***

A major characteristic feature of R7 RGS proteins is their modular organization. These RGS proteins contain four distinct structural domains and form tight stoichiometric complexes with two binding partners. In fact, due to the obligatory nature of the association between three constituent components, R7 RGS proteins are increasingly viewed as heterotrimeric complexes composed of three subunits (Figure 1.1).

The central element of this complex is formed by the RGS molecule itself that shares a common domain organization across all R7 RGS members. The defining feature of all RGS proteins, the catalytic RGS domain, is located at the C-terminus of the molecule and constitutes the only enzymatically active portion of the complex. The RGS domains of all R7 RGS proteins were shown to be capable of stimulating GTP hydrolysis on Gα protein subunits [31-39]. From an enzymatic perspective, this process could be regarded as the conversion of active Gα-GTP species into inactive Gα-GDP species, accompanied by the release of the inorganic phosphate [40] commonly referred to as GAP (GTPase Activating Protein). Interestingly, the RGS domains of the R7 RGS proteins act as potent GAPs, even when isolated from the other, non-catalytic domains (see [31-33, 37] for examples). However, studies with RGS7 and RGS9 indicate that

these other non-catalytic domains contribute to setting the maximal catalytic activity and refining Gα specificity [31-33]. *In vitro* enzymatic studies have demonstrated that full-length R7 RGS proteins containing all non-catalytic domains selectively stimulate GTP hydrolysis on subunits of the $G\alpha_{i/o}$ class of G proteins but not on $G\alpha_{q/11}$, $G\alpha_z$ or $G\alpha_s$ [24, 38].

Crystal structures of isolated RGS homology domains have been solved for RGS7 [41] and RGS9 [42], both alone and, in the case of RGS9, in a complex with activated $G\alpha_t$. Analysis of these structures reveals a high degree of conformity to the all-helical bundle organization observed in a number of other RGS proteins [41, 43-45]. The loops connecting the bundled helices form direct contacts with the switch region of the activated Gα subunit to stabilize it in the transition state of GTP hydrolysis, thereby providing a mechanism for the GAP activity [42]. The RGS domain undergoes very little conformational change upon Gα binding, affecting mainly the α5/6 loop, which contains the catalytically critical Asn residue [42]. Upstream from the RGS domain, R7 RGS proteins carry a second conserved feature, the GGL (G protein Gamma-Like) domain. This domain is structurally homologous to the conventional γ subunits of G proteins [39]. Like all Gγ subunits, the GGL domain binds to its obligatory partner, the Gβ subunit. However, unlike conventional Gγ subunits, this interaction of the GGL domain is incredibly specific, as it is capable of forming a coiled-coil interaction only with Gβ5 (type 5 G protein β subunit), a distant member of the G protein β subunit family [35, 46, 47]. A recently solved crystal structure of the RGS9•Gβ5 complex reveals that the interaction between GGL and Gβ5 closely follows the same orientation and association mechanisms as those observed in conventional Gβγ dimers [48].

Finally, the N-terminus of R7 RGS proteins is formed by the DEP (Disheveled, Egl-10, Pleckstrin) [49] and DHEX (DEP Helical EXtension) [48] domains. While the DEP domain is found in many signaling proteins [49], the DHEX domain is unique to R7 RGS proteins [10]. Both crystal structure [48] and chimeric mutagenesis [50] studies suggest that the DEP and DHEX domains form a single, functional domain in the molecule. Recent studies have revealed that the DEP/DHEX module of R7 RGS proteins

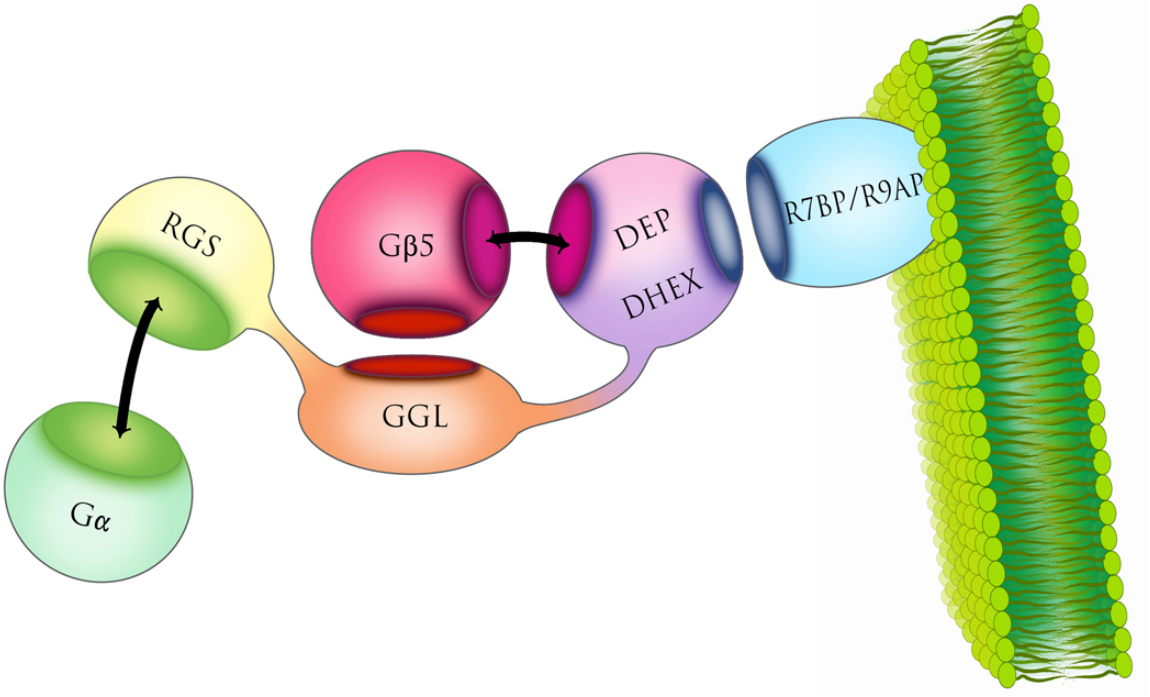

Figure 1.1: Organization of trimeric complexes between R7 RGS proteins and their subunits: R7BP/R9AP and Gβ5.

R7 RGS proteins consist of three functional modules. The N-terminal DEP (Disheveled, EGL-10, Pleckstrin) and DHEX (DEP Helical EXtension) domains mediate binding to the membrane anchors R7BP and R9AP. The central GGL (G Protein gamma-like) domain forms a complex with the Gβ5 (G protein β subunit, type 5). The C-terminal RGS (regulator of G protein signaling) domain mediates transient association with Gα-GTP subunits, during which GTP hydrolysis is stimulated. In addition to the GGL domain, Gβ5 also associates with the DEP/DHEX module.

is responsible for their interaction with two novel membrane proteins, R9AP (RGS9 Anchor Protein) and R7BP (R7 family Binding Protein), which are discussed in detail below.

Increasing evidence suggests that alternative splicing is a powerful mechanism that affects three members of the R7 RGS family: RGS6 [51], RGS9 [52-54] and RGS11 [55]. Combined with the modular principle of R7 RGS organization, differential splicing generates variability in domain composition, leading to the loss or gain of functions mediated by those affected domains. An extreme example of the extensive splicing patterns of R7 RGS proteins was recently provided by studies of RGS6. Alternative splicing of this protein generates 36 isoforms containing virtually all possible combinations of non-catalytic domains in addition to the RGS catalytic domain [51]. Remarkably, several studied isoforms of RGS6 showed differential distribution patterns across cellular compartments [51, 56], suggesting that domain composition may regulate subcellular targeting of RGS6 in cells. The splicing pattern of RGS9 is much less complex, but nonetheless provides the best understood example of functional implications. Two splice variants of RGS9, which differ only in their composition at the C-termini, have been described [52-54]. The short splice isoform, RGS9-1, contains only 18 amino acid residues at the C-terminus and is exclusively expressed in photoreceptors. In the long splice isoform, RGS9-2, the short C-terminus is replaced by a longer region of 209 amino acids. RGS9-2 is expressed in the striatum and is not present in photoreceptors [52, 57]. The ability of the RGS9-1 isoform to recognize its cognate G protein target $G\alpha_t$ is regulated by the effector enzyme of the visual cascade in photoreceptors, PDEγ [58-60], which acts to dramatically enhance the affinity of RGS9-1 for $G\alpha_t$ [61]. As PDEγ is absent in the striatum, G protein recognition is enhanced by the additional C-terminal PDEγ-like domain (PGL) domain that is unique to RGS9-2 [62]. It is likely that future studies on the role of alternative splicing in R7 RGS proteins will yield additional insights into the fundamental principles regulating these proteins.

In summary, R7 RGS proteins are built from the three constituent modules: (i) the catalytic RGS domain, (ii) the GGL domain that recruits the Gβ5 subunit and (iii) the DEP/DHEX domain that mediates interactions with the membrane proteins R7BP and

R9AP. As will be detailed in the following sections, the interplay between these functional domains determines expression level, intracellular localization and ultimately the GAP properties of the R7 family members.

- ***Gβ5, an obligate subunit with an enigmatic functional role***

Gβ5 was first discovered as a novel type of Gβ subunit exclusively expressed in the nervous system [63]. It was shown to selectively interact with Gγ2 *in vitro*, although the existence of this interaction *in vivo* has never been demonstrated [63, 64]. Despite this fact, most subsequent studies focused on analyzing the ability of the Gβ5γ2 complex to mediate classical Gβγ functions such as interactions with Gα subunits and effectors. It was found that Gβ5γ2 has an unusual selectivity for its effectors, as it potently regulates the activities of PLCβ2, N-type calcium channels and GIRK channels, but not PLCβ3, PI3Kγ or adenylate cyclase II [63, 65-69]. Likewise, Gβ5γ2 was shown to interact with GDP-bound Gα subunits [70, 71]. However the specificity of these interactions is more controversial. While one group reported that Gβ5γ2 can bind to $G\alpha_q$ but not to $G\alpha_i$ or $G\alpha_o$ [70], another group detected stable interactions with both $G\alpha_i$ and $G\alpha_o$ [71]. Although no explanation for these discrepancies exists, it was noticed that the complex of Gβ5 with Gγ2 is abnormally weak and prone to spontaneous dissociation, leading to loss of Gβ5 activity [72, 73]. Overall, these findings demonstrate that Gβ5 exhibits some properties that are common to the conventional Gβ subunits, such as interaction with Gα and Gγ subunits as well as with effectors. A recently solved crystal structure supports this idea, as it indicates that most of the critical amino acids that build the protein interaction interface in Gβ5 are conserved [48]. However, the physiological function of Gβ5 remained a mystery until the discovery that Gβ5 readily forms complexes with members of the R7 family of RGS proteins instead of Gγ subunits *in vivo* [46, 47, 74]. Unlike the Gβ5γ2 association, Gβ5•RGS complex formation is very strong and resistant to dissociation in detergent solutions, allowing for its purification by various chromatographic and immunoprecipitation strategies [46, 47, 64]. It should be noted,

however, that the debate on whether Gβ5 can also exist and function in complex with conventional Gγ subunits continues (see [75] for most recent example), as it remains to be established whether Gβ5 can be found outside of the complexes with R7 RGS proteins *in vivo*.

Two splice isoforms of Gβ5 have been described [71]. Gβ5S, a 39 kDa short splice isoform, is ubiquitously expressed in the retina and brain, where it forms complexes with all R7 RGS proteins, except RGS9-1 [46, 64, 76]. The 44 kDa long splice variant, Gβ5L, containing 42 extra amino acids at the N-terminus, is exclusively present in the outer segments of photoreceptors (ROS), where it forms a complex with RGS9-1 [47]. The longer N-terminal portion of the photoreceptor Gβ5L isoform has been shown to contribute to a high affinity to RGS9-1, selectively with a $G\alpha_t$•PDEγ complex, as opposed to free, activated $G\alpha_t$. However, the precise role that alternative splicing of Gβ5 plays for RGS9-1 function is not fully understood.

From early studies on the functional significance of R7 RGS•Gβ5 complex formation, it was unequivocally determined that Gβ5 is essential for the stability and expression of all R7 RGS proteins. Co-expression with Gβ5S was shown to be necessary for achieving high expression levels of RGS6 and RGS7 via protecting them from proteolytic degradation [35, 74], resulting in the enhancement of RGS activity in regulating GIRK channel kinetics [77]. Likewise, experiments with recombinant overexpression in heterologous systems indicate that functionally active proteins can only be obtained when R7 RGS proteins are co-expressed with Gβ5 [32, 34]. Finally, the ultimate proof of the importance of the interaction between R7 RGS proteins and Gβ5 arose from knockout mouse studies that demonstrated that the genetic ablation of Gβ5 resulted in the loss of all R7 RGS proteins [78]. Conversely, deletion of RGS9, the only R7 RGS protein in photoreceptors, results in the degradation of Gβ5. This indicates that, at least in this cell type, Gβ5 exists only in complex with RGS proteins and becomes destabilized in the absence of its interaction with the GGL domain [13]. These observations are reminiscent of the reciprocal stabilization seen in conventional Gβγ subunits, which are thought to form inseparable entities (see [79, 80] for examples).

Overall, most of the accumulated evidence establishes R7 RGS proteins and Gβ5 as obligate subunits of a complex that exists and functions *in vivo* as a single entity.

Delineation of the functional roles that Gβ5 plays as a part of the heterodimeric complex with RGS proteins beyond proteolytic protection has proven to be more difficult. The regulatory effector and Gα binding properties observed for Gβ5γ2 have not been found for Gβ5 in complex with R7 RGS proteins. RGS6•Gβ5 and RGS7•Gβ5 were shown to not modulate either PLCβ or adenylate cyclase [38]. Similarly, recombinant RGS6•Gβ5, RGS7•Gβ5 and RGS9•Gβ5 were demonstrated to be incapable of interacting with GDP-bound $G\alpha_{i/o/t}$ subunits [33, 38, 62]. The crystal structure of the RGS9•Gβ5 complex sheds some light on the apparent discrepancy between the capability of Gβ5 to interact with Gα subunits and effectors when in complex with Gγ2 but not when in complex with RGS proteins [48]. Analysis of the structure indicates that although the protein interaction interface that mediates association of Gβ subunits with Gα subunits and effectors is conserved in Gβ5, it is inaccessible due to its interactions with the N-terminal DEP domain. The DEP domain is intricately interwoven with the adjacent DHEX domain, with both of the domains forming a single structural domain that caps the protein interaction interface of Gβ5. This cap is connected to the rest of the RGS polypeptide via an unstructured hinge region, which is postulated to bear significant conformational flexibility [48]. These observations led to the idea that the complex in the crystal structure was captured in the "closed" conformation, which could be transformed into the "open" state by conformational changes that would disrupt the interactions between the DEP domain and Gβ5 [48, 81]. Indeed, Gβ5 mediates binding of RGS7•Gβ5 complex to G protein-gated potassium channel (GIRK) [82], a classic Gβγ effector channel [83]. Intriguingly, it is speculated that the R7BP and R9AP proteins that bind to the DEP/DHEX domains could impact the equilibrium between "open" and "closed" conformations, thus altering access to the protein-protein interaction interface of Gβ5.

An alternative possibility is that the GGL-Gβ5 module could be employed by RGS complexes to play a role in setting their G protein selectivity, thus regulating the GAP activity of RGS proteins. Indeed, several similar effects of Gβ5 have been reported.

Deletion mutagenesis studies on RGS9-1•Gβ5 complexes indicate that the GGL-Gβ5 module acts to non-specifically reduce the affinity of the RGS catalytic domain to its two G protein targets: free activated $G\alpha_t$ and $G\alpha_t$•PDEγ complexes [33]. In contrast, the non-catalytic domains of RGS9-1 enhance binding specifically for $G\alpha_t$•PDEγ complexes. In conjunction with the function of Gβ5, this activity is thought to be required for setting the high degree of RGS9-1•Gβ5 discrimination for its physiological substrate, $G\alpha_t$•PDEγ, and for preventing short-circuiting of the cascade due to deactivation of $G\alpha_t$ before it can relay the signal to the effector [32, 33]. The ability of Gβ5 to affect RGS interactions with Gα was also observed for RGS7, which was shown to bind to activated $G\alpha_o$ more tightly alone than when in complex with Gβ5 [84]. Finally, Gβ5, in complex with the GGL domain of RGS9, was found to be important for sustaining the high turnover rate of $G\alpha_t$ on the RGS domain of RGS9 [33]. These results suggest that Gβ5 is involved in regulating GAP properties of R7 RGS proteins. However, much of the underlying mechanisms remain to be elucidated.

- ***R7BP and R9AP: Adaptor subunits specifying expression, localization and activity of R7 RGS complexes***

The function of many signaling proteins in cells is determined to a great extent by their targeting to specific subcellular compartments. Photoreceptor neurons have served as a convenient model for delineating compartmentalization mechanisms of several signaling molecules, including that of R7 RGS proteins [85-87]. In these cells, the visual signal transduction pathway is physically restricted to a specialized compartment, the outer segment, which is separated from the rest of the cellular compartments containing other G protein pathways [88]. The outer segment is also the exclusive localization site for RGS9-1, which is tightly bound to the disc membranes [89, 90]. Biochemical reconstitution studies and experiments with transgenic animals have indicated that the association of RGS9-1•Gβ5 with the disc membranes and its specific targeting to the outer segment is mediated by the DEP domain [90, 91]. Proteomic screening for the

molecules that mediate this function in the photoreceptors resulted in the identification of the membrane anchor protein R9AP [92]. Similar to RGS9-1, RGS9-2 also associates with membranes and is specifically targeted to the postsynaptic density site in striatal neurons [93]. The absence of R9AP in the brain led to another proteomic search that identified R7BP, an R9AP homologue that binds to RGS9-2 and all other R7 RGS proteins in striatal neurons [76]. At the same time, R7BP was also independently discovered as a binding partner of R7 RGS proteins via bioinformatics homology searches using R9AP as bait [94]. Although the binding of both R9AP and R7BP to RGS proteins has been shown to be mediated by the DEP domain [50, 76], complex formation exhibits clear interaction specificity. Although all four R7 RGS proteins can bind to R7BP, only RGS9 and RGS11 are capable of forming complexes with R9AP [76, 94].

At the amino acid sequence level, the similarity between R9AP and R7BP is limited to only 30% (15% identity). However, both proteins share a significant homology and similarity in overall architecture with SNARE proteins [90, 95]. SNAREs are membrane-associated proteins involved in the vesicular trafficking and exocytosis that underlie synaptic fusion events (for review, see [96, 97]). Like the SNARE protein syntaxin, R9AP and R7BP are predicted to contain an N-terminal three-helical bundle followed by an extensive coiled-coil domain and a membrane attachment site (Figure 1.2). This similarity invites speculation that the interaction between DEP domains and SNARE-like proteins may be a common principle underlying the targeting of DEP domain-containing proteins, which include numerous signaling proteins [9, 49]. In this context, it is intriguing that in yeast, syntaxin homologues are found among the binding partners of the DEP domain-containing RGS protein, Sst2 [98].

Although both R9AP and R7BP are membrane proteins, the mechanisms of their binding to membranes differ. R9AP is anchored via a single-pass C-terminal transmembrane helix, making it an integral membrane protein [92]. In contrast, association of R7BP with the plasma membrane is mediated by two palmitoyl lipids that are post-translationally attached to the C-terminal cysteine residues, acting synergistically with an upstream polybasic stretch of six amino acids [94, 99]. The labile nature of

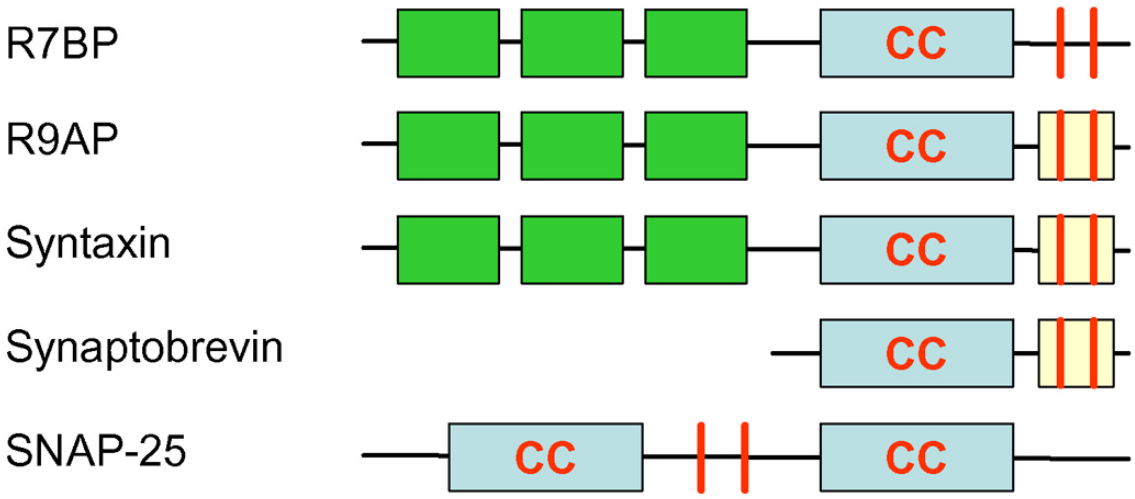

Figure 1.2: Membrane anchors R7BP and R9AP share structural similarities with SNARE proteins. Schematic representation of R7BP and R9AP domain compositions in comparison with three canonical SNARE proteins. Green boxes represent the alpha helical regions, blue boxes indicate conservative coiled-coil domains that participate in SNARE complex formation, yellow boxes indicate transmembrane regions and red lines indicate sites of membrane attachment.

palmitoylation provides R7BP with flexibility in its localization. In cultured cells, it has been shown that de-palmitoylation of R7BP not only removes it from the plasma membrane but also uncovers a nuclear localization signal, resulting in its translocation into the nucleus [94, 99]. This mechanism is thought to contribute to the regulation of R7 RGS protein availability at the plasma membrane [94, 100] in a signaling-dependent manner [101]. However, the exact functional implications of R7BP shuttling from the plasma membrane to the nucleus are unknown. Furthermore, in native neurons R7BP has been primarily found at the plasma membrane compartments [93, 99, 102] and its translocation into the nucleus has not been established despite several reports documenting nuclear localization of R7 RGS proteins *in vivo* [56, 103, 104]. However, more recent study shows 50-70% reduction of nuclear fraction of RGS7•Gβ5 in neurons and brains of R7BP knockouts [105] supporting the role of R7BP in nuclear translocation of the complex *in vivo*.

What does appear to be firmly established is the role of R7BP/R9AP-mediated membrane association in the function of R7 RGS proteins. First, the membrane anchors regulate the activity of R7 RGS proteins. Studies have shown that association of RGS9-1•Gβ5 with R9AP causes a dramatic potentiation of the ability of RGS9-1 to activate transducin GTPase [90, 91, 106]. Under optimal conditions, the degree of this potentiation can be as large as 70-fold [40, 91]. R9AP has also been shown to potentiate GAP activity of RGS11 and therefore inactivation of mGluR6-Go signaling [107]. Similar to R9AP, it was found that co-expression of RGS7•Gβ5 with R7BP in *Xenopus* oocytes enhances the ability of RGS7 to augment M2 receptor-elicited GIRK channel kinetics, presumably due to the stimulation of the catalytic activity of RGS7 [94, 100]. Because the effects of both R7BP and R9AP require the presence of the elements that mediate their membrane attachment, it is reasonable to assume that stimulatory activity of R7BP/R9AP can be attributed to a large extent to concentrating R7 RGS proteins on the membranes and in close proximity to membrane-bound G proteins. However, direct allosteric mechanisms also appear to contribute to the effects of anchors on R7 RGS proteins, as suggested by the observation that R9AP influences not only the catalytic rate of RGS9-1•Gβ5 GAP activity but also its affinity to activated $G\alpha_t$ [108]. Second, R7BP

and R9AP play major roles in dictating the subcellular localization of R7 RGS proteins. In addition to translocation of R7 RGS proteins to the plasma membrane, as observed in transfected cells upon co-expression with R7BP/R9AP [92, 94, 99], membrane anchors target RGS proteins to unique subcellular compartments in neurons. In photoreceptors, R9AP mediates RGS9-1 delivery to the outer segments and excludes it from the axonal terminals [90, 109-111]. In striatal neurons, R7BP specifies the targeting of RGS9-2 to the postsynaptic density [93]. Interestingly, R7BP/R9AP activity is not universally required for targeting all R7 RGS proteins in all cells, as targeting of RGS7•Gβ5 in retinal bipolar neurons relies on binding of RGS7 complexes to an orphan GPCR, GPR179 [112, 113]. Interaction with R7BP has been previously shown to affect GPCR selectivity of RGS7 [114], and it is plausible that interaction with different membrane anchors serves to further promote selectivity in regulation of G protein signaling.

Studies with mouse knockout models revealed that R9AP and R7BP also play an important role in determining the expression levels of R7 RGS•Gβ5 complexes. Knockout of R9AP in mice results in nearly complete elimination of detectable RGS9-1 and RGS11 proteins in the retina [112, 115]. Similarly, knockout of R7BP leads to severe down-regulation of RGS9-2 protein levels in the striatum [93]. At the same time, transcription of the RGS9 and RGS11 genes is unaltered, as evidenced by similar levels of mRNA in both knockout and wild type tissues [93, 115]. The protein levels of RGS9-1, RGS9-2 and RGS11 are reduced by half in the tissues of heterozygous mice carrying one R9AP- or R7BP-deficient allele, which corresponds to the extent of the reduction in R7BP or R9AP expression, respectively. Conversely, overexpression of R9AP in the photoreceptors and R7BP in the striatum led to an increase in the levels of RGS9-1 [20] and RGS9-2 [93], respectively. Examination of the mechanisms by which R7BP/R9AP confer their effects revealed that RGS9 isoforms, even when in complex with Gβ5, are proteolytically unstable proteins with an estimated half life in the cell of less than one hour [50]. RGS9 isoforms carry instability determinants located within their N-terminal DEP/DHEX domains that target they for degradation by cellular cysteine proteases [93]. Binding of R7BP or R9AP to this region is thought to shield these determinants and thus prevent the degradation of RGS9, drastically prolonging its lifetime. The interaction with

the membrane anchors also redistributes RGS complexes from cytosol to the membrane, which might by itself be sufficient for proteolytic protection [110]. In any case, R9AP and R7BP proteins could be viewed as subunits which expression levels ultimately set the levels of RGS9- and RGS11-containing complexes in cells. Interestingly, RGS7 (and likely RGS6) does not possess these instability determinants and is therefore resistant to degradation when present in complex only with Gβ5 [35, 50]. Consistent with this observation, the levels of RGS6 and RGS7 are unaltered in R9AP or R7BP knockout tissues [93, 112]. These observations suggest that RGS9 and RGS11 likely exist as obligate heterotrimeric complexes with either R9AP or R7BP, while RGS7•Gβ5 and RGS6•Gβ5 dimers with could associate with R7BP conditionally. Such remodeling in subunit composition was recently shown in striatum, where the changes in oxygenation or neuronal excitability lead to a dissociation of RGS9-2•R7BP complex, selective degradation of RGS9-2, and an increase in R7BP•RGS7 association as a result [116]. In summary, current evidence indicates that R7BP and R9AP are integral subunits of R7 RGS proteins and play critical roles in regulating the (i) catalytic activity, (ii) GPCR selectivity, (iii) subcellular targeting, and (iv) protein expression levels of R7 RGS complexes.

- ***R7 RGS proteins associate with a wide spectrum of cellular proteins***

As discussed above, R7 RGS proteins form trimeric complexes with R7BP (or R9AP) and Gβ5 subunits. These interactions are intrinsic to all members of the R7 family and have been demonstrated to play critical roles in their activity. Interactions of R7 RGS complexes with their G protein substrates and the Gα subunits of the heterotrimeric G proteins of the $G_{i/o}$ family in the transition state of GTP hydrolysis are equally well established [31, 37, 39, 42, 61, 117]. Interestingly, in addition to these well-accepted interactions, R7 RGSs have been also reported to bind a number of other proteins, suggesting that these RGS proteins are likely integrated into larger macromolecular complexes in cells. Additional interactions were found for all R7 RGS proteins including both splice isoforms of RGS9 (Table 1). In contrast to the conventional complexes of R7

Table 1. Interactions of R7 RGS proteins outside of the complexes with Gβ5 and membrane anchors R7BP/R9AP.

Interaction partner	R7 RGS	System	Method	Domain	Reference
μ-opioid receptor	RGS9-2	PC12	Co-IP	N/A	[118]
		periaqueductal gray matter	Co-IP	N/A	[119]
M3 receptor	RGS7	CHO-K1	PD	DEP	[120]
mGluR6 receptor	RGS11	HEK293	Co-IP	N/A	[121]
GPR179	RGS7	HEK293	Co-IP	N/A	[113]
GPR158	RGS7	brain, HEK293	Co-IP	DEP	[113]
β-arrestin	RGS9-2	PC12	Co-IP	N/A	[118]
α-actinin-2	RGS9-2	HEK293, brain	Y2H, Co-IP	N/A	[122]
NMDAR, subunit NR1	RGS9-2	HEK293, brain	Co-IP	N/A	[122]
14-3-3	RGS7	HEK293, brain	Co-IP, PD	RGS	[123]
	RGS9-2	periaqueductal gray matter; dorsal spinal cord	Co-IP	N/A	[119, 124]
DMAP1, DNMT1	RGS6	COS-7, SH-SY5Y, brain	Y2H, Co-IP, PD	GGL	[125]
SCG10	RGS6	COS-7	Y2H, Co-IP	GGL	[126]
Snapin	RGS7	CHOK1	Co-IP, PD	DEP	[127]
Polycystin	RGS7	HEK293	Co-IP, PD	GGL	[128]
Spinophilin	RGS9-2	striatum	Co-IP	N/A	[129]
GRK2	RGS9-2	striatum	Co-IP	N/A	[129]
Guanylyl cyclase	RGS9-1	bovine ROS	Overlay	N/A	[130]

RGS proteins with R9AP, R7BP and Gβ5, most interactions reported in Table 1 were shown only for some members of the family, and their universality is unknown. Furthermore, for most of these interactions, it is unknown whether the binding occurs directly or is mediated by other proteins. Information about the binding determinants is often missing, and most of these interactions were not considered in the context of constitutive R7 RGS complexes with Gβ5 and R7BP or R9AP. Despite these limitations, analysis of the patterns of these interactions may be productive, as it may suggest not only a potential involvement of R7 RGS proteins in the regulation of discrete cellular processes, but may also provide models of the regulation of RGS protein function. Interaction partners of R7 RGS proteins can be divided into three groups: (i) components of G proteins receptor complexes, (ii) signaling proteins outside of classical GPCR pathways and (iii) proteins that modulate RGS function.

The first consistent theme of R7 RGS proteins is the association with components of GPCR signaling complexes. In brain lysates, RGS9-2 was co-precipitated with the μ-opioid receptor [118, 119]. Furthermore, targeting of RGS9-2 to membrane compartments required the presence of its DEP domain and co-transfection with μ-opioid [118] or D2 dopamine [131] receptors in transfected cells. Similarly, RGS7 was shown to directly interact with the intracellular loops of the muscarinic M3 receptor and GPR158 through its N-terminus [113, 120]. Additionally, mGluR6 has been recently identified as a binding partner of RGS11 required for proper localization of the complex to the dendritic tips of bipolar cells in retina, as well as for its proteolytic stabilization [121]. The interactions of mammalian R7 RGS proteins with GPCRs are further supported by the observation that the DEP domain of the yeast RGS protein Sst2 directly interacts with the C-terminal domain of its cognate receptor, Ste2 [132]. Hypothetically, the RGS•GPCR pairing can serve as a powerful mechanism that provides the specificity of RGS activity and shapes the kinetics of the response. In this respect, it is important to note the discovery of the polypeptide that contains both GPCR and RGS domains, which allow it to effectively modulate cell proliferation [133]. Interestingly, binding partners of R7 RGS proteins also include proteins that are normally found in complexes with GPCRs. Receptor kinase GRK2, β-arrestin, and the GPCR scaffold spinophilin were

found to co-immunoprecipitate with RGS9-2 in brain tissue [118, 129]. Although it is unclear whether these interactions occur directly or are mediated by μ-opioid receptors, they are thought to contribute to the regulation of receptor internalization and the development of tolerance, both of which are influenced by RGS9-2 [27, 118, 129].

The second large group of R7 RGS binding partners is composed of the non-conventional interactions of R7 RGS proteins with signaling proteins outside of G protein signaling pathways. For example, a yeast two hybrid screen has revealed interactions between RGS6 and the transcriptional repressor complex DMAP1/DNMT1 [125], an observation that is consistent with the previously reported localization of RGS6 in the nucleus [56]. Nuclear localization has also been reported for other R7 RGSs [103, 104, 134] and is thought to be mediated by R7BP, which can serve as a membrane-nuclear shuttle in a palmitoylation-dependent fashion [99, 100]. This raises the possibility that additional interactions of R7 RGS proteins with components of signaling pathways in the nucleus exist. The discovery of these interactions may provide significant insight into the function of these proteins in the nucleus. In the cytoplasm, RGS6 was found to be associated with the microtubule destabilizing protein SCG10. This interaction that was shown to result in the enhancement of neurite outgrowth when studied in transfected cells [126]. Similarly, RGS9-2 was reported to be associated with another cytoskeletal protein, α-actinin-2 [122]. In transfected cells, this interaction was demonstrated to link RGS9-2 to the regulation of NMDA receptor function [122]. Finally, RGS7 was found to bind a component of the synaptic fusion complex, snapin, leading to the hypothesis that R7 RGS proteins can also regulate exocytosis [95, 127]. More studies will be needed to delineate the exact roles of R7 RGS proteins in mediating these signaling processes and fully validate these novel interactions. Likewise, it remains to be established whether the non-conventional functions of R7 RGS proteins are mediated by G proteins or occur via other, yet undetermined pathways.

The last group of R7 RGS binding partners consists of the proteins that serve to regulate RGS proteins themselves. Although there are only two reported observations in this category, the number of examples is expected to grow substantially as the organization of R7 RGS proteins and their reliance on protein-protein interactions for

determining their cellular function are complex. In studies of the established interactions with R7BP/R9AP and Gβ5, association with other cellular proteins was shown to affect catalytic activity and proteolytic stability of R7 RGS proteins. This is a recurring theme for the regulation of this RGS family. Indeed, the binding partner of RGS7, polycystin, was shown to protect it from rapid proteolytic degradation by the ubiquitin proteasome system [128], whereas association with the 14-3-3 protein was shown to inhibit RGS7 activity in a phosphorylation-dependent manner [123].

- ***Physiological roles of R7 RGS proteins in regulation of CNS function***

Most of what we know about the physiological roles of R7 RGS proteins comes from studies on selective elimination or overexpression of R7 RGS proteins in murine models. Among the four R7 RGS proteins, the function of RGS9 is best understood due to its localized expression and the abundance of mouse genetic models. The functional role of this member can serve as a valuable example of the other R7 RGS family members, the physiological roles of which remain largely unknown.

Targeting of the RGS9 gene produced a line of knockout mice that lack the expression of both splice isoforms: RGS9-1 in the retina and RGS9-2 in the brain [13]. Elimination of RGS9-1 in the retina resulted in a substantial delay in the termination of photoreceptor responses to light, a process mediated by the GPCR phototransduction cascade [13]. In this pathway, the activated receptor (photoexcited rhodopsin) triggers the activation of the G protein transducin ($G\alpha_t$), which in turn stimulates the activity of the effector enzyme cGMP phosphodiesterase. This leads to transient membrane hyperpolarization, a major response of the photoreceptor to light (reviewed in [25, 135]). Following extinction of light excitation, wild type rod photoreceptors quickly return to the resting state, with an average time constant of approximately 200 ms. This rapid recovery requires G protein inactivation in the cascade and is critical for the high temporal resolution of our vision [136]. In contrast, rods of mice lacking RGS9-1 show recovery kinetics that is an order of magnitude slower (time constant ~ 2.5 s) [13]. This phenotype is thought to result from delayed transducin inactivation, which is mediated by RGS9-1. This suggests that this regulator is the GAP in the phototransduction cascade.

Similar recovery deficiencies were also described in cone cells, suggesting that this function of RGS9-1 is conserved in all photoreceptor cells [137]. Consistent with its obligatory trimeric organization, the function of RGS9-1 in providing timely transducin deactivation has been shown to depend on its association with R9AP and Gβ5 subunits. Elimination of these subunits in mice results in an identical slow photoreceptor deactivation phenotype [115, 138]. In line with the observations in mice, mutations disrupting RGS9-1 and R9AP were found to cause the human visual disease bradyopsia, which disrupts the ability of those affected to adapt to changes in luminance and to recognize moving objects [139-141]. Conversely, overexpression of RGS9-1•Gβ5•R9AP in mouse rods results in an acceleration of photoresponse inactivation, demonstrating that it serves as a key rate-limiting enzyme in the cascade of recovery reactions that bring photoreceptors to a resting state [20].

The other splice isoform, RGS9-2, was found to be enriched in the striatum, a region commonly associated with reward and motor control functions. It was also found, albeit at much lower levels, in the periaqueductal gray matter, the dorsal horns of the spinal cord and the cortex, which are structures that mediate nociception [27, 122, 142, 143]. This expression pattern has prompted several groups to evaluate the contribution of RGS9-2 to specific behaviors controlled by these systems. RGS9 knockout mice had the following phenotypic properties: (i) increased sensitivity to the rewarding properties of cocaine, amphetamine and morphine [12, 27, 144], (ii) increased sensitivity to the anti-nociceptive action of morphine [27, 118] (similar observation were also made with the down-regulation of RGS9-2 expression by antisense oligonucleotides [142], (iii) delayed development of tolerance to the administration of morphine [27], (iv) enhanced severity of withdrawal symptoms following the cessation of morphine administration [27] (v) rapid development of tardive dyskinesia in response to suppression of dopaminergic signaling [131] and (vi) deficits in motor coordination and working memory [145]. Conversely, viral-mediated overexpression of RGS9-2 in the rat striatum resulted in the reduction of locomotor activity potentiation in response to cocaine administration [12]. Similarly, overexpression of RGS9-2 in a MPTP monkey Parkinson's model has been reported to diminish L-DOPA-induced dyskinesia symptoms [146]. Despite the long list,

these deficiencies are likely to arise from alterations in specific pathways, as RGS9 knockout mice are quite normal in many behavioral aspects. They exhibit unaltered basal locomotor activities, cognitive function, fear conditioning and pre-pulse inhibition [12, 27, 145].

These described phenotypic observations suggest a model in which the function of RGS9-2 in the striatum negatively regulates the sensitivity of the signaling pathways that process reward and nociceptive cues. Indeed, growing pharmacological evidence supports the idea that RGS9-2 moderates signaling via D2 dopamine and μ-opioid receptors, two prominent systems that are thought to critically regulate reward, nociception and locomotor functions [12, 27, 131, 144, 146-148]. Moreover, signaling through D2 and μ-opioid receptors appears to be connected to RGS9-2 expression through feedback mechanisms that adjust the level of this negative regulator, thus allowing dynamic modulation of the signaling intensity [12, 27, 149, 150]. Furthermore, the RGS9-2 complex physically associates with D2 and μ-opioid receptors (see previous chapter and Table 1), although it is currently unknown what mediates this interaction.

The role of RGS9-2 in regulation of dopamine and opioid signaling has been established primarily using the knockout model, and did not take into consideration the possibility of redistribution of released R7BP to complexes with other R7 RGS proteins available and the effect it might have on the overall signaling [116]. Recent findings indicate that sensitivity of motor stimulation to cocaine is instead controlled by RGS7, which function is negatively affected by R7BP•RGS7 complex formation upon down-regulation of RGS9-2 expression levels [114]. Furthermore, ablation of R7BP does not lead to an increased morphine withdrawal, a characteristic of RGS9 knockout model [151], suggesting a possible contribution of complex remodeling.

In contrast to the thorough understanding of the role of RGS9-1 in the phototransduction cascade, the mechanistic picture of RGS9-2 activity and the second messengers and effector systems that are involved in this activity are far less clear. Studies that have addressed this issue have found that introduction of the catalytically active portion of the RGS9 protein into the striatal cholinergic interneurons reduced the modulation of N-type voltage gated calcium channels by dopamine, suggesting that ion

channels that regulate neuronal excitability are a potential target of RGS9-2 activity [147]. This observation is in line with reconstitution studies in *Xenopus* oocytes that demonstrated that full length RGS9-2, both alone and in complex with Gβ5, can powerfully modulate the kinetics of GIRK channel gating [12, 77]. Studies with RGS9 knockout mice also revealed enhanced D2 dopamine receptor-mediated suppression of NMDA currents in striatal medium spiny neurons lacking RGS9-2. Furthermore, RGS9-2 was found to regulate Ca^{2+}-dependent NMDA inactivation via complex formation with α-actinin-2 in transfected cells [122]. Although the mechanisms by which RGS9-2 controls these reactions are unclear, these studies implicate RGS9-2 in the regulation of excitatory glutamatergic transmission and potentially synaptic plasticity. Finally, RGS9-2•Gβ5 was reported to diminish ERK1/2 kinase activation in response to the activation of μ-opioid receptor in transfected cells [118]. While these studies outline the range of the effector systems that can be regulated by RGS9-2, much of the underlying mechanisms remain unclear. Among key unanswered questions are whether the effects of RGS9-2 require its GAP activity (as, for example, in the regulation of calcium channels [147]) or if these effects can be explained by direct association with receptors (as, for example, in the regulation of μ-opioid receptor internalization [118]). Equally important is the question whether RGS9-2 is a specific regulator of select receptors or if it can function as a universal regulator of several GPCRs in neurons (discussed in [152]). Finally, since RGS9-2 forms a constitutive complex with Gβ5 and R7BP, elucidating the contribution of these subunits to its activity and selectivity will have a significant impact on our understanding of RGS9-2 function.

Our knowledge of the physiological roles played by other R7 RGS members is substantially more limited. Knockdown studies using antisense oligonucleotides have implicated RGS6, RGS7, and RGS11 in regulating nociception mediated by μ- and δ-opioid receptors and the development of tolerance to morphine administration [28, 153]. In addition, the expression levels of these R7 RGS proteins have been reported to be modulated in response to changes in signaling via a range of pathways (for examples see [154-157]). Broad expression profiles across the nervous system [30, 39, 74] and the ability to regulate responses elicited by a variety of GPCRs that are coupled not only to

$G_{i/o}$ [34, 38, 39, 77] but also to G_q [158, 159] suggest that R7 RGSs may be critical regulators in a range of signaling pathways. Indeed, the development of the Gβ5 knockout mouse provides a glimpse into the range of dysfunctions that are caused by the elimination of all R7 family members at once [78]. Many of Gβ5 knockout defects, including motor coordination deficit were previously attributed to the loss of RGS9. However, additional contribution from other R7 RGS is possible. Loss of RGS6 for example leads to a similar motor deficit phenotype (abnormal gait and ataxia) due to potentiation of GABA-B (γ-aminobutyric acid) signaling in cerebellum [160]. Aside from that, Gβ5 knockout mice exhibit a range of developmental anomalies. Homozygous mice lacking Gβ5 are smaller in size at birth, gain weight at a slower rate, do not gain body weight in the critical period prior to weaning between postnatal days 15 to 20 and exhibit a high pre-weaning mortality rate (up to ~60%) by 21 days of age [78]. In addition, retinas of Gβ5 knockout mice are unable to relay light excitation from rod photoreceptors to downstream ON-bipolar cells, as revealed by the lack of the characteristic b-wave on electroretinograms [161]. This deficiency in synaptic transmission is underlined by the failure of ON-bipolar cells to establish synaptic contacts with rod terminals during the critical developmental window [161]. Recently several groups have connected these morphological and functional deficits in bipolar cells to a combined loss of RGS11 and RGS7 function [162-166]. Interestingly, synaptic transmission remains largely intact if either protein is ablated individually. In light of the widespread developmental deficiencies upon Gβ5 loss, it is interesting to note that the expression of R7BP, a universal subunit of R7 RGS proteins, is tightly and developmentally controlled. R7BP mRNA and protein are largely undetectable at birth and exhibit a rapid and dramatic induction, peaking around the age of weaning [93, 102]. Delineating the roles of R7 RGS complexes in regulating the specific pathways that shape developmental processes and the establishment of synaptic connectivity will be an exciting future direction.

- ***Role of RGS proteins in regulation of cardiovascular physiology***

G protein signaling pathways are indispensable for the regulation of many cardiovascular functions including heart rate, contractility, and vascular tone. These functions are mediated by a number of important neurotransmitters, including acetylcholine (ACh), epinephrine and norepinephrine, angiotensin II (AngII), vasopressin, and others, which activate GPCRs on cardiomyocytes, vascular smooth muscle cells (VSMCs), and endothelial cells to exert their effect. Regulation of blood pressure is primarily dependent on the balance of $G_{q/11}$-mediated vasoconstriction upon activation of AngII or α1-adrenoreceptors of VSMCs and G_s-mediated vasodilatation when M1, M3 or β-adrenoreceptors are stimulated (see [167] for a review). Two members of RGS family have been implicated in regulation of peripheral vascular resistance: RGS2 and RGS5. Down-regulation of blood pressure by RGS2 appears to be due to its negative regulation of AngII type 1 receptor [168, 169], as well as NO-mediated vascular relaxation [11, 170], which results in a development of hypertensive phenotype in RGS2 knockout mice [169, 171]. Furthermore, RGS2 mRNA and protein expression show a negative correlation with blood pressure in humans [172-174]. The physiological role of RGS5, on the other hand, is much less clear. The protein is specifically expressed in pericytes [175, 176] and predominantly arterial VSMC [175, 177], where it negatively regulates a number of G_i- and G_q-mediated pathways, including AngII [176, 178, 179]. However, contrary to the prediction based on these initial observations, RGS5 knockout mice exhibit a mild hypotensive phenotype [17, 180] with an unknown mechanism.

More pertinent to the current dissertation are the mechanisms regulating chronotropic function of the heart. Cardiac automaticity is regulated by two branches of autonomic nervous system, parasympathetic and sympathetic (rev. in [181]). ACh released from post-ganglionic parasympathetic neurons provides regulatory input by acting primarily on M2 muscarinic receptors (M2R) to reduce heart rate and conduction velocity in sinoatrial (SA) and atrioventricular (AV) nodes. Presence of additional types of MR (types 1,3-5) has been shown in cardiac tissue [182, 183], but their role in

parasympathetic regulation of heart rate has been a source of a major discussion (rev. in [181]). Recent studies using knockout mice lacking M2R and/or M3R unambiguously established role of M3R in mediating positive chronotropic effects of high doses of carbamoylcholine (CCh), ACh analogue [184]. However, physiological role of this effect remains to be established.

Over 90% of muscarinic receptors in mammalian heart are represented by M2R [183], which appears to be the only mediator of ACh-evoked bradycardia [184]. M2R is a seven-transmembrane-domain receptor coupled to PTX-sensitive $G_{i/o}$ proteins, and, according to more recent findings - primarily to G_{i2} [185, 186]. Activation of M2R in SAN cells produces negative chronotropic effect through (i) cellular hyperpolarization and (ii) decreasing the rate of spontaneous depolarization (rev in [187, 188]). The latter is a result of the inhibition of cAMP-gated I_f pacemaker current due to G_i-dependent inhibition of adenylate cyclase (AC) and cAMP level decrease [189, 190]. Additionally, a direct inhibition of I_f by G_o proteins has been proposed [191]. Hyperpolarization of maximum diastolic potential upon M2R stimulation also leads to a decrease in spontaneous firing rates of SAN cells [15, 190, 192]. It is produced by Gβγ-dependent activation of I_{KACh} current [193, 194], which accounts for approximately half of negative chronotropic effect of vagal stimulation [195].

Previous *in vitro* studies [196], as well as more recent data obtained in RGS-insensitive transgenic mice [185, 197] show strong modulation of M2 muscarinic response by RGS proteins. RGS 1-5, 7 and 8 have been reported to play an important role in rapid deactivation of ACh-evoked I_{KACh} current reconstituted in *Xenopus* oocytes [196, 198-201] and transfected cells [202]. However, in most of these studies GIRK1/2 subunit composition of I_{KACh} was used rather than cardiac-specific GIRK1/4 [203]. Taking into consideration recent findings showing RGS•GIRK complex formation [82, 204] the difference in GIRK subunit composition could serve as one of the factors defining *in vivo* RGS specificity or/and efficacy.

Twenty members of RGS family are expressed in mammalian myocardium, and many of them were shown to accelerate GTPase activity of $G_{i/o}$ proteins *in vitro* (rev. in

[205]) making them potential regulators of M2 response. Despite that our knowledge of specific physiological roles of various RGS proteins in parasympathetic regulation of HR *in vivo* is significantly lagging behind.

One of RGS family members that received a significant attention as an important regulator of cardiac function is RGS4. In addition to its role in cardiac hypertrophy [206-208] and heart failure [209, 210] it has been shown to interact with both M2R [204] and GIRK1 subunit of I_{KACh} channel [211] implicating RGS4 in modulation of parasympathetic regulation of heart rate. Indeed, loss of RGS4 in RGS4 knockout mice results in increased sensitivity to bradycardic effect of CCh *in vivo*, *ex vivo* in isolated hearts, and in isolated SAN cells *in vitro* as determined by reduced action potential firing rate [15]. At the molecular level RGS4 ablation significantly reduced I_{KACh} desensitization and deactivation kinetics, and hyperpolarized maximum diastolic potential in SAN cells upon CCh treatment [15]. This establishes RGS4 as the only known RGS protein regulating M2-mediated parasympathetic effects in heart.

Nevertheless, there is little doubt that with at least 20 members of RGS family being expressed in cardiac tissue, it is very likely that more modulators of parasympathetic regulatory input will be identified.[1]

[1] We thank Mr. Perry Anderson for his help with illustrations. Studies on R7 RGS proteins in our laboratory are supported by the NIH grants EY018139 and DA 021743. Garret Anderson is a recipient of the Ruth L. Kirschstein National Research Service Award DA024944.

Chapter 2 – Proteomic identification of HSC70 as a mediator of RGS9-2 degradation by *in vivo* interactome analysis

Ekaterina Posokhova[1], Vladimir Uversky[2,3], and Kirill A. Martemyanov[1]

From: [1]Department of Pharmacology, University of Minnesota, Minneapolis, MN 55455 USA; [2]Institute for Intrinsically Disordered Protein Research, Department of Biochemistry and Molecular Biology, Indiana University School of Medicine, Indiana, IN 46202 USA; [3]Institute for Biological Instrumentation, Russian Academy of Sciences, 142290 Pushchino, Moscow Region, Russia

Content taken from the published manuscript:

Posokhova E., Uversky V., Martemyanov K.A. Proteomic identification of HSC70 as a mediator of RGS9-2 degradation by *in vivo* interactome analysis. *Journal of Proteome Research,* 2010. 9(3):1510-1521.

Specific contributions: ENP data is presented in Figures 2.1, 2.2, 2.3, 2.4, 2.5B-E, 2.6, and Table 2.

Changes in interactions between signaling proteins underlie many cellular functions. In the mammalian nervous system a member of the Regulator of G protein Signaling family, RGS9-2 is a key regulator of dopamine and opioid signaling pathways that mediate motor control and reward behavior. Dynamic association of RGS9-2 with a neuronal protein R7BP has been found to be critically important for the regulation of the expression level of the complex by proteolytic mechanisms. Changes in RGS9-2 expression are observed in response to a number of signaling events and are thought to contribute to the plasticity of the neurotransmitter action. In this study, we report an identification of molecular chaperone HSC70 (Heat Shock Cognate protein 70) as a critical mediator of RGS9-2 expression that is specifically recruited to the intrinsically disordered C-terminal domain of RGS9-2 following its dissociation from R7BP. HSC70 was identified by a novel application of the quantitative proteomics approach developed to monitor interactome dynamics in mice using a set of controls contributed by knockout strains. We propose this application to be a useful tool for studying the dynamics of protein assemblies in complex models, such as signaling in the mammalian nervous system.

- ***Introduction***

Assembly of proteins into macromolecular complexes is a fundamental property that underlies a vast number of cellular signaling reactions involving ion channels, transcriptional machinery and receptor signaling pathways. Individual subunits often contribute unique properties making re-arrangement of the complex composition a powerful mechanism for the regulation of cellular responses. Cells, in turn, tightly regulate the assembly, composition and interaction stoichiometries within these complexes by an array of mechanisms. Controlled protein degradation is one of the central mechanisms that allow rapid changes in the makeup of macromolecular complexes and thus determines their functional dynamics in cells.

Multi-subunit organization shaped by proteolysis is a consistent theme in the regulation of G protein signaling in the nervous system by the members of the R7 family of RGS (Regulator of G protein signaling) proteins [212]. R7 RGS proteins act to accelerate the inactivation of G protein signaling by stimulating the rate of the GTP hydrolysis on the alpha subunits of heterotrimeric G proteins thus speeding up termination of the cellular response following GPCR activation. The best studied member of the R7 RGS proteins, RGS9-2, is selectively enriched in the striatum region of the brain and has been demonstrated to play critical roles in controlling nociception, locomotion and reward behavior by controlling the activity of μ-opioid and dopamine receptor signaling (see [212-214] for recent reviews). RGS9-2 forms trimeric complex with its two other subunits, the type 5 G protein beta subunit (Gβ5) [76-78] and the SNARE-like R7 Binding Protein (R7BP) [76, 94]. Association with Gβ5 is strictly required for the expression of RGS9-2, as well for all other R7 RGS proteins, and genetic knockout of Gβ5 in mice results in the elimination of R7 RGS proteins [78]. Similarly, association with R7BP is also required for achieving a high expression level of RGS9-2 in the striatum [50] and elimination of R7BP in mice makes RGS9-2 susceptible to degradation by cellular cysteine proteases substantially reducing its levels [93]. However, in contrast to Gβ5 elimination, R7BP knockout does not affect the expression of other R7 RGS proteins and leaves readily detectable amounts of RGS9-2 [93] suggesting that

association with R7BP serves as regulatory mechanism that selectively modulates the abundance of the RGS9-2•Gβ5 complex. Indeed, changes in neuronal activity and oxygenation status were found to reduce RGS9-2 expression concomitant with the decrease in RGS9-2•Gβ5 coupling to R7BP [116], while viral-mediated over-expression of R7BP results in the elevation of RGS9-2 levels [93]. Furthermore, RGS9-2 expression in the striatum is uniquely sensitive to the administration of psychostimulants and morphine [12, 27, 215] which is believed to be an important feedback mechanism underlying adaptations in the striatum upon the development of drug addiction [214]. Together, these findings suggest that the dynamic coupling/un-coupling of RGS9-2•Gβ5 with R7BP serves as a critical regulatory event that determines the abundance of this signaling regulator by post-translational mechanisms involving protein degradation. What remains unknown however are the molecular details of processes that control and/or mediate RGS9-2•Gβ5 degradation.

In this study we report the identification of molecular interactions that underlie RGS9-2•Gβ5 instability upon dissociation of R7BP from the complex. We have developed an iTRAQ®-based proteomics approach that allows quantification of changes in the composition of protein complexes induced by genetic manipulations in mice. This method was applied to identify the interactions of RGS9-2•Gβ5 complex that are up-regulated in the striatum of the R7BP knockout mouse. Based on the changes in the interactome we detected, we propose a model of molecular events controlling RGS9-2 degradation where the key role is played by molecular chaperone HSC70.

- ***Materials and Methods***

Antibodies, Recombinant Proteins, DNA Constructs and Mouse Strains - Generation of sheep anti-R7BP (N-terminal epitope) and sheep anti-RGS9-2CT (C-terminal epitope) has been described previously [76]. Antibodies were affinity purified and stored in PBS buffer containing 50% glycerol. Rabbit anti-Gβ5 (SGS) antibodies were a generous gift from Dr. William Simonds, NIDDK. Rat monoclonal anti-HSC-70 (clone 1B5) antibodies were from Assay Designs (Ann Arbor, MI). Mouse monoclonal

anti-β-actin (clone AC-15) antibodies were purchased from Sigma (St. Louis, MO). Mouse monoclonal anti-c-myc (clone 9E10) antibodies were from Roche Applied Sciences (Indianapolis, IN). The Anti-HA tag antibody was a mouse monoclonal from Millipore (Temecula, CA). All general chemicals were purchased from Sigma Aldrich.

The recombinant C-terminus of RGS9-2 protein was purified from Sf9 cells. The DNA region encoding amino acids 467-675 of mouse RGS9-2 was appended at the 5'end with the his-tag encoding sequence by PCR and cloned into a baculovirus shuttle vector, pVL1392, that was used to generate recombinant baculovirus. A high titer baculoviral stock was applied to 2 liters of Sf9 cell culture at MOI=3. Following 3 days of post-infection incubation, cell were collected, disrupted in lysis buffer (20 mM Tris-HCl, pH=8.0, 150 mM NaCl supplemented with Complete (Roche) protease inhibitors and the recombinant C-terminus was purified on Ni-NTA beads as described previously [33]. Protein quantification was performed using Bradford reagent (Sigma) according to the manufacture's specifications using BSA as a standard (Pierce).

Cloning of full length R7BP, Gβ5, RGS9-2 was described previously [62, 76]. For expression in mammalian cells, the HA-tag was added at the 5'-end of the RGS9-2 C-terminus (aa 467-675) by PCR and the cassette was cloned into the pcDNA3.1 vector between EcoRI and Not restriction sites. The rat N-terminal myc-tagged HSC70 construct was a generous gift from Dr. Cam Patterson, UNC, and it was further subcloned into the pcDNA3.1/V5-His-TOPO (Invitrogen) mammalian expression vector according to the manufacture's specifications. The HA-tagged N-terminus (aa 1-209) of the RGS9 protein was cloned into the pcDNA3.1/V5-His-TOPO (Invitrogen) mammalian expression vector according to the manufacture's specifications. All constructs were propagated using an *E.coli* Top-10 strain (Invitrogen), isolated using Maxiprep kits (Qiagen) and sequenced.

The generation of the R7BP knockout mouse has been described previously [93]. RGS9 knockout mice [13] have been generously provided by Dr. Jason Chen (Virginia Commonwealth University). Mice were housed in groups on a 12h light/dark cycle with food and water available *ad libitum.* All procedures were carried out in accordance with the National Institute of Health guidelines and were granted formal approval by the Institutional Animal Care and Use Committee of the University of Minnesota.

Preparative immunoprecipitation of RGS9-2 complexes from mouse striatum – For the preparation of brain lysates, punches of striatal tissue were dissected from mouse brains immediately upon sacrificing. Tissue was homogenized in immunoprecipitation (IP) buffer composed of PBS (pH=7.4, ThermoFisherScientific) supplemented with an additional 150 mM NaCl, 1% Triton X-100, Complete protease inhibitors (Roche) and Phosphatase Inhibitor Cocktails I and II (Sigma) by passing it through a series of needles decreasing in gauge. Following a 30 minute incubation at 4ºC, insoluble material was removed by centrifugation at 200,000 x g for 15 minutes. Supernatants were incubated for 1 hour at 4^0C with 50 μg of anti-RGS9-2 CT antibody covalently coupled to 10 μl of protein G beads (GE Healthcare) with Bis(Sulfosuccinimidyl)suberate (BS3) (Pierce) as described previously [76]. The beads were washed three times with ice-cold IP buffer and proteins were eluted with 200 ml of 5% NH_4OH, lyophilized using a SpeedVac concentrator, and processed for mass-spectrometric analysis as described in the following sections.

Pull-down of brain proteins with recombinant C-terminus of RGS9-2 – Whole brain extract from wild-type mice was prepared by homogenizing the tissue in pull-down (PD) buffer (1xPBS, 150 mM NaCl, 0.1% n-Dodecanoylsucrose and protease inhibitors) in a glass homogenizer and passing the suspension through a series of needles with varying gauge sizes. Following a 30 minute incubation at 4ºC, the lysate was centrifuged for 15 minutes at 14,000 x g. The supernatant was incubated for 90 minutes at 4ºC with 20 μl beads covalently bound to 35 μg of recombinant RGS9-2 C-terminus by SulfoLink kit (Pierce) according to the manufacturer's protocol, except that all coupling procedures were performed in 20 mM Tris, pH 7.8 supplemented with 300 mM NaCl, 10% glycerol and protease inhibitors. Non-conjugated beads were used as a negative control. Following incubation, beads were washed 3 times with the PD buffer, bound proteins were eluted with 5% NH_4OH, lyophilized using a SpeedVac concentrator, and processed for mass-spectrometric analysis as described in the following sections.

iTRAQ® labeling and preparation of samples for mass-spectrometry – Samples from preparative IP were dissolved in 0.5 M triethylammonium bicarbonate (pH 8.5) containing 0.1% SDS, reduced with 5mM tris-(2-carboxyethyl) phosphine for 1hr at 60°C

and alkylated with 10 mM methyl methanethiosulfonate for 10 minutes at room temperature. Proteins were digested with 10 μg of modified porcine trypsin (Promega) at 37ºC for 16 hrs. iTRAQ® labeling reagents (Applied Biosystems) were reconstituted in ethanol, added to tryptic digests (wild-type, iTRAQ® 114; R7BP knockout, iTRAQ® 115; RGS9 knockout, iTRAQ® 116) and incubated at room temperature for 1 hr. Differentially labeled peptide mixtures were combined and dried out in a SpeedVac. In some experiments iTRAQ® 116 labeled samples (RGS9 knockout) were not mixed with other samples and were processed separately. Labeled peptide mixtures were reconstituted in 0.2% formic acid (Pierce) and applied to an MCX cartridge (Waters) pre-equilibrated with methanol/water (1:1, vol/vol). The cartridge was washed with 0.1% formic acid in 5% methanol followed by a 100% methanol wash. Peptides were eluted from MCX resin in 1 ml of 1.5% NH_4OH in methanol, dried by SpeedVac and subjected to separation by liquid chromatography as described below.

Samples from pull-down experiments were dissolved in 20 ml of SDS sample buffer (62mM Tris, 10% glycerol, 2%SDS, 5% β-ME), and resolved by SDS-PAGE (Lonza). Gels were fixed with 5% acetic acid in 50% methanol for 20 minutes and stained with NOVEX Colloidal Blue staining kit (Invitrogen) overnight. Band(s) present in RGS9-2 C-terminus pull-down sample were cut out with a razor blade. A corresponding piece of gel of a matching molecular weight was also excised from the control sample where empty beads were used for the pull-down. In-gel digestion with porcine sequencing grade modified trypsin (Promega) was performed following sample reduction, alkylation and destaining as described previously [216]. Final samples were dissolved in 10 μl of 0.1% trifluoroacetic acid (TFA) in 50% acetonitrile (ACN) and 0.7 μl of each sample was mixed with an equal amount of 6 mg/ml α-cyano-4-hydroxycinnamic acid (Fluka) in an ACN:H_2O mixture (75:25 v/v), 0.1% TFA, 10 mM ammonium phosphate and spotted on a MALDI target in 384-spot format.

Liquid Chromatography and MALDI mass-spectrometry – The Tempo™ LC MALDI spotting system (ABI) was used to separate iTRAQ®-labeled peptides and deposit LC eluates into fractions robotically spotted onto LC MALDI targets in a 1232-spot format. Peptides were dissolved in 0.1% formic acid in a 98:2 ratio, water:ACN

mixture, loaded onto a ProteoCol™ C18 trap cartridge (SGE Analytical Science, Victoria, Australia: 300 Å pore size, 300 μm internal diameter, 10 mm length). The cartridge was washed with a loading buffer for 18 minutes at 9 μl/min with loading buffer and then connected to a C18 analytical column made of ~12 cm of 100 μm Integrafrit™ tubing (New Objective, Woburn, MA) packaged with Magic 5 μm 200 Å C18AQ (Michrom BioResources, Auburn, CA). Peptides were eluted at 500 nl/min flow rate by gradually increasing the ratio of elution buffer (98:2, ACN:water, 0.1% TFA) to the starting buffer (98:2, water:ACN, 0.1% TFA) according to the following profile. From 0 to 5 min concentration of elution buffer increased to 15%, by 52 min to 35%, by 54 min to 80% at which point it was held constant at an 80% level for 10 minutes. Peptide elution was monitored by UV absorbance at 214 nm. Eluted fractions were mixed prior to spot deposition with a matrix solution (6 mg/mL alpha-cyano-4-hydroxycinnamic acid) at a rate of 1 μl/min using a Harvard Apparatus (Holliston, MA) syringe pump and deposited in 24 second intervals.

All mass-spectrometric data were acquired on a 4800 MALDI TOF/TOF™ analyzer (ABI) with a 200 Hz repetition rate Nd:YAG laser. TOF MS spectra were acquired from 800 – 4000 *m/z*. A total of 800 to 1000 laser pulses were accumulated for each TOF MS spectrum fixed laser setting following an optimization protocol. Tandem MS mode was operated with 2kV collision energy with CID gas (air) over a range of 10 *m/z* to 95% of the precursor mass value. Precursor mass window was 250 ppm (FWHM) in relative mode. A minimum of 800 and a maximum of 4000 laser shots were accumulated with laser stop conditions set at 6 product ion peaks of S/N > 60 (signal to noise ratio) and an optimized, fixed laser setting. The metastable suppressor setting was on. Data dependent tandem MS settings included acquisition of the top 10 most intense ion signals per spot (top 25 for gel-derived samples). In the cases where 2 or more consecutive spots in an LC run showed identical precursor *m/z* values (within 200 ppm tolerance), tandem MS was acquired exclusively from the spot with the maximum S/N, as determined from the TOF MS spectra.

Database searches and MS data analysis - Tandem mass spectra were searched using ProteinPilot™ 2.0.1 software, revision number 67476 (Applied Biosystems, Inc.)

with the ParagonTM search algorithm against the National Center for Biotechnology Information's Reference Sequence mouse subset protein database (ver. 11-01-07; http://www.ncbi.nlm.nih.gov/), which contained 34,715 proteins including 179 contaminant proteins from Thermo Scientific. Parameters for preparative IP samples were "iTRAQ® 4plex (peptide labeled)" sample type, MMTS-cysteine modifications, trypsin digest, thorough search with biological modifications ID focus, and 66% protein confidence threshold. Search parameters for pull-down samples were the same except for sample type ("gel-based ID") and cysteine modifications (iodoacetomide). Protein identifications with at least 95% confidence as determined by ProteinPilot software were considered significant.

In each separate quantification experiment, the ratio for all proteins was normalized to the 115:114 of RGS9-2. To perform the normalization, manual bias correction was applied to 115/114 iTRAQ® ratios. The manual bias correction was calculated from the product of the 115/114 value for RGS9-2 and the auto-bias value provided by ProteinPilot^{TM} software. The normalization accounted for both the difference in total sample amounts and amounts of precipitated RGS9-2. Protein summary data that included, but was not limited to, ProteinPilot scores for protein identification, percent coverage, iTRAQ® ratios and their p-values were exported from ProteinPilot as tab-delimited text with manual bias correction applied.

Normalized data from both experiments was pooled together. Proteins identified from immunoprecipitations with RGS9 knockout samples were considered non-specific and excluded from the dataset. Only proteins that showed a statistically significant change in levels between wild-type and R7BP knockout samples (p-value 115/114 < 0.05, EF<2) were included in the final report. The EF is a measure of how well a mean protein ratio was determined (a reflection of the variance and the number of peptide measurements), and is used to calculate the 95% confidence interval (CI) of the average iTRAQ® ratio for each protein [EF = 95% CI, where 95% CI range = (ratio x EF) – (ratio / EF)].

Cell culture, transfections and RNA interference - HEK293FT cells were obtained from Invitrogen and cultured at 37°C and 5% CO_2 in DMEM (Dulbecco's Modified

Eagle Medium; GIBCO) supplemented with 100 units of penicillin and 100 mg of streptomycin, 10% FBS, 1x MEM non-essential amino acids (GIBCO), 1mM sodium pyruvate and 4 mM L-glutamine.

Cells were transfected at ~ 70% confluency, using Lipofectamine LTX (Invitrogen) according to the manufacturer's protocol. The ratio of Lipofectamine to DNA used was 6.25 μl : 2.5 μg per 10 cm^2 cell surface. Cells were grown for 24-48 hours post-transfection. Equal amounts of each construct were transfected, balanced when necessary by empty pcDNA3.1 vector. In experiments testing the ability of C-terminus of RGS9-2 to protect RGS9-2 from degradation, 0.25 μg RGS9-2 and 0.25 μg Gβ5 constructs were co-transfected with or without 2 μg of construct encoding C-terminus of RGS9-2.

The following siRNA duplexes were purchased from Quiagen: human HSPA8, sense (r(AAG CUG CUA UAG UAA GUU A)dTdT) and antisense (r(UAA CUU ACU AUA GCA GCU U)dAdA). siRNAs (0.4 nmol) of HSPA8 or equivalent amount of non-silencing AllStars control siRNA (Qiagen) were transfected when cells were at ~40% confluence using Lipofectamine 2000 (Invitrogen) according to the manufacturer's protocol. The ratio of Lipofectamine to siRNA used was 4 μl : 0.4 nmol per 10 cm^2 cell surface. Cells were allowed to grow for 24 hrs before transfection with RGS9-2/Gβ5 complex. Cells were collected for analysis 24 hrs following transfection with RGS9-2•Gβ5, lysed and protein expression was analyzed by quantitative Western blotting using an Odyssey infrared imager (LiCor).

Co-immunoprecipitation assays and Western blotting – Cellular or striatal lysates were prepared in IP buffer lacking phosphatase inhibitors and centrifuged for 15 minute at 14,000 x g. The resulting extracts were incubated with 3 μg of antibodies and 10 μl of protein G beads (GE Healthcare) for 1 hour at 4^0C. After 3 washes with ice-cold binding buffer proteins bound to the beads were eluted with SDS-sample buffer. Eluates were resolved on 12.5% SDS-PAGE gel, transferred onto PVDF membrane (Millipore) and subjected to Western blot analysis using HRP conjugated secondary antibodies and an ECL West Pico (Pierce) detection system. For quantification, samples were analyzed by infrared Western blotting using IRDye680 and IRDye800 labeled secondary antibodies

(Li-Cor Biosciences) according to the manufacturer's protocol. Detection and quantification of specific bands was performed on an Odyssey Infrared Imaging System (Li-Cor Biosciences). The integrated intensity of each band of interest was measured in a corresponding channel with a top-bottom background setting. Integrated intensity of β-actin was used for data normalization.

Bioinformatics – Disorder predictions were done using a recently developed Various Short-Long version 2 algorithm of the Predictor Of Natural Disordered Regions (PONDR®-VSL2). This algorithm consists of an ensemble of logistic regression models that predict per-residue order-disorder [217, 218]. The predictor assigns a score ranging from 0 to 1 to each residue reflecting the likelihood for a given residue to adopt disordered conformation, with scores above the threshold of 0.5 corresponding to residues predicted to be disordered.

- ***Results***

Analysis of changes in the RGS9-2 interactome in R7BP knockout mice – In order to identify proteins that differentially interact with RGS9-2 when R7BP is removed from the complex, we have developed a proteomic approach based on differential labeling with iTRAQ® reagents (Figure 2.1). Although iTRAQ® has become a standard tool for quantitative proteomic analysis [219], we, for the first time to our knowledge, attempt to analyze system wide changes in the interaction network of the signaling regulator using genetic mouse knockouts. RGS9-2 was immunoprecipitated, in parallel, from striatal tissue lysates obtained from wild-type and R7BP knockout mice. In addition, precipitation from RGS9 knockout tissue lysates served as a control to account for non-specific interactions. Proteins present in eluates were digested with trypsin and resulting peptides were differentially labeled with iTRAQ® reagents (Figure 2.1). At this point samples were combined and peptides were separated by liquid chromatography (Figure 2.2A) followed by mass-spectrometric identification of peptides by MALDI TOF/TOF (Figure 2.2B). The experiment was conducted twice and the results of both experiments were reviewed together. A total of 680 unique peptides were identified, of which 519 had

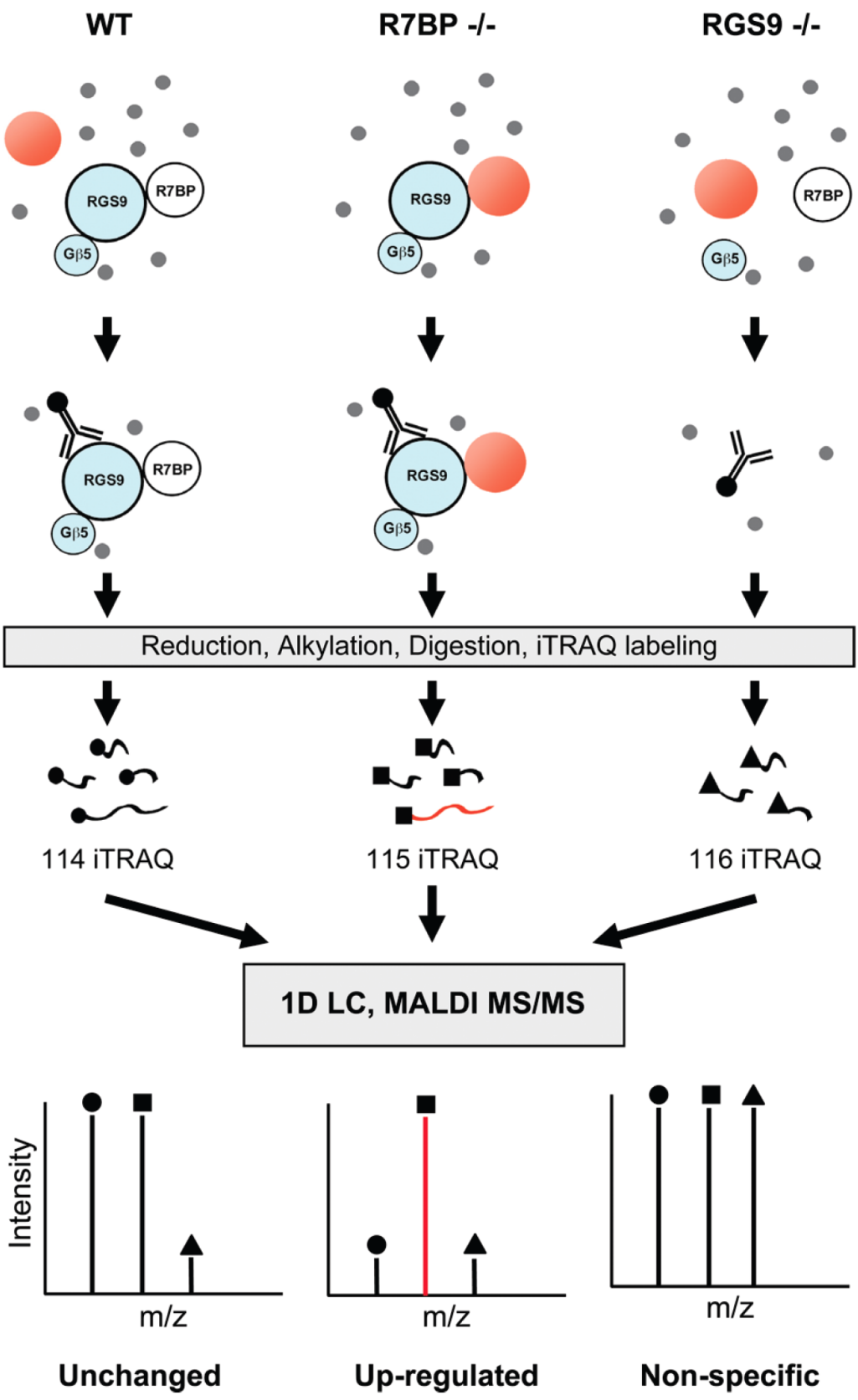
WT
R7BP -/-
RGS9 -/-
RGS9
R7BP
Gβ5
Reduction, Alkylation, Digestion, iTRAQ labeling
114 iTRAQ
115 iTRAQ
116 iTRAQ
1D LC, MALDI MS/MS
Intensity
m/z
Unchanged
Up-regulated
Non-specific

Figure 2.1: Approach for quantitative and comparative analysis of changes in the RGS9-2 interactome in genetic mouse models.

Striatal lysates were prepared from wild-type (WT), R7BP knockout (R7BP-/-), or RGS9 knockout (RGS9-/-) animals. RGS9-2 containing complexes were purified in parallel with specific antibodies that recognize the C-terminus of RGS9-2, and eluates were reduced, alkylated and digested with trypsin. Peptides were differentially labeled with iTRAQ® labels, as indicated, i.e. iTRAQ®114 label (●) was used for WT, iTRAQ®115 (■) - for R7BP knockout, and iTRAQ®116. (▲) - for RGS9 knockout samples. Samples were combined and the mixture was resolved by one dimensional liquid chromatography (1D LC), mixed with matrix solution and continuously spotted on a MALDI target. Samples were analyzed by tandem mass spectrometry using ABI 4800 MALDI TOF/TOF analyzer followed by protein identification and quantification using ProteinPilot software. It is theoretically expected that interactions that are up-regulated in R7BP knockout samples will show higher intensity of iTRAQ®115 ions. Non-specific interactions that are found in RGS9 knockout samples and do not show differences in iTRAQ® label intensities are excluded from the analysis.

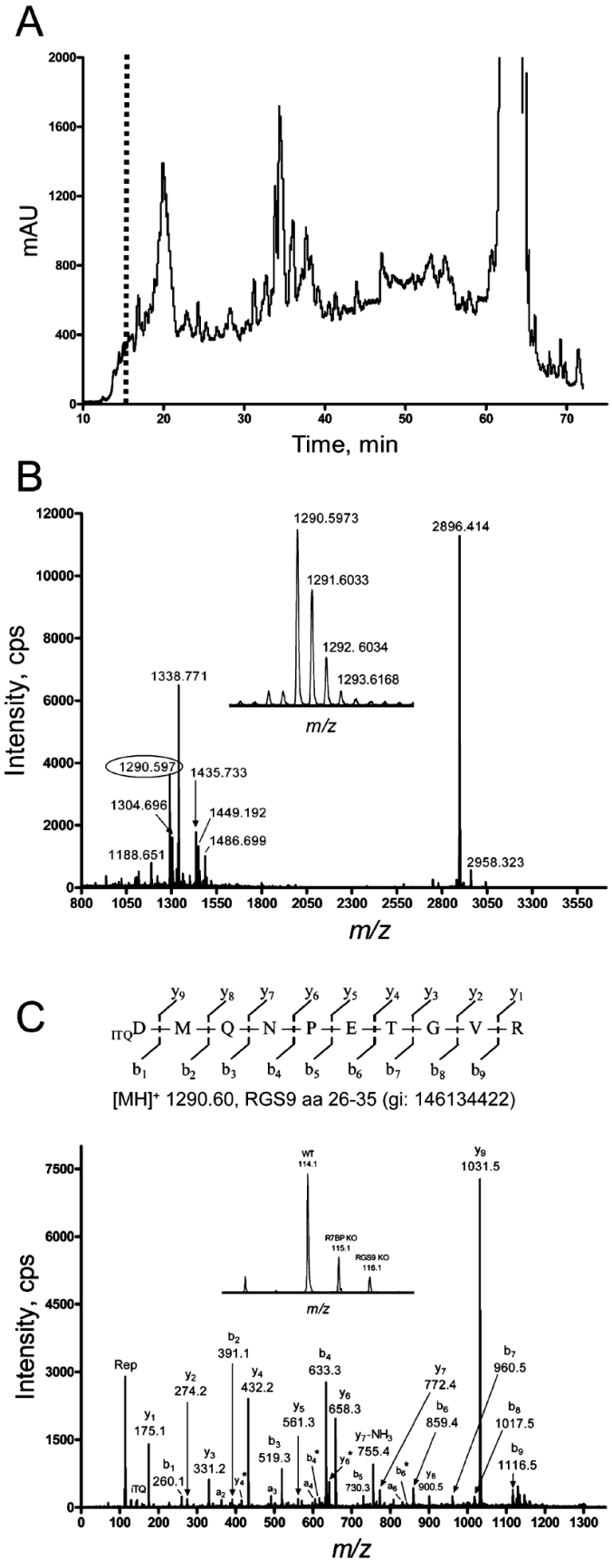

Figure 2.2: Identification and quantification of changes in RGS9-2 interaction partners.

A, Separation profile of the peptide elution from analytical C18 as detected by absorption at l=214. The dashed vertical line indicates a representative fraction subjected to MS analysis (*panel B*, below). **B**, A representative full scan MS spectrum of the fraction/spot eluted from analytical C18 column at the time point indicated in *panel A*. *Insert*: high resolution graph showing precursor region of the ion selected for tandem MS/MS shown in *panel C*. **C**, representative MS/MS fragmentation spectrum, generated by precursor ion at m/z 1290.60. Continuous series of both b- and y-ions allowed high confidence assignment of the amino acid sequence DMQNPETGVR, corresponding to aa 26-35 of RGS9-2 sequence. *Insert*: high resolution graph showing iTRAQ® reporter region. All graphs were exported as ASCII files and peaks were labeled in GraphPad Prism. Abbreviations are: mAU, milliabsorbance units; aa, aminoacids; cps, counts per second; Rep, iTRAQ® reporter ions.

peptide confidence scores ≥ 95% as determined by ProteinPilot™'s Paragon scoring algorithm [220]. Protein inference from peptide hits resulted in the identification of 134 distinct mouse proteins with ≥66% confidence threshold as defined by ProteinPilot™ software, which proportionally weighs contributions of individual peptide scores to the protein identification confidence. iTRAQ® label was present on more than 96% of identified peptides. A typical MS/MS spectrum acquired on the TOF/TOF and used for quantification is presented in Figure 2.2C. Fragmentation of the peptide $_{iTQ}$DMQNPETGVR from RGS9-2 protein (Figure 2.2C, *insert*) showed strong iTRAQ® reporter ion signals with signal intensity variation that was consistent with changes in RGS9-2 expression levels in different samples as determined by Western blotting (Figure 2.3B). Comparison of iTRAQ® reporter ion signal intensities (114/115) revealed 4.85-fold ($p<0.001$) difference in the abundance of RGS9-2 present in the wild-type as compared to R7BP knockout samples (Figure 2.3A). This is in a good agreement with a 3.5±0.2-fold difference ($p<0.001$) detected by quantification of the Western blotting data (Figure 2.3B). In addition to RGS9-2, we readily detected its known interaction partners, R7BP and Gβ5 by both Western blotting and mass-spectrometry (Figure 2.3A,B). Furthermore, decrease in levels of RGS9-2 in R7BP knockout samples resulted in a similar decrease in amount of co-precipitated Gβ5 as measured by iTRAQ® technology (115/114 ratio of 0.313 vs. 0.206, Figure 2.3A). This result is consistent with previously reported quantification of the Western blotting data [93] and indicates unchanged stoichiometry of RGS9-2 interaction with Gβ5, upon the removal of R7BP from the complex. Mass spectrometric signals from the 116 reporter ions from RGS9-2 peptides were substantially reduced (116/114 ratio of 0.162, $p=3.01x10^{-20}$; Figure 2.3A), but did not disappear completely as would be expected given the absence of RGS9-2 in RGS9 knockout samples. Similar observations were made with 115 reporter for R7BP peptides (115/114 ratio is 0.192, $p=0.0008$; Figure 2.3A). This likely reflects an ion suppression effects inherent to the application of iTRAQ® to complex mixtures [221]. In this scenario, other peptides within the ion selector mass tolerance window (5 Da) from the precursor peptide serve as source of the reporter ions while only precursor peptide is identified due to the ion suppression of others. These effects limit the application of this

A

Name	% Cov (p-value)	Number of peptides	115:114 (p-value)	116:114 (p-value)
RGS9-2 (gi: 146134422)	**65.78** ($5.32x10^{-100}$)	**72**	**0.206** ($4.02x10^{-28}$)	**0.162** ($3.01x10^{-20}$)
Gβ5 (gi: 6754018, 41281679)	**40** ($8.63x10^{-29}$)	**22**	**0.313** ($5.04x10^{-7}$)	**0.350** (0.002)
R7BP (gi: 119360350)	**29.18** ($9.96x10^{-11}$)	**7**	**0.192** (0.0008)	**0.247** (0.015)

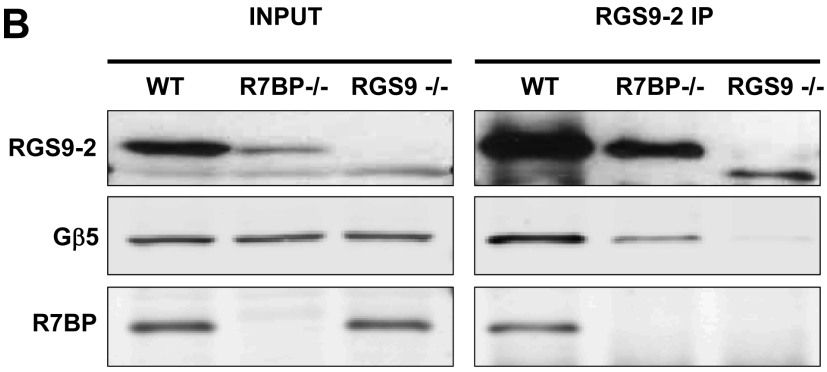

Figure 2.3: Quantification of the composition of the RGS9-2 core complex by iTRAQ® and Western blotting.

A, Summary of identification and iTRAQ®-based quantification of known binding partners of RGS9-2 performed by ProteinPilot software. In cases where a set of peptides could be assigned to more than one protein, all accession numbers are listed. Percent coverage and number of peptides refer to the peptides with at least 95% identification confidence according to ProteinPilot. *p-values* for the identification and change significance are as reported by Protein Pilot software. **B**, Quantitative immunoblotting of RGS9-2 containing complexes immunoprecipitated from wild-type (WT), R7BP knockout (R7BP-/-), and RGS9 knockout (RGS9-/-) striatal tissues. Whole cell extracts (Input) and eluates from beads conjugated to RGS9-2 antibodies (RGS9 IP) were analyzed by quantitative Western blotting using secondary antibodies labeled with IRDye680 and IRDye800 fluorescent dyes and detected by an Odyssey (LiCor) infrared scanner. Immunoprecipitation and elution was performed as described in Materials and Methods. Equal protein amounts of striatal extracts and volumes of eluates were loaded on the gel.

Table 2. Proteins showing up-regulated binding to RGS9-2 in R7BP-/- samples.

Protein Name	Accession	Fold increase	Normalized 114/115 ratio	p-value of ratio	Number of peptides	% Coverage	ID score	p-value of ID
predicted hypothetical protein similar to Igh-1a	gi|149274201	5.6	0.179	$2.5x10^{-4}$	5	38.22	10.02	$9.5x10^{-11}$
p21 (CDKN1A)-activated kinase 7	gi|134949024	5.4	0.184	$3.9x10^{-8}$	7	21.56	17.34	$4.5x10^{-18}$
heat shock protein 8 (Hsc70)	gi|31981690	5.2	0.192	$5.6x10^{-8}$	7	18.27	14	$9.9x10^{-15}$
2',3'-cyclic nucleotide 3' phosphodiesterase	gi|6753476	5.2	0.193	0.0201	2	9.05	4	$1.0x10^{-4}$
ribosomal protein L13	gi|33186863	5	0.202	$1.5x10^{-4}$	4	23.70	8.09	$8.1x10^{-9}$
calcium/calmodulin-dependent protein kinase II a2	gi|28916677	4.9	0.204	0.0123	1	3.14	2.31	0.0049
predicted hypothetical protein similar to IgG	gi|149255583	4.5	0.224	0.006	3	29.75	6	$1.0x10^{-6}$
β actin	gi|6671509	4.1	0.243	$2.4x10^{-9}$	12	54.40	22.87	$1.3x10^{-23}$
heat shock protein 9 (Hsp70)	gi|6754256	3.9	0.254	0.0011	4	21.06	8	$1.0x10^{-8}$
MAP/microtubule affinity-regulating kinase 4	gi|26986591	3.9	0.259	0.0067	1	6.91	2.09	0.0081
Predicted hypothetical protein similar to ribosomal protein L23	gi|149255181	3.8	0.264	$9.6x10^{-5}$	2	60.40	4.96	$1.1x10^{-5}$
Solute carrier family 25, member 4 (ADP/ATP translocase)	gi|148747424	3.7	0.274	0.0014	3	21.81	6.03	$9.3x10^{-7}$
Predicted protein similar to ribosomal protein L10-like	gi|82942312	3.3	0.300	0.0155	1	9.81	2.09	0.0081
Predicted hypothetical protein similar to ribosomal protein S5	gi|94404463	3.2	0.314	$9.7x10^{-4}$	4	35.84	8	$1.0x10^{-8}$
ribosomal protein S11	gi|21426889	3.2	0.317	$4.8x10^{-4}$	2	20.25	4.11	$7.7x10^{-5}$
Hypothetical ankyrin repeat containing protein LOC383787	gi|126517480	3.1	0.320	0.0209	2	11.79	4	$1.0x10^{-4}$
tubulin, beta 4	gi|31981939	3.1	0.320	0.0093	16	47.07	9.05	$8.9x10^{-10}$
Predicted hypothetical protein similar to ribosomal protein S13	gi|82919239	2.9	0.349	0.0049	2	19.21	4.55	$2.8x10^{-5}$
RAB11 family interacting protein 5, isoform 1	gi|52421788	2.8	0.352	0.0025	4	8.65	8	$1.0x10^{-8}$
ribosomal protein S9-like	gi|33504483	2.7	0.369	0.0066	3	19.07	5	$1.0x10^{-5}$
Predicted protein similar to histone H4	gi|94378251	2	0.501	0.0274	4	25.32	7.52	$3.0x10^{-8}$

method for the quantification of proteins whose levels are down-regulated more than ~5 fold thus reaching the background (116/114 ratio ~ 0.2). Since unequal amounts of RGS9-2 were precipitated from R7BP knockout and wild-type tissues, the data were normalized to bring 115:114 ratio of RGS9-2 protein to 1:1. The same correction factor was then applied to all proteins in the dataset using bias correction function built into the ProteinPilot™ software. Finally, in order to reliably account for the interactions that are not mediated by RGS9-2, but the level of which could non-specifically change between samples, we conducted additional immunoprecipitation experiments with RGS9 knockout samples only. Proteins identified in these control experiments were excluded from the iTRAQ® dataset.

The final dataset revealed 21 binding partners of RGS9-2 that exhibit statistically significant upregulation upon elimination of R7BP (Table 2). The range of observed changes in levels varied from 2 to nearly 6 fold. Most of the identified proteins can be grouped into four distinct classes based on their roles in cellular processes. The largest class is represented by ribosomal proteins followed by equally represented cytoskeletal components, protein kinases, and molecular chaperones. In summary, we have developed a quantitative proteomics method for analyzing interactome changes induced by genetic manipulation of mice and applied it to identify a distinct set of protein-protein interactions of RGS9•Gβ5 complex unregulated in response to the loss of its binding partner, R7BP.

HSC70 is a new binding partner of RGS9-2 upregulated upon R7BP elimination - We have reasoned that decreased stability of RGS9-2 observed upon elimination of R7BP could be caused by the enhanced association of the complex with factors that mediate degradation of the RGS9-2•Gβ5 complex. This brought our attention to chaperone HSC70, also known as heat shock protein 8, a molecule that has been extensively implicated in protein degradation (reviewed in [222, 223]). HSC70 shows ~5 fold upregulation in R7BP knockout samples and it is confidently identified by tandem mass-spectrometry screen with 7 peptides (15.2% sequence coverage) and 99% protein identification confidence as determined by ProteinPilot™ (see Figure 2.4A for the representative MS/MS spectrum).

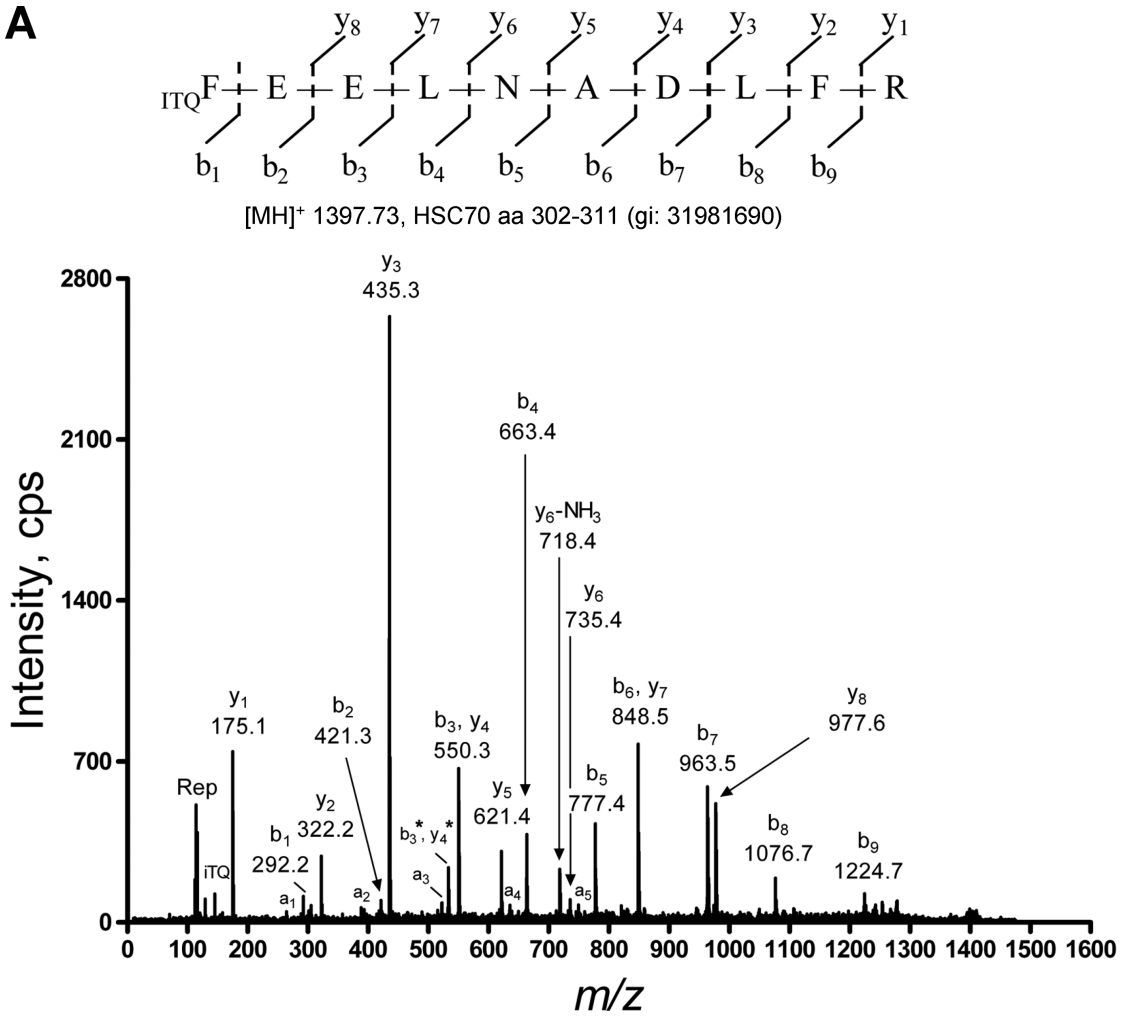
A
ITQ F E E L N A D L F R
y8 y7 y6 y5 y4 y3 y2 y1
b1 b2 b3 b4 b5 b6 b7 b8 b9
[MH]+ 1397.73, HSC70 aa 302-311 (gi: 31981690)
Intensity, cps
m/z
y3 435.3
b4 663.4
y6-NH3 718.4
y6 735.4
b6, y7 848.5
y8 977.6
b7 963.5
b5 777.4
y5 621.4
b3, y4 550.3
b2 421.3
y1 175.1
y2 322.2
b1 292.2
Rep
iTQ
b8 1076.7
b9 1224.7

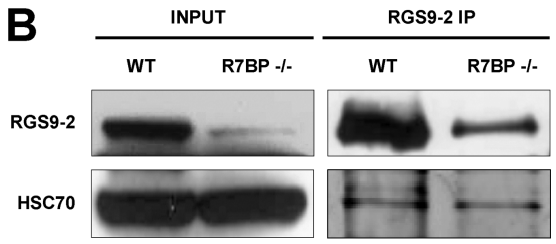
B
INPUT
RGS9-2 IP
WT
R7BP -/-
WT
R7BP -/-
RGS9-2
HSC70

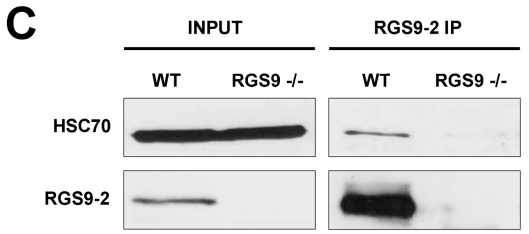
C
INPUT
RGS9-2 IP
WT
RGS9 -/-
WT
RGS9 -/-
HSC70
RGS9-2

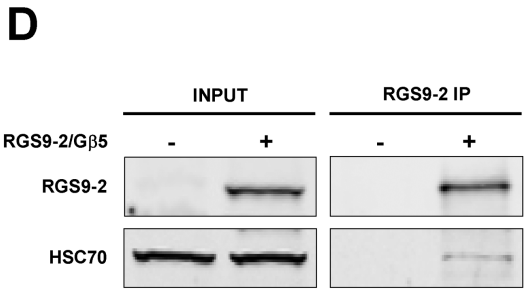
D
INPUT
RGS9-2 IP
RGS9-2/Gβ5
-
+
-
+
RGS9-2
HSC70

Figure 2.4: HSC70 is a binding partner of RGS9-2.

A, Representative MS/MS spectrum and deduced amino acid sequence of an HSC70-derived peptide found in RGS9-2 immunoprecipitation. **B**, Co-immunoprecipitation of HSC70 with RGS9-2 from wild-type (WT) and R7BP knockout (R7BP-/-) striatal tissues. RGS9-2 was immunoprecipitated and eluates were subjected to Western blot analysis as described under *Experimental Procedures*. **C**, HSC70 is absent from the eluates from RGS9 knockout samples indicating specific interaction between RGS9-2 and HSC70. RGS9-2 was precipitated with a specific antibody from striatal lysates of wild-type (WT) and RGS9 knockout (RGS9-/-) mice and analyzed by Western blotting. **D**, HSC70 interacts with RGS9-2 in transfected cells. HEK293FT cells were co-transfected with equal amounts of either RGS9-2•Gβ5 complex or empty pcDNA3.1 vector. RGS9-2 was precipitated with a specific antibody and eluates were analyzed by Western blotting.

Western blot analysis revealed the presence of similar amounts of HSC70 in the eluates from the immunoprecipitation experiments conducted with wild type and R7BP knockout samples (Figure 2.4B). Because substantially less RGS9-2 is precipitated from R7BP knockout samples as compared to wild type, this result indicates an increase in co-immunoprecipitation of HSC70 with RGS9-2 in the absence of R7BP. Indeed, quantification of several Western blotting experiments revealed no statistically significant differences in HSC70 levels between wild-type and R7BP knockout samples (ratio of band densities is 1.3±0.6, p=0.447). Therefore, when normalized to the 3.5-fold difference in RGS9-2 levels, these data indicate that the amount of HSC-70 co-immunoprecipitated with RGS9-2 is increased by at least 3-fold, which is in good agreement with 5-fold HSC70 upregulation quantified based on the iTRAQ® data.

The specificity of the HSC70•RGS9-2 interaction in native neurons was validated by conducting the RGS9-2 immunoprecipitation experiments with striatal extracts obtained from RGS9 knockout mice. The results presented in Figure 2.4C show that while easily detectable in the wild-type eluates, HSC70 is absent from the RGS9 knockout samples confirming that the anti-RGS9-2 antibodies do not precipitate HSC70 non-specifically. We further tested the interaction in transfected mammalian HEK293FT cells (Figure 2.4D). As in native striatal neurons, RGS9-2•Gβ5 complex co-precipitated with HSC70 endogenously expressed in HEK293 cells suggesting a direct nature of the binding that does not require the presence of specific neuronal proteins.

HSC70 is recruited to the intrinsically disordered C-terminus of RGS9-2 - We next addressed which molecular determinants in RGS9-2 mediate interaction with HSC70. Previous studies have hypothesized that the loss of R7BP exposes KFERQ sequences confined to the N-terminal DEP/DHEX domains of RGS9-2 [93]. KFERQ motifs are known elements that confer HSC70 recruitment [224]. Alternatively, HSC70/HSP70 chaperones have been shown to bind to the regions of high conformational flexibility known as intrinsic disorder regions [225, 226]. Analysis of RGS9-2 sequence by PONDR VSL2 algorithm [217, 218] of residue-by-residue prediction of the intrinsic disorder probability indicated that a proline-rich C-terminus is very likely to be intrinsically disordered (Figure 2.5A). Most of the amino acid sequence

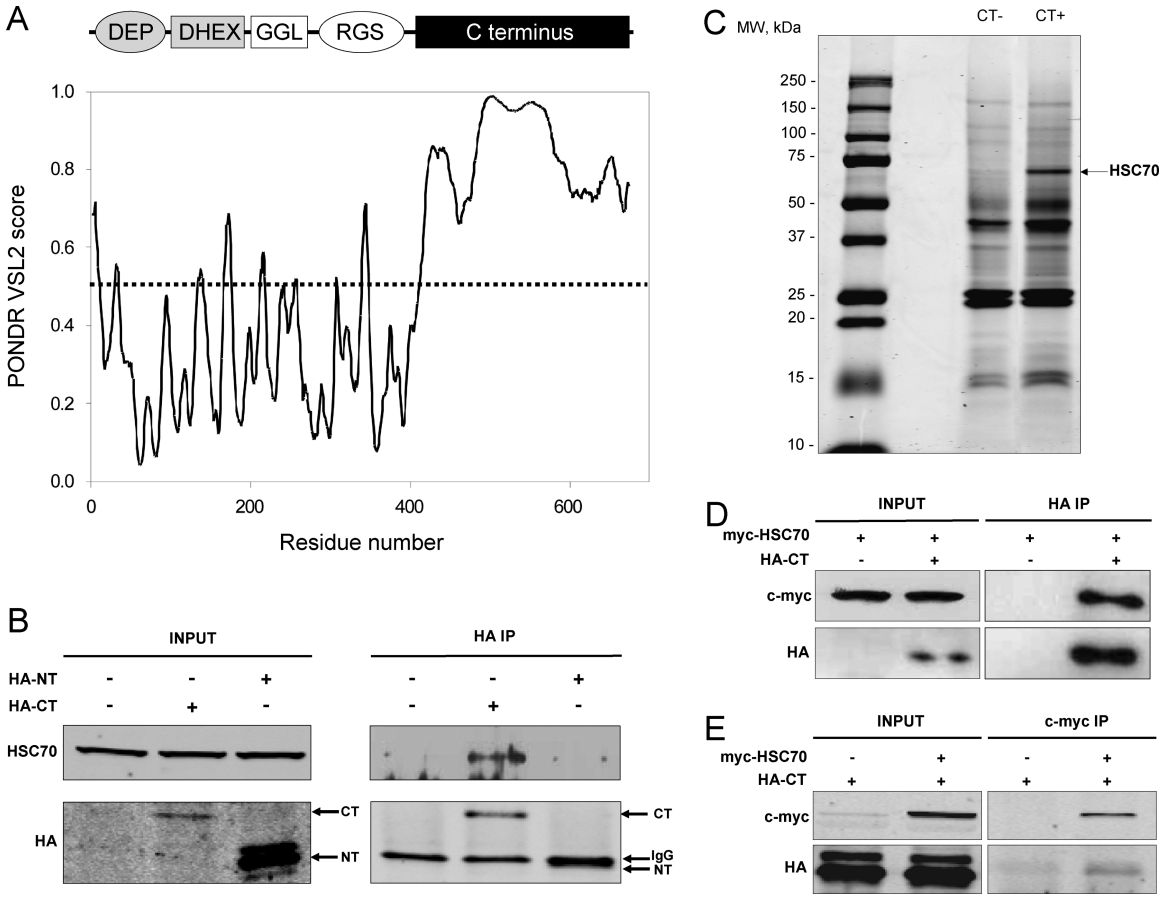

Figure 2.5: The interaction of HSC70 with RGS9-2 is mediated by the C-terminus of RGS9-2.

A, Intrinsic disorder prediction for RGS9-2 sequence using PONDR VSL2 algorithm. A dashed line represents an arbitrary threshold for disorder set at 0.5 value. Gray shading represents N-terminus and black marks the C-terminal fragments of RGS9-2 used in the subsequent experiments (panels B,C,D,E). **B**, Comparison of HSC70 binding to N-terminal (NT) and C-terminal (CT) fragments of RGS9-2. HEK293 cells were transfected with either C-terminus or N-terminus. Both the C- and N-terminus were tagged with an HA tag, which was used for their precipitation from cellular lysates, followed by analysis with Western blotting. **C,** A Coomassie stained gel showing separation of proteins pulled-down from whole brain extracts by either empty SulphoLink beads (-CT) or SulphoLink beads conjugated to the recombinant C-terminus of RGS9-2 (+CT). Arrow indicates a position of the band specifically present in +CT but not -CT samples. MALDI MS/MS analysis identified HSC70 as a major protein present in the band. **D**, Co-immunoprecipitation of HA-tagged C-terminus of RGS9-2 (HA-CT) with myc-tagged HSC70 (myc-HSC70) from transfected HEK293 cells using anti anti-HA antibody, followed by Western blotting analysis. **E**, Reciprocal co-immunoprecipitation of HA-tagged C-terminus of RGS9-2 with myc-tagged HSC70 from transfected HEK293FT cells using anti c-myc antibody, followed by Western blotting analysis.

of the C-terminal domain scores near a maximal probability value (PONDR VSL2 score 1), well above the score of the rest of the domains, which are close to the threshold value of 0.5. These observations are additionally supported by the previously observed structure/functional similarity of RGS9-2 C-terminus to the gamma subunit of phosphodiesterase (PDE6γ) [62], a known intrinsically disordered protein [227, 228]. Therefore we have analyzed the interaction of HSC70 with both of its potential binding sites in RGS9-2, the N-terminal fragment consisting of DEP and DHEX domains and C-terminal region (Figure 2.5B). In transfected cells, the C-terminal domain of RGS9-2 co-precipitated with endogenous HSC70. In contrast, immunoprecipitation of the N-terminal fragment did not reveal HSC70 in the eluates above the amount that bound non-specifically to the beads, suggesting that its binding to HSC70, if any, is much weaker than that of the C-terminus (Figure 2.5B, right panels). Interestingly, binding of HSC70 to RGS9-2 fragments inversely correlated with their expression levels in the cells (Figure 2.5B left panels), consistent with the role of HSC70 in mediating protein degradation.

Further proof that the C-terminus of RGS9-2 recruits HSC70 was obtained from unbiased pull-down assays in which the His-tagged recombinant C-terminal fragment purified from Sf9 cells was covalently cross-linked to beads and incubated with total brain extract. Separation of the eluates by SDS PAGE followed by Coomassie staining revealed the presence of a single major band retained by the protein-conjugated beads that was absent in the control experiment with empty beads (Figure 2.5C). Tandem MS/MS mass-spectrometric analysis identified that this band contains a mixture of two chaperone proteins: HSC70 (12 unique peptides) and its inducible homologue HSP70 (9 unique peptides).

In the next set of experiments we have confirmed the specificity of the HSC70 interaction with the C-terminus of RGS9-2 by performing forward and reciprocal co-immunoprecipitation experiments (Figure 2.5D,E). Upon co-transfection in HEK293FT cells, c-myc-tagged HSC70 construct was effectively co-precipitated with HA-tagged C-terminus of RGS9-2 when either c-myc or HA antibodies used for the immunoprecipitation but not in the control experiments in which cells were transfected

only with one construct. Taking these data together, we conclude that intrinsically disordered C-terminus of RGS9-2 is a specific site mediating its binding to HSC70.

HSC70 regulates RGS9-2 expression - Our observation that HSC70 specifically binds to destabilized RGS9-2 together with a known role of HSC70 in protein degradation has prompted us to evaluate whether HSC70 has an effect on RGS9-2 expression levels. We have first asked whether stabilization of RGS9-2•Gβ5 complex by R7BP affects its association with HSC70. Consistent with earlier report [50], higher levels of RGS9-2 were detected in cells co-transfected with R7BP (Figure 2.6A). Concomitantly, the presence of R7BP significantly reduced the amount of HSC70 co-precipitating with RGS9-2•Gβ5 indicating that protective effects of R7BP involve down-regulation of HSC70 binding to the complex (Figure 2.6A,B).

We have next used an RNA interference approach to specifically knock-down HSC70 and examine its effects on RGS9-2 levels. Transfection of cells with siRNA matching HSC70 mRNA sequence resulted in 20.5±11.6% decrease in HSC70 expression levels (Figure 2.6C,D) as compared to control siRNA transfection ($p=0.015$, $n=6$, t-test). The modest degree of knockdown efficiency of HSC70 is expected based on a critical housekeeping role that this protein plays for cellular survival [229]. Concomitant with HSC70 down-regulation the levels of RGS9-2 increased by 17.4±6.1% ($p=0.002$, $n=6$, t-test) as evidenced by statistical analysis of quantitative Western blotting (Figure 2.6D).

Further, we have employed a "dominant-negative" strategy aimed at inhibiting RGS9-2 interaction with HSC70. The cells were additionally transfected with an excess of the construct encoding C-terminal domain of RGS9-2, which constitutes the main binding site for HSC70 and therefore expected to compete with full-length RGS9-2 for binding to endogenous HSC70. Data in Figure 2.6 (panels E and F) show that the expression of C-terminus in 2.5±0.3 -fold excess over full-length RGS9-2 (quantified by Western blotting) resulted in 2.0±0.3 -fold ($p=0.016$, $n=4$, t-test) increase in RGS9-2 expression. These data indicate that HSC70 negatively regulates RGS9-2 expression consistent with their increased association upon RGS9-2 destabilization *in vivo*.

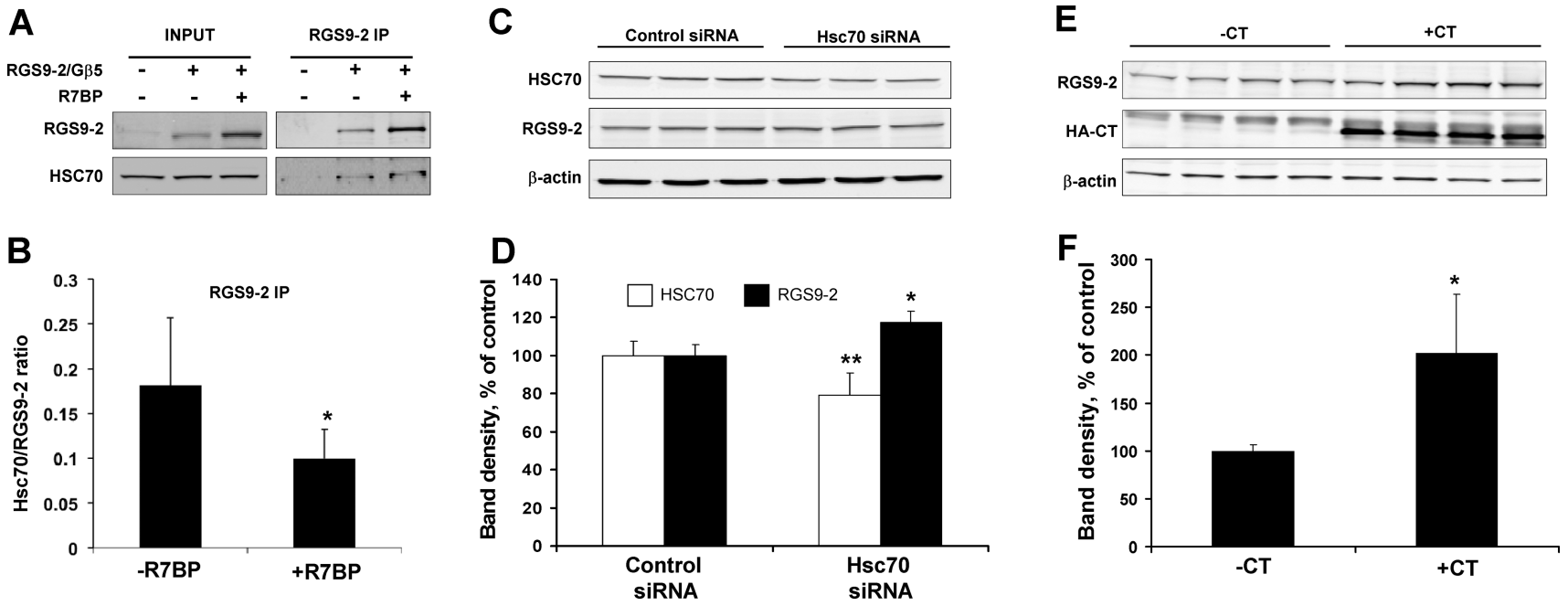

Figure 2.6: HSC70 is a negative regulator of RGS9-2 expression.

A, Down-regulation of HSC70 binding to RGS9-2•Gβ5 upon co-expression with R7BP. HEK293 cells were transfected with RGS9-2•Gβ5 complex with either R7BP or empty pcDNA3.1 vector. RGS9-2 containing complexes were immunoprecipitated from cell lysates and eluates were analyzed using specific antibodies. **B,** Quantification of changes in HSC70 binding analyzed as described in panel A. Band densities were quantified by Odyssey infrared imaging system and integrated intensities were normalized to the amounts of precipitated RGS9-2. **C**, Up-regulation of RGS9-2 expression upon knock-down of HSC70. HEK293FT cells were transfected with either negative control siRNA or specific siRNA targeting HSC70 expression, followed by transfection with RGS9-2•Gβ5 complex. Twenty-four hrs post transfection, cell lysates (20 μg/lane) were analyzed for protein expression using specific antibodies. **D**, Quantification of changes in expression levels of proteins analyzed as described in panel C. Band densities were quantified by Odyssey infrared imaging system and integrated

intensities were normalized to β-actin. **E**, Up-regulation of RGS9-2 expression upon co-expression of the C-terminus of RGS9-2 (CT). HEK293FT cells were transfected with RGS9-2•Gβ5 complex (0.25 mg each/10 cm^2) with either C-terminus (+CT) or empty pcDNA 3.1 vector (-CT) (2 mg/10 cm^2). 24 hrs after transfection cell lysates (20 μg/lane) were analyzed for protein expression using RGS9-2 and β-actin antibodies. **F**, Quantification of changes in expression levels of proteins, presented in panel E. Band densities were quantified by Odyssey infrared imaging system and normalized to β-actin. *$p<0.05$

- ***Discussion***

Proteomics approach for the analysis of changes in protein interaction networks in mouse genetic models - Many cellular functions are built on the principle of complex networks of protein-protein interactions. Recent studies in simple model organisms have indicated that most signaling proteins interact transiently and/or simultaneously with several partners [230]. While some interactions are static, growing evidence suggests that the majority of proteins are part of macromolecular assemblies where individual components transiently interact with each other [230, 231]. Thus, it is the dynamic re-organization of these networks that is thought to be responsible for mediating a variety of cellular reactions including signal transmission, biogenesis and trafficking of molecules, and formation of cellular structures [232, 233].

The interaction dynamics of signaling proteins in mammals is relatively uncharted territory. It is generally recognized that the logic behind addressing such questions in a complex signaling networks, such as those in neurons for example, is to study perturbations in the cellular interactome that occur following specific protein changes (see [234] for discussion). An increasing number of studies have reported changes in protein expression following specific manipulations (see [235, 236] for recent examples) as well as comprehensive information about the interactome for individual proteins [237, 238]. However, the analysis of the changes in the interaction profiles following precise intervention at the level of a single molecule is substantially lagging, although such studies are expected to provide valuable insights into the operational logic of the signaling pathways and the mechanisms of their regulation.

Genetic mouse models represent potentially powerful tools for examining the interactome changes in mammalian systems. A variety of mouse knockout and transgenic strains offer precise control over the expression of a single gene often with an exquisite spatial and temporal resolution making them uniquely suited for delineating dynamic interactions in complex signaling networks but also for performing interaction specificity controls critical for validation of interactome data. In this study, we report the development of a proteomics approach to quantify changes in the protein interactions

induced by genetic knockout, and demonstrate its application for studying the mechanisms mediating the degradation of RGS9-2, a key regulator of G protein signaling in the striatum. The platform for this approach is antibody-based affinity purification of protein complexes followed by differential iTRAQ® labeling of samples, and subsequent mass-spectrometric identification and quantification of binding proteins. The use of two separate types of mouse knockouts is critical for the success of the approach. The first line lacks the component whose influence on the interaction network is being studied. The second line lacks the target protein for the affinity purification, and therefore provides the ideal control for interaction specificity. Following mass-spectrometric quantification and normalization to the levels of purified proteins, the resulting interactome database is expected to reveal three groups of proteins whose interaction within the complex are: (i) up-regulated, (ii) down-regulated, or (iii) unchanged. Grouping these proteins by homology or functional relevance provides insight into how changes in the interactions of the central protein of interest translate into regulation of its functional homeostasis and/or changes in signaling networks. In our application of the approach, we have focused on identifying interactions that are upregulated upon decrease in the levels of signaling protein undergoing degradation. Due to the large decrease in target protein levels, the identification of the interactome alterations was limited to up-regulated interactions, as down-regulated associations fell close to the threshold for identification set by the non-specificity control provided by the knockout of the target protein and therefore could not be considered reliable. Nevertheless, we believe this approach may be successfully used for the identification of changes in the interactome in both directions providing that the levels of the target proteins do not exhibit substantial differences. Given the nature of the alteration in the knockout mouse of interest, the results reported in the present study primarily describe the identification of the mechanisms for regulation of signaling protein homeostasis. However, we envision that future applications of the described approach to other signaling systems could also result in the identification of a range of functional interaction changes.

Insights into mechanisms of RGS9-2 degradation from interactome analysis - The abundance of RGS9-2 in the striatum has been demonstrated to influence sensitivity of

reward and motor circuits in D2-dopamine and μ-opioid receptor signaling pathways [12, 27, 118]. Interestingly, stimulation of the receptors by psychostimulants and morphine [12, 27, 118, 215], changes in neuronal excitability and oxygenation status [116] have been shown to result in rapid changes in RGS9-2 expression, which is thought to constitute an important feedback mechanism underlying the plasticity of striatal signaling [214]. Dynamic association with the membrane anchor R7BP has been shown to play a key role in controlling the expression of RGS9-2 by altering proteolytic stability of the complex [93, 116]. The key observation of this study is the identification of a molecular chaperone HSC70 that is a critical factor negatively regulating RGS9-2 expression levels that are upregulated upon the loss of R7BP binding. How can HSC70 association lead to the degradation of RGS9-2? HSC70 is a major housekeeping isoform of the HSP70 family of chaperone proteins [239, 240]. Abundant evidence indicates that, in addition to protein folding, HSC70 plays a major role in protein degradation. There are two distinct mechanisms by which HSC70 is known to assist in protein degradation. On the one hand, HSC70 recruits the E3 ubiquitin ligase CHIP to its substrate protein facilitating ubiquitination and subsequent proteasomal degradation [223, 241]. On the other hand, HSC70 in complex with co-chaperone proteins binds to the LAMP2a channel and targets proteins for import into the lysosomes where they undergo degradation through a process called chaperone-mediated autophagy [222, 242]. Proteolysis of RGS9-2 in the striatum of R7BP mice can be prevented by blocking cysteine proteases but not the proteasome, suggesting that the lysosomal pathway is likely to be responsible for the degradation of RGS9-2 [93]. However, in transfected cells, RGS9-2 was also found to be ubiquitinated in R7BP-sensitive manner [116]. These observations suggest that the mechanism of RGS9-2 degradation might be complex and involve post-translational modifications, i.e. ubiquitination, in addition to HSC70-based chaperone mediated autophagy. For example, three protein kinases found on the list of the up-regulated interactions could also be involved in specifying the pathway of RGS9-2 degradation *in vivo*. In any event, we believe that the involvement of HSC70 in both pathways makes it a key regulator of RGS9-2 expression.

We have shown that the main site of HSC70 binding is located within the intrinsically disordered C-terminus of RGS9-2. This observation is consistent with a previous report that HSC70 is recruited to an intrinsically disordered domain of the TNF-α regulator SIMPL [226] and further implicates HSC70 as a sensor of the intrinsic disorder regions in proteins. Previously, the only universal consensus site in proteins for HSC70 binding was thought to be formed by so-called 'KFERQ' sequences. These motifs have poor conservation and high variability between different proteins, the hallmark feature of which is a hydrophobic, highly positive and highly negative stretch of 5-6 amino acids [242]. Interestingly, the N-terminus of RGS9-2 was predicted to contain several KFERQ-like motifs located within the local intrinsic disorder peaks. Several KFERQ-like sequences were also predicted within the C-terminal domain, which incidentally exhibits much longer regions of disorder. Because C-terminal domain of RGS9-2 binds HSC70 much stronger than the N-terminal region we conclude that a combination of high intrinsic disorder propensity with the presence of the "KFERQ"-like motif is a stronger predictor of HSC70 recruitment than the presence of the 'KEFRQ'-like sequences alone. In fact, our analysis of intrinsic disorder indicates that 'KFERQ'-like sequences are extremely likely to be unstructured suggesting that these sequences represent local disorder hot-spots. Therefore, the intrinsic disorder domains in proteins are likely to serve as the primary determinant for the interaction of target proteins with HSC70 chaperons, thus determining their rate of turnover in the cell.

Beyond HSC70, ribosomal proteins were a major group of RGS9-2 binding proteins that were upregulated in R7BP knockout tissue. The crystal structure of the ribosome [243] indicates that most of the ribosomal proteins we isolated are clustered on the surface of the ribosomal subunits suggesting that they likely reflect the interaction of the nascent RGS9-2 chain with ribosomes. In fact, ribosomal proteins often serve as the initial interaction partners for newly synthesized proteins, thus assisting in their folding (see [244] for recent review). This suggests a co-translational mechanism of RGS9-2 complex assembly with R7BP. Furthermore, chaperones of the HSP70 family, including HSC70 are found bound to the ribosomes where they are thought to facilitate folding and macromolecular complex assembly [245, 246]. This leads us to hypothesize a scenario

for co-translational checkpoint control of the formation of the RGS9-2•R7BP complex. We speculate that newly emerging DEP/DHEX domains of RGS9-2 bind to R7BP causing this complex to be quickly targeted to its destination in the post-synaptic density. In the absence of R7BP, lingering transient interactions with ribosomal proteins lead to the recruitment of ribosome associated HSC70 to the C-terminus of RGS9-2 resulting in degradation. Finally, increased association of RGS9-2 with cytoskeletal proteins in the absence of R7BP could be explained by the fact that both ribosomes and HSP70 chaperones are organized by the cytoskeleton [247, 248]. In conclusion, we believe that precise delineation of the pathways and regulatory cues that are responsible for triggering RGS9-2 proteolysis will be an exciting future direction, and we hope further investigation of the regulated RGS9-2 binding partners our study has uncovered will provide insight into this process.[2]

[2] We are indebted to Dr. LeeAnn Higgins at the Center for Mass-Spectrometry and Proteomics, University of Minnesota for the acquisition of the mass-spectrometry data, discussions and critical comments on the manuscript. We are grateful to Drs. Brock Grill, Nick Skiba and Garret Anderson for critical comments on the manuscript. We also thank Dr. William Simonds (NIH) for the generous gift of anti-R7BP and anti-Gβ5 antibodies, Dr. Jason Chen (Virginia Commonwealth University) for providing RGS9 knockout mice, Dr. Cam Patterson for providing HSC70 construct, Dr. Keqiang Xie for cloning HA-tagged N-terminus of RGS9-2. This work was supported in part by NIH grants DA021743 (K.A.M.), DA026405 (K.A.M.), LM007688 (V.N.U.) and GM071714 (V.N.U.), McKnight Land-Grant Professorship award (K.A.M.), and a grant from the Program of the Russian Academy of Sciences "Molecular and Cellular Biology" (V.N.U.). We gratefully acknowledge core resources provided by Minnesota Supercomputing Institute and the support of the IUPUI Signature Centers Initiative. National Science Foundation for Major Research Instrumentation grants 9871237 and NSF-DBI-0215759 was used to purchase the instruments described in this study.

Chapter 3 - RGS6·Gβ5 complex accelerates I_{KACh} gating kinetics in atrial myocytes and modulates parasympathetic regulation of heart rate

Ekaterina Posokhova, Nicole Wydeven, Kevin L. Allen, Kevin Wickman, Kirill A. Martemyanov

From the Department of Pharmacology, University of Minnesota, 6–120 Jackson Hall, 321 Church Street S.E. Minneapolis, MN 55455 USA

Content taken from the published manuscript:

Posokhova E., Wydeven N., Allen K.L., Wickman K., Martemyanov K.A. RGS6·Gβ5 complex accelerates I_{KACh} gating kinetics in atrial myocytes and modulates parasympathetic regulation of heart rate. *Circulation Research,* 2010. 107(11):1350-1354.

Specific contributions: ENP data is presented in Figures 3.2, 3.3, 3.4, 3.7, 3.8, 3.9.

Rationale - The parasympathetic reduction in heart rate (HR) involves the sequential activation of M2 muscarinic cholinergic receptors (M2R), pertussis toxin-sensitive ($G_{i/o}$) heterotrimeric G proteins, and the atrial potassium channel I_{KACh}. Molecular mechanisms regulating this critical signal transduction pathway are not fully understood.

Objective - To determine whether the G protein signaling regulator RGS6•Gβ5 modulates M2R-I_{KACh} signaling and cardiac physiology.

Methods and Results - Cardiac expression of RGS6, and its interaction with Gβ5, was demonstrated by immunoblotting and immunoprecipitation. RGS6 knockout mice were generated by gene targeting, and the cardiac effects of RGS6 ablation were analyzed by whole-cell recordings in isolated cardiomyocytes and electrocardiogram (ECG) telemetry. Loss of RGS6 yielded profound delays in M2R-I_{KACh} deactivation kinetics in both neonatal atrial myocytes and adult sino-atrial nodal cells. RGS6 knockout mice exhibited mild resting bradycardia and altered HR responses to pharmacologic manipulations that were consistent with enhanced M2R-I_{KACh} signaling.

Conclusions - The cardiac RGS6•Gβ5 complex modulates the timing of parasympathetic influence on atrial myocytes and HR in mice.

- ***Introduction***

Cardiac output is shaped to a great extent by sympathetic and parasympathetic influences. Parasympathetic input tempers heart rate (HR) and counteracts the pro-arrhythmic effects of sympathetic activation, and is mediated by acetylcholine (ACh) [249]. ACh is released from post-ganglionic parasympathetic neurons and binds to M2 muscarinic receptors (M2R) on pacemaker cells and atrial myocytes, triggering activation of pertussis toxin-sensitive ($G_{i/o}$) heterotrimeric G proteins [250]. Once activated, G proteins dissociate into Gα-GTP and Gβγ subunits, leading to modulation of adenylyl cyclase and multiple ion channels. Central among these reactions is the binding of Gβγ to the atrial potassium channel I_{KACh}, a heterotetramer composed of GIRK1 and GIRK4 subunits [251]. Binding of Gβγ to I_{KACh} enhances its gating which leads to cell hyperpolarization and ultimately, decreased HR [195].

The duration of G protein signaling is controlled by members of the Regulator of G protein Signaling (RGS) family [252]. RGS proteins stimulate inactivation of Gα-GTP, facilitating its re-assembly with Gβγ. RGS proteins play a critical role in shaping bradycardic effects of M2R receptor activation [15, 185, 197]. Indeed, eliminating RGS influence by expressing Gα subunits insensitive to RGS action results in a substantial enhancement of I_{KACh} regulation by M2R signaling, via both Ga_o and Ga_{i2} pathways [185, 197]. Although more than 30 RGS proteins have been identified, the involvement of specific RGS proteins in the regulation of parasympathetic input is not fully-understood. Here, we report an unexpected role of the RGS6•Gβ5 complex, previously thought to be neuron-specific regulator, in the temporal regulation of M2R-I_{KACh} signaling.

- ***Materials and Methods***

Antibodies, Recombinant Proteins, DNA Constructs - Sheep anti-RGS6 antibodies (αRGS6-FL) were generated against recombinant fragment containing amino acids 263-

472 of mouse RGS6 that was expressed and purified from *E.coli* as described [253]. Antibodies were affinity-purified on the epitope-conjugated column and stored in PBS buffer containing 50% glycerol. Rabbit anti-Gβ5 (SGS) and rabbit anti-R7BP (TRS) antibodies were a generous gift from Dr. William Simonds, NIDDK. Rabbit polyclonal anti-AU1 tag (GenScript, Piscataway, NJ), mouse monoclonal anti-AU5 (MMS-135R; Covance, Princeton, NJ), goat polyclonal anti-RGS4 (Santa Cruz Biotechnology, Santa Cruz, CA), rabbit polyclonal anti-PSD95 (Millipore, Billerica, MA) rabbit polyclonal anti-$G\alpha_{i1/2}$ (Thermo Fisher Scientific, Rochford, IL) and rabbit polyclonal anti-Ga_o (K20; Santa Cruz Biotechnology, Santa Cruz, CA) were purchased. All general chemicals were purchased from Sigma Aldrich (St. Louis, MO).

Cloning of full-length mouse Gβ5S and RGS6 was described previously [62, 76]. The open reading frame of Gβ5S was subcloned into pcDNA3.1/TOPO (Invitrogen) mammalian expression vector, and RGS6 was cloned into pcDNA3.1NT-GFP-TOPO (Invitrogen) creating an N-terminal fusion with GFP. Cloning of GIRK1-AU5 and GIRK4-AU1 into mammalian expression vectors has been described [254]. All constructs were propagated using an *E.coli* Top-10 strain (Invitrogen), isolated using Nucleobond kits (Macherey-Nagel; Bethlehem, PA), and sequenced.

Mouse Strains - The generation of R7BP [93], Gβ5 [78], and GIRK4 knockout [195] mice has been described previously. Gβ5 knockout mice were generously provided by Dr. Jason Chen (Virginia Commonwealth University). These three strains of mice were out-bred onto the C57BL/6 background for at least 5 generations. RGS6 knockout mice were generated by Lexicon Pharmaceuticals using 129SvEvBrd embryonic stem cells. Chimeric offspring were mated with C57BL/6 strain and the resulting heterozygous progeny were inbred to generate null mutant and wild-type littermates. Mice were housed in groups on a 12h light/dark cycle with food and water available *ad libitum*. Littermate mice were used for all experiments in this study. All procedures were carried out in accordance with the National Institute of Health guidelines and were granted formal approval by the Institutional Animal Care and Use Committee of the University of Minnesota. All efforts were made to minimize the use of animals in this study, as well as their suffering. All animals used in this study were bred on-site.

Cell culture and transfections - HEK293FT cells were obtained from Invitrogen (Carlsbad, CA) and cultured at 37°C and 5% CO_2 in DMEM (Dulbecco's Modified Eagle Medium; GIBCO) supplemented with 100 units of penicillin and 100 mg of streptomycin, 10% FBS, 1x MEM non-essential amino acids (GIBCO; Carlsbad, CA), 1 mM sodium pyruvate and 4 mM L-glutamine. Cells were transfected at ~70% confluency, using Lipofectamine LTX (Invitrogen) according to the manufacturer's protocol. The ratio of Lipofectamine to DNA used was 6.25 μl : 2.5 μg per 10 cm^2 cell surface. Cells were grown for 24-48 hours post-transfection. Equal amounts of each construct were transfected, balanced when necessary by empty pcDNA3.1 vector.

Immunoprecipitation assays and Western blotting - Cellular and tissue lysates were prepared in immunoprecipitation (IP) buffer (1XPBS (Fisher Scientific), 150 mM NaCl, 1% Triton X-100, protease inhibitors (Roche; Indianapolis, IN)) and centrifuged for 15 min at 14,000 x g. Protein concentration was determined in the resulting extracts using BSA assay (Pierce; Rockford, IL) and equal amounts of protein were incubated with 3 μg of antibodies and 10 μl of protein G beads (GE Healthcare; Waukesha,WI) for 1 h at 4^0C. After 3 washes with ice-cold IP buffer proteins bound to the beads were eluted with SDS-sample buffer. Eluates were resolved on 12.5% SDS-PAGE gel, transferred onto PVDF membrane (Millipore; Billerica, MA) and subjected to Western blot analysis using HRP conjugated secondary antibodies and an ECL West Pico (Pierce) detection system. For quantification, samples were analyzed by infrared Western blotting using IRDye680 and IRDye800 labeled secondary antibodies (Li-Cor Biosciences; Lincoln, NE) according to the manufacturer's protocol. Detection and quantification of specific bands was performed on an Odyssey Infrared Imaging System (Li-Cor Biosciences). The integrated intensity of each band of interest was measured in a corresponding channel with a top-bottom background setting.

Adult cardiomyocyte isolation - Atrial cardiomyocytes were isolated from adult mice (1 m.o.). Hearts were excised into Tyrode's solution (in mM): 140 NaCl, 5.4 KCl, 1.2 KH_2PO_4, 1.0 $MgCl_2$, 1.8 $CaCl_2$, 5.5 glucose, 5 HEPES, pH 7.4 with NaOH. Atria were dissected, cut into strips and placed into a modified Tyrode's solution containing (in mM): 140 NaCl, 5.4 KCl, 1.2 KH_2PO_4, 0.2 $CaCl_2$, 50 taurine, 18.5 glucose, 5 HEPES,

0.1% BSA, pH 6.9 with NaOH, with elastase (0.3 mg/ml; Worthington Biochemical Corp.), collagenase II (0.21 mg/ml; Worthington Biochemical Corp.) and proteinase XIV (0.2 mg/ml; Sigma). Tissue was digested at 37°C for 1 hr, with occasional inversion, and then washed twice in a solution containing (in mM): 100 L-glutamic acid/potassium salt, 10 L-aspartic acid/potassium salt, 25 KCl, 10 KH_2PO_4, 2 $MgSO_4$, 20 taurine, 5 creatine, 0.5 EGTA, 20 glucose, 5 HEPES, 0.1% BSA, pH 7.2 with KOH. Atrial tissue was then triturated in the wash solution, and cell pellet (50 x g, 5 min) was washed twice with PBS (Fisher Scientific) and lysed in IP buffer (PBS, 150 mM NaCl, 1% Triton, protease inhibitor cocktail (Roche).

Whole-cell electrophysiology - Primary cultures of atrial myocytes were generated from neonatal mice (P2-4) as described [255, 256], using the Neonatal Cardiomyocyte Isolation System (Worthington Biochemical Corp., Lakewood, NJ). Atrial myocytes were used for electrophysiological analysis after 1-3 d in culture. Sinoatrial nodal cells were isolated from adult mice (3 months) as described [15], and used within 8 h of isolation. In brief, hearts were excised into Tyrode's solution (in mM): 140 NaCl, 5.4 KCl, 1.2 KH_2PO_4, 1.0 $MgCl_2$, 1.8 $CaCl_2$, 5.5 glucose, 5 HEPES, pH 7.4 with NaOH. The sinoatrial node (SAN) was identified as the narrow band of tissue located on the inner wall of the right atrium, medial to the crista terminalis and between the superior and inferior vena cava. Two incisions were made to the superficial side of the superior and inferior vena cava, followed by a longer cut along the outer atrial wall, to expose the SAN region. SAN-containing tissue was excised into a modified Tyrode's solution containing (in mM): 140 NaCl, 5.4 KCl, 1.2 KH_2PO_4, 0.2 $CaCl_2$, 50 taurine, 18.5 glucose, 5 HEPES, 0.1% BSA, pH 6.9 with NaOH, with elastase (0.3 mg/ml; Worthington Biochemical Corp.) and collagenase II (0.21 mg/ml; Worthington Biochemical Corp.). SAN tissue was digested at 37°C for 30 min, with occasional inversion, and then washed three times in a solution containing (in mM): 100 L-glutamic acid/potassium salt, 10 L-aspartic acid/potassium salt, 25 KCl, 10 KH_2PO_4, 2 $MgSO_4$, 20 taurine, 5 creatine, 0.5 EGTA, 20 glucose, 5 HEPES, 0.1% BSA, pH 7.2 with KOH. SAN tissue was then triturated in the wash solution and plated onto poly-L-lysine coated coverslips for electrophysiological studies.

Coverslips containing atrial myocytes or SAN cells were transferred to a chamber containing a low-K^+ bath solution (in mM): 140 NaCl, 4 KCl, 2 $CaCl_2$, 2 $MgCl_2$, 10 D-glucose, 10 HEPES/NaOH (pH 7.4). Cardiac cells were visualized using an Olympus IX-70 microscope. The dominant population of atrial myocytes with spherical shape (typical capacitance, 10-20 pF) was targeted for this study. SAN cells were identified as the thin striated cells exhibiting spontaneous contractions (typical capacitance, 25-40 pF) (see Figure 3.6B, inset). Membrane potentials and whole-cell currents were measured with hardware (Axopatch-200B amplifier, Digidata 1320) and software (pCLAMP v. 9.2) from Molecular Devices (Sunnyvale, CA). Borosilicate patch pipettes (3-5 MΩ) were filled with (in mM): 130 gluconate, 2 $MgCl_2$, 1.1 EGTA/KOH (pH 7.2), 5 HEPES/KOH (pH 7.2), 2 Na_2ATP, 5 phosphocreatine, 0.3 Na-GTP.

Upon achieving whole-cell access, input resistance, capacitance, and resting membrane potentials were measured. Neonatal atrial myocytes and SAN cells from wild-type and knockout mice did not differ with respect to these parameters. CCh-induced currents were measured at a holding potential of -70 mV using a high-K+ bath solution (in mM): 120 NaCl, 25 KCl, 2 $CaCl_2$, 2 $MgCl_2$, 10 D-glucose, 10 HEPES/NaOH (pH 7.4). The high-K^+ bath solution (+/-CCh) was applied with an SF-77B rapid perfusion system (Warner Instruments, Inc.; Hamden, CT). In pilot studies, we found no difference in current amplitudes evoked by 10 and 100 μM CCh, irrespective of genotype or cell type. As such, 10 μM CCh was taken as the saturating CCh concentration for these studies. All currents were low-pass filtered at 1 kHz, sampled at 2 kHz, and stored on computer hard disk for analysis. Steady-state current amplitudes were measured for each experiment by subtracting the baseline current from the current measured just prior to the return to drug-free solution. Activation and deactivation time constants were extracted from appropriate regions of current traces, which were fit with a 1-term Boltzmann equation using the Levenberg-Marquardt search method, sum of squared errors minimization method, and no weighting (Figure 3.1). Only those experiments for which the access resistances were stable and low (<15 MΩ) were included in the final analysis.

Telemetry - Wild-type (n=5) and RGS6 knockout (n=5) littermates aged 4-5 months were used for *in vivo* ECG monitoring. Biopotential telemetry transmitters ETA-

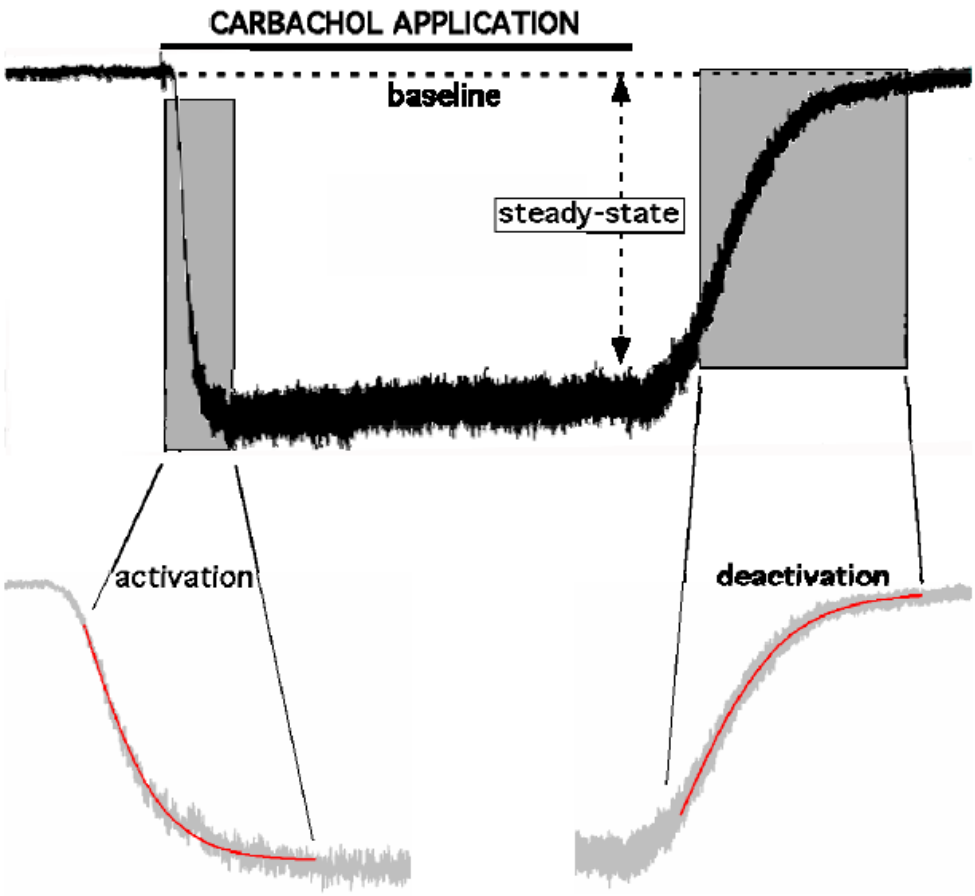

Figure 3.1: Depiction of measured parameters for the whole-cell CCh-induced current studies.
A typical response of a wild-type neonatal atrial myocyte to 10 mM CCh is shown, with the horizontal line showing the duration of CCh application. Current amplitude and density determinations involved steady-state currents, measured relative to baseline just prior to the removal of CCh. Shaded rectangles identify the regions of the trace used for determination of current activation and deactivation kinetics. The fit curves, derived from a 1-term standard Boltzmann equation, are shown in red.

F10 (Data Sciences International; Saint Paul, MN) were implanted intraperitoneally under kethamine/xylazine anesthesia (60 and 12 mg/kg correspondently). ECG leads were externalized and abdominal wall was closed with Prolene 5-0 (Ethicon; Somerville, NJ) incorporating suture rib of the transmitter into the closure. ECG leads were tunneled under the skin into lead II position and sutured to the abdominal wall by Prolene 5-0. Skin incisions were closed using Vicryl 5-0 (Ethicon). Upon termination of anesthesia, animals received a single intraperitoneal injection of ketoprofen (5 mg/kg), followed by administration of ibuprofen and amoxicillin in drinking water during recovery period (days 1-10). Upon recovery, recordings were performed in a scheduled manner, for 20 s each min, following 1-h acclimation using Dataquest ART 4.2 acquisition software (Data Sciences International). On day 11, 6 h of baseline ECG data were recorded. On day 12, after 30 min of baseline recording, animals were injected i.p. with 0.9% saline solution (10 ml/kg) as a vehicle control. Atropine sulfate was injected 2 h later (1 mg/kg, i.p.; Hospira, Lake Forest, IL), followed by 3 h of recording. On day 13, following 30 min of baseline recording, animals were injected first with 0.9% saline solution and 2 h later with CCh (0.1 mg/kg, i.p.; Acros Organics, Geel, Belgium). Recording proceeded for 3 h, after which animals were sacrificed by CO2 inhalation. Transmitters were explanted, cleaned with 1% Tergazyme enzymatic detergent (Alconox; White Plains, NY), sterilized with Cidex activated dialdehyde solution (Ethicon), and reused.

Statistical Analysis - Statistical analyses were performed using Prism (GraphPad Software, Inc.; La Jolla, CA) and SigmaPlot 11 (Systat Software Inc; San Jose, CA). EC_{50} values were calculated with the Hill coefficient set to 1. The impact of genotype on CCh-induced current responses (steady-state current density and kinetics) was evaluated using one-way (single-saturating concentration study) and two-way (concentration-response study) ANOVA. The impact of genotype on CCh- and atropine-induced heart rate response was evaluated using two-way (time-response study) ANOVA. Tukey's Multiple Comparison (one-way ANOVA) and Bonferroni (two-way ANOVA) post hoc tests were used as appropriate. For all analyses, the level of significance was set at $P < 0.05$.

- ***Results***

Profiling RGS6 protein expression across mouse tissues revealed its readily detectable levels in the heart in addition to abundant presence in the brain (Figure 3.2A and Figure 3.3). RGS6 protein was enriched in atria, where it was found predominantly in myocytes (Figure 3.4), consistent with a recent report [257], and similar to the distribution of GIRK1, an integral subunit of I_{KACh} (Figure 3.2B). To begin exploring the role of RGS6 in cardiac physiology, we obtained RGS6 knockout mice where exons 5 to 7 encoding the critical N-terminal portion of the protein were eliminated (Figure 3.2C,D). Immunoblotting verified the complete absence of RGS6 protein in the hearts of RGS6 knockout mice (Figure 3.2E).

RGS6 interacts with the type 5 G protein β subunit (Gβ5) and the R7 Binding Protein (R7BP) in the CNS [212] (Figure 3.2E). In the mouse heart, however, only Gβ5 is available for the interaction with RGS6 (Figure 3.2E). RGS6 was undetectable in hearts from Gβ5 knockout mice, indicating that the physical association with Gβ5 is critical for the expression and/or stability of RGS6 (Figure 3.2F). Similarly, Gβ5 levels were dramatically reduced in the RGS6 knockout heart but not brain, indicating that in the heart RGS6 is the predominant RGS bound to Gβ5. No effect on RGS6 or Gβ5 levels was observed upon elimination of R7BP or GIRK4. Notably, we detected no compensatory changes in either $G\alpha_{i/o}$ proteins or RGS4, a protein previously implicated in regulation of the M2R-I_{KACh} signaling [15].

Given the co-enrichment of RGS6 and I_{KACh} in atria and the role of R7 RGS•Gβ5 complexes in GPCR-GIRK signaling in the CNS [82], we next measured the impact of RGS6 ablation on M2R-I_{KACh} signaling in neonatal atrial myocytes, which exhibit robust inward current triggered by the non-selective muscarinic agonist carbachol (CCh). While CCh evoked currents with comparable potency in atrial myocytes from wild-type mice, current deactivation kinetics were notably slower across all CCh concentrations tested in myocytes from RGS6 knockout mice (Figure 3.5).

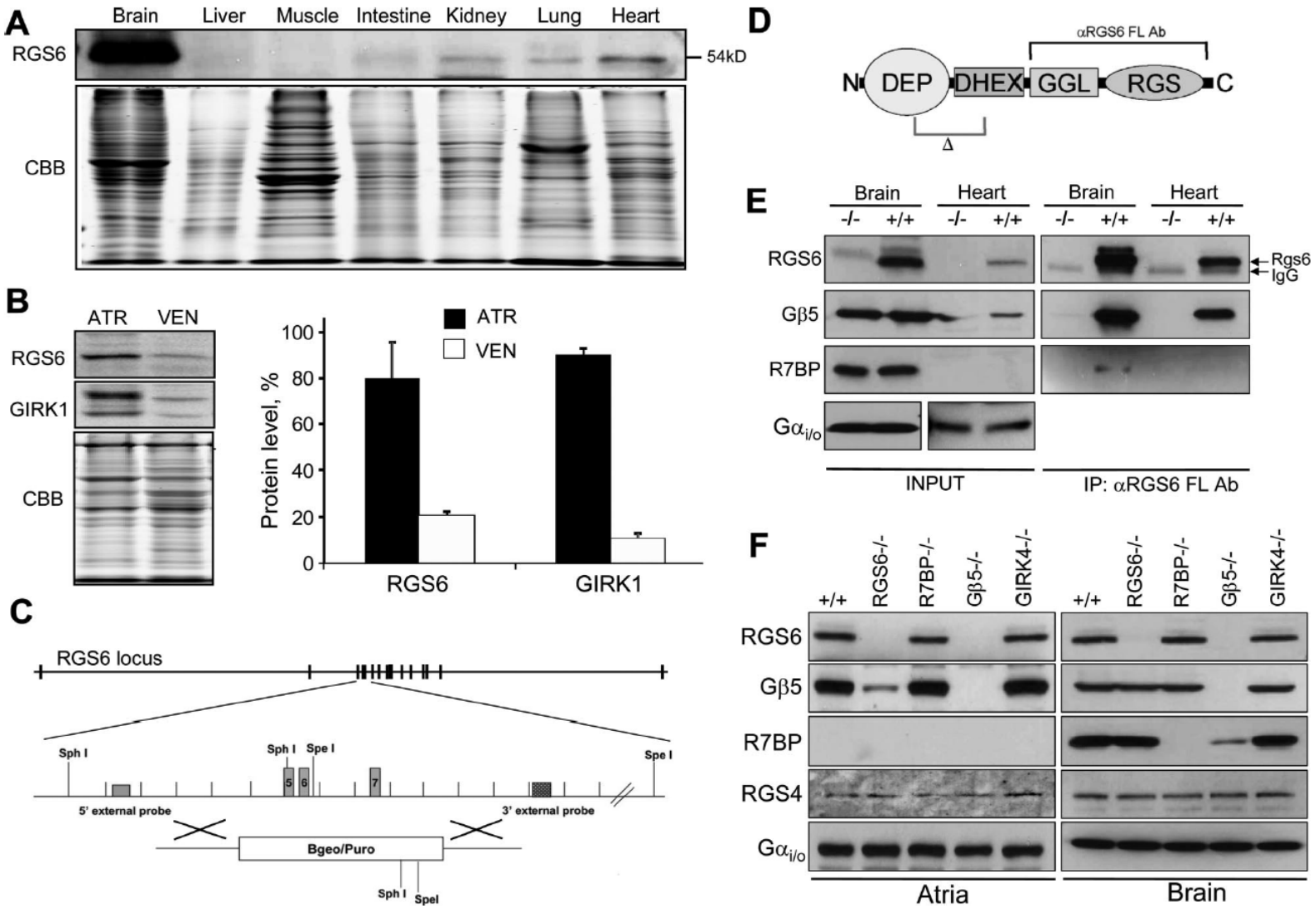
A
Brain
Liver
Muscle
Intestine
Kidney
Lung
Heart
RGS6
54kD
CBB
B
ATR
VEN
RGS6
GIRK1
CBB
ATR
VEN
Protein level, %
100
80
60
40
20
0
RGS6
GIRK1
C
RGS6 locus
Sph I
Sph I
Spe I
Spe I
5
6
7
5' external probe
3' external probe
Bgeo/Puro
Sph I
SpeI
D
αRGS6 FL Ab
N
DEP
DHEX
GGL
RGS
C
Δ
E
Brain
Heart
Brain
Heart
-/-
+/+
-/-
+/+
-/-
+/+
-/-
+/+
RGS6
Gβ5
R7BP
Gαi/o
Rgs6
IgG
INPUT
IP: αRGS6 FL Ab
F
+/+
RGS6-/-
R7BP-/-
Gβ5-/-
GIRK4-/-
+/+
RGS6-/-
R7BP-/-
Gβ5-/-
GIRK4-/-
RGS6
Gβ5
R7BP
RGS4
Gαi/o
Atria
Brain

Figure 3.2: RGS6 protein level and complex formation in the mouse heart.

A, RGS6 protein levels across mouse tissues as analyzed by Western blotting. Equal amounts of total protein (20 μg) were loaded in each lane. Coomassie staining (CBB) was used as a loading control. **B,** RGS6 is co-enriched with GIRK1 in the atria. Atrial (ATR) and ventricular (VEN) lysates were analyzed by Western blotting (upper panels). CBB staining confirms equal protein loading. *Graph:* Quantification of RGS6 and GIRK1 band densities. **C,** Strategy for *Rgs6* ablation by homologous recombination. **D,** Structural organization of RGS6. Frames designate the deleted region (D) and recognition site of the RGS6 FL antibody (αRGS6 FL Ab) used throughout the study. Colored boxes designate known structural domains. **E,** Co-immunoprecipitation of RGS6 with Gβ5 and R7BP from heart and brain tissues. **F,** Co-dependence of RGS6 and Gβ5 expression in the heart and brain as analyzed by Western blotting.

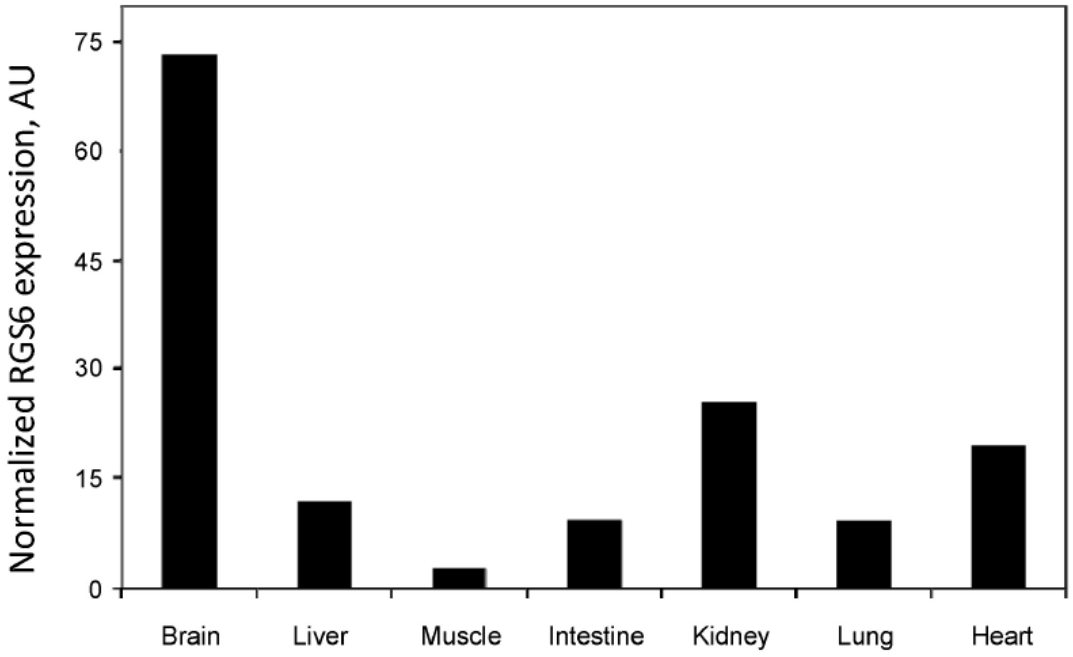

Figure 3.3: Quantitative analysis of RGS6 distribution across tissues.

RGS6 band densities from Western blot experiment presented in Figure 3.2A have been determined by densitometry using Image J software and normalized to the total protein content determined from CBB stained gel (Figure 3.2A). Resulting values representing relative abundance of RGS6 proteins across tissues are plotted as a bar graph.

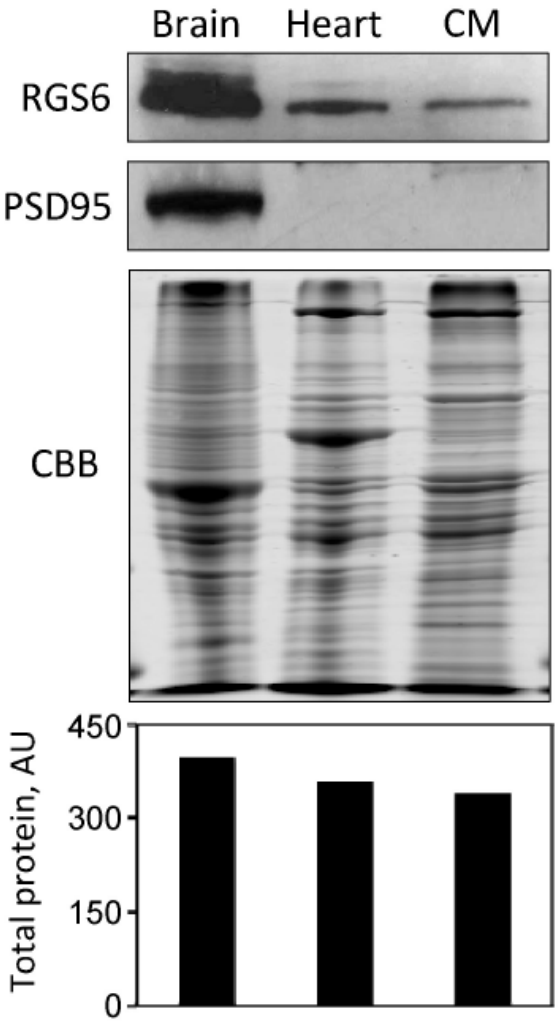

Figure 3.4: RGS6 is present in isolated atrial cardiomyocytes.

Cardiomyocytes were isolated from adult mice as described in Methods section above. Following lysis in SDS sample buffer, 25 μg of total protein was loaded on the gel. RGS6 expression was detected by Western blotting with specific anti-RGS6-FL antibodies. Brain tissue was used as a control. The absence of the immunoreactivity for the neuronal specific marker PSD95 in isolated cardiomyocyte fraction (CM) demonstrate that RGS6 is predominantly expressed in the myocytes. Protein loading was verified by Coomassie Brilliant Blue (CBB) following separation on SDS-PAGE gel. Densitometric analysis of the total protein content quantified from the CBB-stained gel is presented in the lower panel.

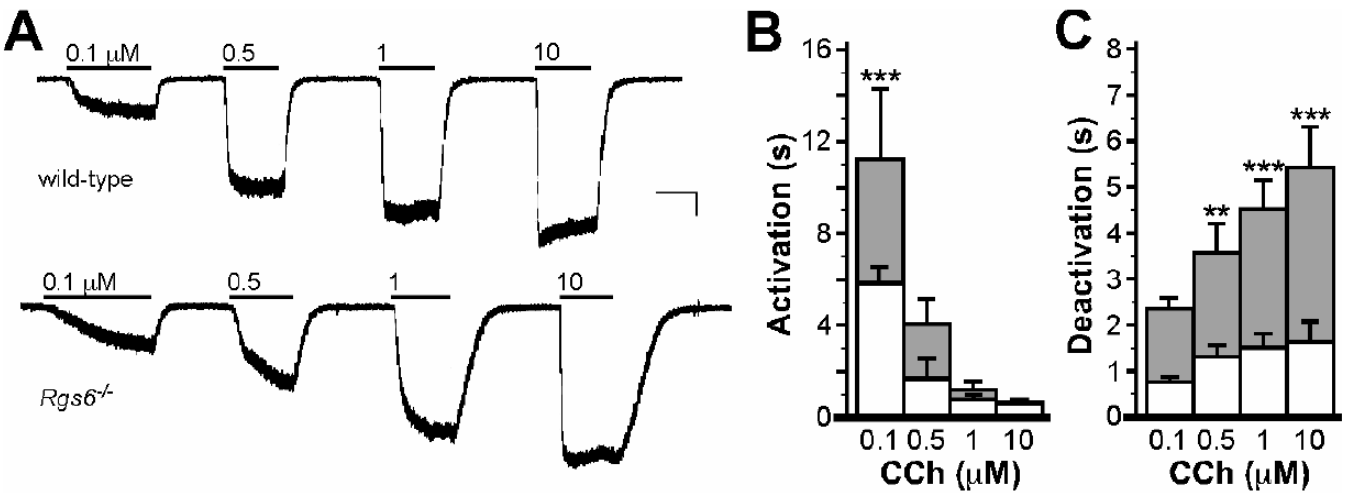

Figure 3.5: Impact of RGS6 ablation on M2R-I_{KACh} signaling in atrial myocytes.

A, Inward currents evoked by CCh (0.1-10 μmol/L) in atrial myocytes from wild-type and RGS6 knockout mice. Scale bars: 15 s/100 pA. Evoked currents developed gradually at 0.1 μmol/L CCh and saturated at 10 μmol/L CCh (responses to 10 μmol/L CCh are not shown). Half-saturating parameters were for wild-type: EC_{50} = 0.25 to 0.49 μmol/L (95% CI) and for *Rgs6*$^{-/-}$: EC_{50} = 0.21 to 0.62 μmol/L (95% CI). Steady-state current densities did not differ between RGS6 knockout (-36±4 pA/pF at 10 μmol/L CCh, n=7) and wild-type (-42±6 pA/pF, n=7) myocytes. **B,** Summary of M2R-I_{KACh} activation kinetics in atrial myocytes from wild-type and RGS6 knockout mice. Main effects of concentration ($F_{3,43}$=25.5; P<0.001) and genotype ($F_{1,43}$=13.3; P<0.001) were observed, as well as a concentration x genotype interaction ($F_{3,43}$=4.1; P<0.05). Symbols: *** P<0.001 vs. wild-type (within dose). **C,** Summary of M2R-I_{KACh} deactivation kinetics in atrial myocytes from wild-type and RGS6 knockout mice. Main effects of concentration ($F_{3,44}$=5.5; P<0.01) and genotype ($F_{1,44}$=58.9; P<0.001) were observed, and there was no concentration x genotype interaction ($F_{3,44}$=1.7; P=0.17). Symbols: *,** P<0.05 and 0.01, respectively, vs. wild-type (within dose).

Current activation kinetics were also delayed in RGS6 knockout myocytes, though only for the lower CCh concentrations tested.

We next compared CCh-induced currents in sinoatrial node (SAN) cells, the key anatomic substrate for parasympathetic control of heart rate (Figure 3.6). While some differences in the density and kinetics of CCh-induced responses between adult SAN cells and neonatal atrial myocytes were evident, RGS6 ablation correlated with significantly delayed deactivation rates in both cell types. Under the same conditions, no differences in CCh-induced steady-state current density or activation kinetics were observed between genotypes in either atrial myocytes or SAN cells (Figure 3.6). Furthermore, deletion of the Gβ5 replicated prolonged deactivation kinetics seen in RGS6 knockout myocytes (Figure 3.6E), indicating that regulation of the M2R-I_{KACh} signaling in heart atria is mediated by the RGS6•Gβ5 complex rather than RGS6 by itself.

The striking impact of RGS6 ablation on M2R-I_{KACh} signaling kinetics in atrial myocytes and SAN cells, prompted us to test whether RGS6•Gβ5 can physically associate with the I_{KACh} channel. In transfected HEK293 cells, we detected robust co-immunoprecipitation of the RGS6•Gβ5 complex with GIRK4 but not GIRK1 by both forward and reverse precipitation strategies (Figure 3.7). Thus, the involvement of RGS6•Gβ5 in M2R-I_{KACh} signaling is likely aided by a direct protein-protein interaction mediated by the cardiac-specific GIRK subunit, GIRK4.

The delay in I_{KACh} deactivation kinetics triggered by RGS6•Gβ5 elimination is expected to enhance M2R-I_{KACh} signaling as the channel would stay open longer which would potentiate the parasympathetic regulation of HR. We addressed this possibility by analyzing cardiac function in mice using ECG telemetry, at baseline and following pharmacologic manipulation. Analysis of ECG traces did not reveal gross abnormalities in cardiac physiology in RGS6 knockout mice (Figure 3.8A and Figure 3.9). RGS6 knockout mice did, however, display a mild resting bradycardia (511±13 vs. 476±4 bpm, $P<0.05$), consistent with the effect of RGS6•Gβ5 ablation on M2R-dependent signaling in atrial myocytes (Figure 3.8B). While CCh administration (0.1 mg/kg, i.p.) triggered a

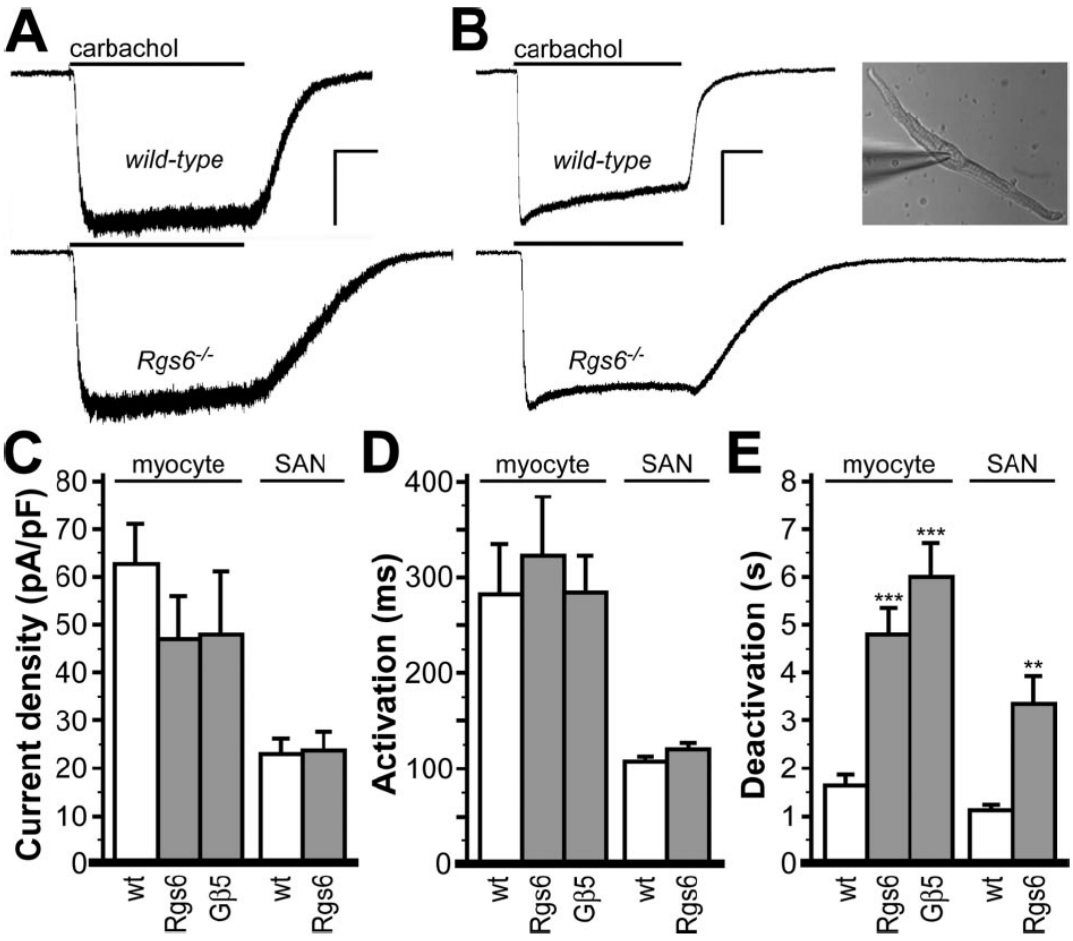

Figure 3.6: Impact of RGS6 ablation on M2R-I_{KACh} signaling in atrial myocytes and SAN cells.

A, Inward currents evoked by CCh (10 μmol/L) in atrial myocytes from wild-type and RGS6 knockout mice. Scale bars: 5 s/200 pA. **B,** Inward currents evoked by CCh (10 μmol/L) in SAN cells from wild-type and RGS6 knockout mice. Scale bars: 5 s/400 pA. Inset: image of the wild-type SAN cell evaluated in the adjacent trace. Summary of steady-state CCh-induced current density **(C)**, activation kinetics **(D)**, and deactivation kinetics **(E)** in wild-type, RGS6, and Gβ5 atrial myocytes (n=5-11 per group), and in wild-type and RGS6 knockout SAN cells (n=10-12 per genotype). Genotype did not impact current density (atrial myocytes: $F_{2,21}$=1.9, P=0.18; SAN cells: t(20)=0.13, P=0.90) or activation kinetics (atrial myocytes: $F_{2,21}$=1.0, P=0.38; SAN cells: t(20)=1.69, P=0.11), but did influence deactivation kinetics (atrial myocytes: $F_{2,21}$=24.8, P<0.001; SAN cells: t(20)=3.71, P<0.01). Symbols: **, *** P<0.01 and 0.001, respectively, vs. wild-type (within cell type).

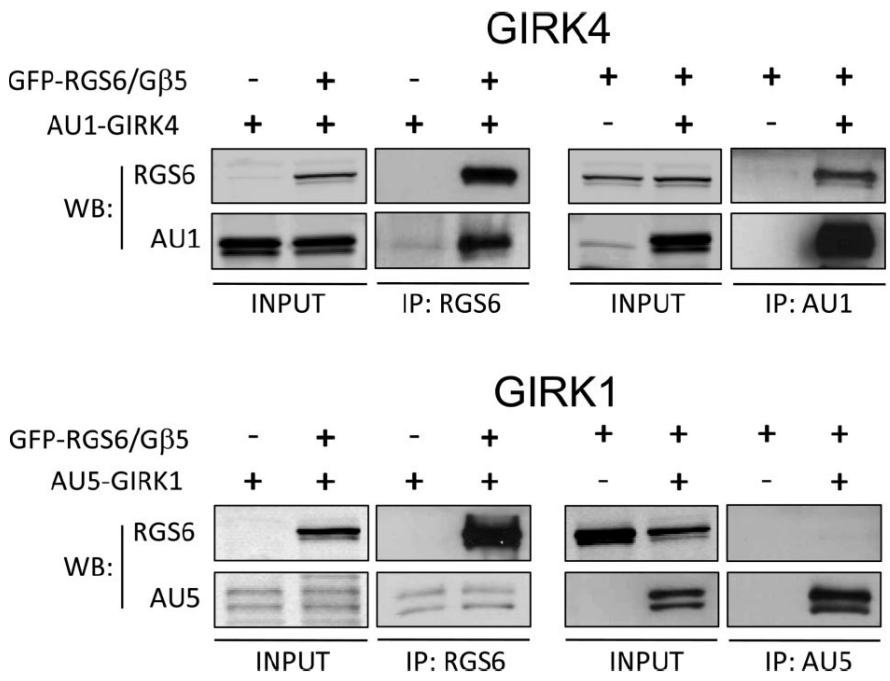

Figure 3.7: RGS6•Gβ5 forms a complex with GIRK4.

RGS6 and Gβ5 were co-expressed with either AU1-tagged GIRK4 or AU5-tagged GIRK1 in HEK293 cells. Forward and reciprocal co-immunoprecipitation assays were performed as described in the *Methods* using indicated antibodies. Eluates were analyzed using Western blotting.

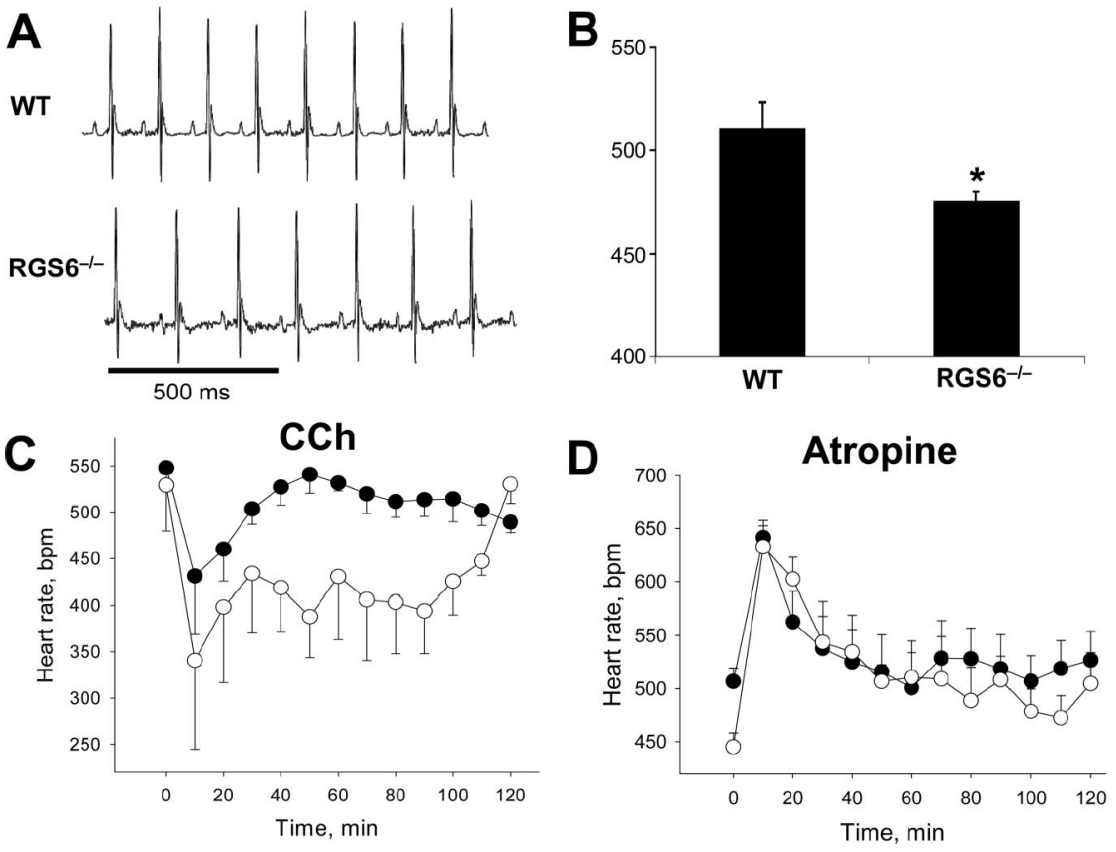

Figure 3.8: Effect of RGS6 ablation on resting HR and muscarinic regulation.

A, Baseline ECG recorded during light phase from conscious, unrestrained wild-type (WT, n=5) and RGS6 knockout mice (n=5). **B,** Average HR as determined from the analysis of the ECG recordings (6hr). Symbols: * $P<0.05$ vs. wild-type. **C**, Effect of CCh (0.1 mg/kg, i.p.) on HR, analyzed and plotted as simple moving average with a period of 10 min. HR at 0 min corresponds to the 30-min average baseline HR on the day of the experiment. Two-way ANOVA analysis (genotype and time) of the 120-min post-injection interval revealed main effects of genotype ($F_{1,104}=21.6$; $P<0.001$). **D,** Effect of atropine (1 mg/kg, i.p.) on HR, analyzed and plotted as simple moving averages with a period of 10 min. No significant difference in HR was observed during the 60-min post-injection interval ($F_{1,56}=0.02$; $P=0.89$).

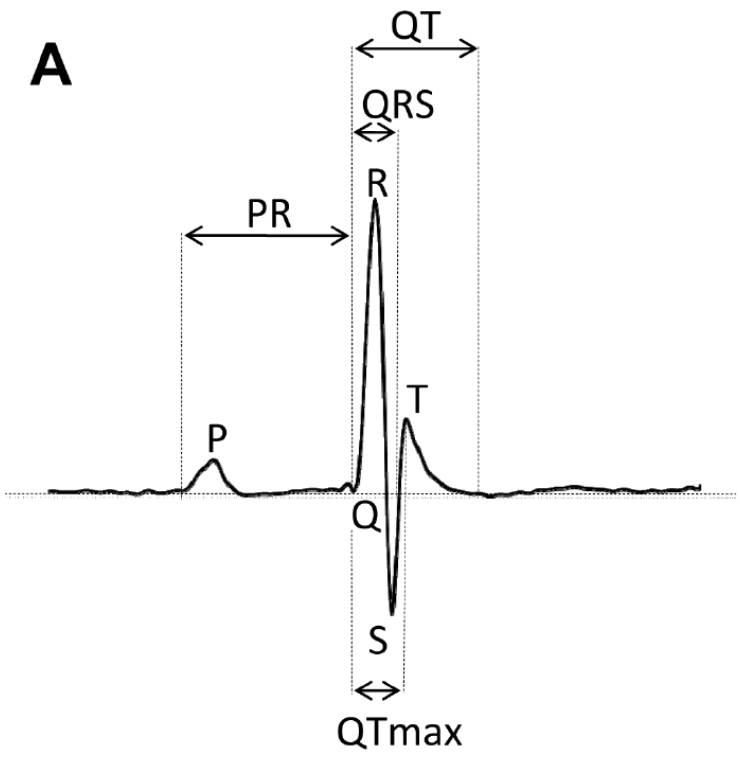

B

Interval, ms±SEM	RGS6$^{+/+}$	RGS6$^{-/-}$
PR	39.41±1.08	40.94±2.12
QRS	9.68±0.49	10.14±0.55
QT	44.12±1.91	38.75±2.08
QTmax	12.06±0.60	11.88±0.29

Figure 3.9: Quantitative analysis of ECG intervals in RGS6 knockout mice.

A, Representative ECG trace obtained from RGS6 knockout mice. Peaks and intervals used for the quantitative analysis are annotated. **B,** Quantitative analysis of the ECG traces. Data derived from the analysis of total 500 representative traces from 3 to 5 mice of each genotype. Values were averaged separately for each animal. Group sizes were defined as a number of unique animals used for the analysis (n=3-5). Errors are s.e.m values.

rapid decrease in HR in wild-type and RGS6 knockout animals, the effect was significantly larger and persisted longer in RGS6 knockout mice (Figure 3.8C). Similarly, parasympathetic blockade with atropine (1 mg/kg, i.p.) had a positive chronotropic effect in both groups, with a significantly larger effect seen in RGS6 knockout mice (Figure 3.8D). Importantly, there was no difference in HR immediately following atropine administration, indicating that the bradycardia seen in RGS6 knockout mice results from enhanced intrinsic M2R signaling.

- ***Discussion***

Here, we report that RGS6•Gβ5 negatively regulates M2R-I_{KACh} signaling in atrial myocytes by accelerating I_{KACh} deactivation kinetics. These observations, together with the effect of RGS6 ablation on HR and responses to pharmacologic manipulation, indicate that RGS6•Gβ5 represents a key node of regulation in the parasympathetic control of cardiac output. Since dysregulation of the parasympathetic tone by deficiencies in I_{KACh} function is increasingly accepted as a major factor in the pathogenesis of the atrial fibrillation [249], our study introduces RGS6•Gβ5 complex as an attractive candidate for better understanding of cardiac pathophysiology and development of corrective therapies.

RGS6 belongs to the R7 family of RGS proteins, members of which were thought to be expressed exclusively in the nervous system, where they play roles in nociception, vision, reward behavior and locomotion [212]. Although RGS6 expression was reported previously in the heart [74, 257, 258], our study documents for the first time the functional relevance of RGS6 to cardiac physiology. In the CNS, RGS6 forms complexes with two proteins, Gβ5 and R7BP that specify its stability, subcellular distribution, and activity [212]. Here we show that cardiac RGS6 forms a complex with Gβ5, but not with R7BP, which is undetectable in the heart. The obligate and functionally-relevant nature of the RGS6•Gβ5 interaction was underscored by the mutual dependence of RGS6 and Gβ5 levels on their co-expression, and the phenotypic similarities in M2R-I_{KACh} signaling in myocytes from RGS6 and Gβ5 knockout mice. In neurons, Gβ5 recruits R7 RGS proteins

to GIRK channels, resulting in accelerated channel kinetics associated with $GABA_B$ receptor activation [82]. Thus, the present work reveals the conservation of this compartmentalization mechanism by showing that RGS6•Gβ5 can likewise regulate M2R-I_{KACh} signaling.

Previous work has identified RGS4 as a critical regulator of M2R-I_{KACh} signaling in sinoatrial nodal cells [15]. Indeed, the deficiencies in M2R-I_{KACh} signaling linked to RGS6 ablation reported herein are reminiscent of those reported in RGS4 knockout mice [15]. Therefore, murine sinoatrial nodal cells may employ parallel approaches involving RGS4 and RGS6•Gβ5 to regulate M2R-I_{KACh} signaling. It is possible, for example, that RGS4 and RGS6•Gβ5 selectively regulate different G protein subtypes involved in I_{KACh} gating. Indeed, studies with knock-in mice expressing RGS-insensitive G proteins reveal a differential contribution of $G\alpha_{i2}$ and $G\alpha_o$ to M2R-dependent actions [185, 197]. Furthermore, RGS6•Gβ5 shows selectivity towards $G\alpha_o$ over $G\alpha_{i2}$ *in vitro* [34]. However, while the role of $G\alpha_{i2}$ in mediating M2R-I_{KACh} coupling is well established [185], the involvement of $G\alpha_o$ in this process is less certain. Moreover, it remains possible that other proteins of more than 30-member RGS family also play roles in this regulation. Delineating the mechanisms of the functional involvement of RGS proteins in controlling M2R-I_{KACh} signaling in the mouse models and their relevance to human physiology will serve as an exciting future research direction.[3]

[3] This work was supported by NIH grants DA026405 (KAM), MH061933 (KW), DA011806 (KW), and T32 DA07234 (KA), and a McKnight Land–Grant Award (KAM).

Chapter 4 - Conclusion

The findings described in this dissertation identify novel aspects of G protein signaling regulation by two members of R7 RGS protein family, RGS9-2 and RGS6. This protein family has received significant attention for its involvement in regulation of neuronal signaling. Although all of the R7 RGS family members are enriched in neuronal tissues, the physiological roles of all but one of them remain unclear.

In contrast, RGS9-2 has a well-established role in regulation of movement and reward. Changes in RGS9-2 expression levels have a dramatic impact on behavioral outcomes and are controlled by its dynamic association with R7BP. However, until now the molecular mechanisms regulating RGS9-2 levels upon dissolution of the RGS9-2•R7BP complex had not been investigated.

We identified 21 proteins whose interaction with RGS9-2 is upregulated in the absence of R7BP. We focused our attention on one of the candidates, HSC70 and demonstrated that it plays a significant role in regulating RGS9-2 expression by binding to the intrinsically disordered C-terminal domain of the protein. We think that HCS70 acts by targeting RGS9-2 to lysosomal degradation through a previously described mechanism of chaperone-mediated autophagy. Testing this possibility further would be an exciting future direction.

Another open question pertains to the cellular location of the regulatory influence imposed by HSC70. Ribosomal proteins were the biggest group of upregulated interactions of RGS9-2 following the loss of R7BP. Because R7BP is required for targeting RGS9-2 to the postsynaptic density (PSD) compartment, it is plausible that in R7BP knockout tissues newly synthesized RGS9-2 remains associated with ribosomes until the assembly of the degradation complex. This brings up an important question of whether similar mechanisms are responsible for RGS9-2 degradation after it has been properly targeted. The role of HSC70 in the regulation of RGS9-2 levels upon stimuli promoting its degradation in PSD will likely be an interesting line for further investigations.

Interestingly, HSC70 and R7BP bind to different sites in RGS9-2. The stabilizing subunit, R7BP is known to be recruited to the N-terminal DEP/DHEX domain, while degradation-promoting HSC70 is recruited to the C-terminus of RGS9-2 in a manner sensitive to the presence of R7BP interaction. This implies existence of a "communication" mechanism between the two termini of RGS9-2, where uncoupling of R7BP from DEP/DHEX domain ultimately leads to an increased association of HSC70 with C-terminal domain. Such mechanism could be a conformational change in C-terminus triggered either by the loss of interaction with R7BP exclusively or in combination with post-translational modifications. HSC70 has been previously shown to bind proteins in a phosphorylation-dependent manner, and coincidentally, we identified increased complex formation between RGS9-2 and three different kinases in R7BP knockout tissues. Interaction with calcium/calmodulin-dependent protein kinase IIα (CaMKIIα) was one of the most significantly upregulated. Taken together with the presence of three CaMKIIα consensus phosphorylation sites in the C-terminus of RGS9-2 (Thr^{429}, Ser^{515}, Ser^{557}) and the essential role of calcium in RGS9-2 degradation, CaMKIIα appears to be one of the most promising candidates for the investigation of the additional mechanisms. My pilot experiments indicated that CaMKIIα can indeed bind and phosphorylate RGS9-2 *in vitro*, however the results of the ex vivo studies with brain slices were inconclusive. As such, further studies are necessary to investigate the mechanism underlying increased affinity of HSC70 for the C-terminus of RGS9-2 in the absence of R7BP. It is possible that uncovering the role of other identified interactions could provide an insight into this problem, and it would make another exciting direction to pursue.

The second part of this dissertation demonstrates the cardiac expression of RGS6 and its role in regulation of M2 receptor signaling and parasympathetic control of heart rate. Importantly, it shows for the first time that: (i) R7 RGS proteins express and function to regulate physiological processes outside of the nervous tissue and (ii) RGS6 serves as a classical negative regulator of G protein signaling in native tissues as opposed to presumed unconventional roles in the nucleus. It is also to be expected that more

functional roles in peripheral tissues will be identified for RGS6 and possibly, other R7 RGSs.

There are several important scientific questions related to the role of RGS6 in cardiac physiology that remain to be explored but fall beyond the scope of this dissertation. First, regulation of M2R signaling has been previously attributed to RGS4. RGS4 knockout mice reportedly have a cardiac phenotype similar to that of RGS6 knockouts. RGS4 and RGS6 show different G protein selectivity *in vitro*. While RGS6 is more selective towards $G\alpha_o$ and RGS4 is more selective towards $G\alpha_i$, an observation that can potentially explain a non-redundant function of both RGS proteins in controlling M2 pathway. However, the relative contribution of the two RGS proteins, as well as the role of the cAMP component in heart rate control by each of these RGS proteins remains to be established. Second, GIRK channel opening upon M2R activation is recognized as a source of heart rate variability (HRV). HRV is a physiological phenomenon where time between two consecutive heartbeats varies on a beat-to-beat basis. Abnormal HRV has an established prognostic value for cardiac-related mortality and is thought to contribute to arrhythmia development. As a negative regulator of GIRK channels, RGS6 is likely to have a negative impact on HRV as well. Since our current understanding of the molecular mechanisms guiding the periodicity of HR is very limited, it would be exciting to see the role of RGS6 in HRV addressed in future studies. Third, according to the NCBI SNP (single nucleotide polymorphism) database there are around 30 missense mutations identified in RGS6 in humans. A number of them are mapped to the Gβ5 interaction surface or RGS domain of RGS6, and can potentially affect protein expression levels or catalytic activity of the protein. Future studies connecting this genotyping data with predicted cardiac phenotype would allow for translation of our phenotypic observations in mice into humans and could potentially establish RGS6 as a marker for bradycardia and dysregulation of the parasympathetic control.

In summary, the results of research included into this dissertation expand our understanding of mechanistic principles of G protein regulation by R7 RGS proteins, as well as of the physiological processes they regulate. This provides a foundation for further work in the fields of molecular cardiology and neuroscience, as well as novel

molecular targets for the development of pharmacological interventions for drug abuse and addiction, motor coordination deficits, and cardiac arrhythmias.

Bibliography

1. Hepler, J.R. and A.G. Gilman, *G proteins.* Trends Biochem Sci, 1992. **17**(10): p. 383-7.
2. Neer, E.J., *G proteins: critical control points for transmembrane signals.* Protein Sci, 1994. **3**(1): p. 3-14.
3. Cabrera-Vera, T.M., et al., *Insights into G protein structure, function, and regulation.* Endocr Rev, 2003. **24**(6): p. 765-81.
4. Offermanns, S., *G-proteins as transducers in transmembrane signalling.* Prog Biophys Mol Biol, 2003. **83**(2): p. 101-30.
5. Gainetdinov, R.R., et al., *Desensitization of G protein-coupled receptors and neuronal functions.* Annu Rev Neurosci, 2004. **27**: p. 107-44.
6. Clapham, D.E. and E.J. Neer, *G protein beta gamma subunits.* Annu Rev Pharmacol Toxicol, 1997. **37**: p. 167-203.
7. Bourne, H.R. and L. Stryer, *G proteins. The target sets the tempo.* Nature, 1992. **358**(6387): p. 541-3.
8. Berman, D.M. and A.G. Gilman, *Mammalian RGS proteins: barbarians at the gate.* J Biol Chem, 1998. **273**(3): p. 1269-72.
9. Burchett, S.A., *Regulators of G protein signaling: a bestiary of modular protein binding domains.* J Neurochem, 2000. **75**(4): p. 1335-51.
10. Ross, E.M. and T.M. Wilkie, *GTPase-activating proteins for heterotrimeric G proteins: regulators of G protein signaling (RGS) and RGS-like proteins.* Annu Rev Biochem, 2000. **69**: p. 795-827.
11. Sun, X., et al., *RGS2 is a mediator of nitric oxide action on blood pressure and vasoconstrictor signaling.* Mol Pharmacol, 2005. **67**(3): p. 631-9.
12. Rahman, Z., et al., *RGS9 modulates dopamine signaling in the basal ganglia.* Neuron, 2003. **38**(6): p. 941-52.
13. Chen, C.K., et al., *Slowed recovery of rod photoresponse in mice lacking the GTPase accelerating protein RGS9-1.* Nature, 2000. **403**(6769): p. 557-60.
14. Xie, Z., et al., *RGS13 acts as a nuclear repressor of CREB.* Mol Cell, 2008. **31**(5): p. 660-70.
15. Cifelli, C., et al., *RGS4 regulates parasympathetic signaling and heart rate control in the sinoatrial node.* Circ Res, 2008. **103**(5): p. 527-35.
16. Iankova, I., et al., *Regulator of G protein signaling-4 controls fatty acid and glucose homeostasis.* Endocrinology, 2008. **149**(11): p. 5706-12.
17. Cho, H., et al., *Rgs5 targeting leads to chronic low blood pressure and a lean body habitus.* Mol Cell Biol, 2008. **28**(8): p. 2590-7.
18. Martin-McCaffrey, L., et al., *RGS14 is a mitotic spindle protein essential from the first division of the mammalian zygote.* Dev Cell, 2004. **7**(5): p. 763-9.
19. Huang, X., et al., *Pleiotropic phenotype of a genomic knock-in of an RGS-insensitive G184S Gnai2 allele.* Mol Cell Biol, 2006. **26**(18): p. 6870-9.
20. Krispel, C.M., et al., *RGS expression rate-limits recovery of rod photoresponses.* Neuron, 2006. **51**(4): p. 409-16.

21. Wettschureck, N. and S. Offermanns, *Mammalian G proteins and their cell type specific functions.* Physiol Rev, 2005. **85**(4): p. 1159-204.
22. Farfel, Z., H.R. Bourne, and T. Iiri, *The expanding spectrum of G protein diseases.* N Engl J Med, 1999. **340**(13): p. 1012-20.
23. Burchett, S.A., *Psychostimulants, madness, memory... and RGS proteins?* Neuromolecular Med, 2005. **7**(1-2): p. 101-27.
24. Hooks, S.B., K. Martemyanov, and V. Zachariou, *A role of RGS proteins in drug addiction.* Biochem Pharmacol, 2008. **75**(1): p. 76-84.
25. Burns, M.E. and V.Y. Arshavsky, *Beyond counting photons: trials and trends in vertebrate visual transduction.* Neuron, 2005. **48**(3): p. 387-401.
26. Koelle, M.R. and H.R. Horvitz, *EGL-10 regulates G protein signaling in the C. elegans nervous system and shares a conserved domain with many mammalian proteins.* Cell, 1996. **84**(1): p. 115-25.
27. Zachariou, V., et al., *Essential role for RGS9 in opiate action.* Proc Natl Acad Sci U S A, 2003. **100**(23): p. 13656-61.
28. Garzon, J., A. Lopez-Fando, and P. Sanchez-Blazquez, *The R7 subfamily of RGS proteins assists tachyphylaxis and acute tolerance at μ-opioid receptors.* Neuropsychopharmacology, 2003. **28**(11): p. 1983-90.
29. Psifogeorgou, K., et al., *A unique role of RGS9-2 in the striatum as a positive or negative regulator of opiate analgesia.* J Neurosci, 2011. **31**(15): p. 5617-24.
30. Gold, S.J., et al., *Regulators of G-protein signaling (RGS) proteins: region-specific expression of nine subtypes in rat brain.* J Neurosci, 1997. **17**(20): p. 8024-37.
31. Rose, J.J., et al., *RGS7 is palmitoylated and exists as biochemically distinct forms.* J Neurochem, 2000. **75**(5): p. 2103-12.
32. He, W., et al., *Modules in the photoreceptor RGS9-1·Gβ5L GTPase-accelerating protein complex control effector coupling, GTPase acceleration, protein folding, and stability.* J Biol Chem, 2000. **275**(47): p. 37093-100.
33. Skiba, N.P., et al., *RGS9-Gβ5 substrate selectivity in photoreceptors. Opposing effects of constituent domains yield high affinity of RGS interaction with the G protein-effector complex.* J Biol Chem, 2001. **276**(40): p. 37365-72.
34. Hooks, S.B., et al., *RGS6, RGS7, RGS9, and RGS11 stimulate GTPase activity of Gi family G-proteins with differential selectivity and maximal activity.* J Biol Chem, 2003. **278**(12): p. 10087-93.
35. Witherow, D.S., et al., *Complexes of the G protein subunit Gβ5 with the regulators of G protein signaling RGS7 and RGS9. Characterization in native tissues and in transfected cells.* J Biol Chem, 2000. **275**(32): p. 24872-80.
36. Wall, M.A., et al., *The structure of the G protein heterotrimer Gi α1 β1 γ2.* Cell, 1995. **83**(6): p. 1047-58.
37. McEntaffer, R.L., M. Natochin, and N.O. Artemyev, *Modulation of transducin GTPase activity by chimeric RGS16 and RGS9 regulators of G protein signaling and the effector molecule.* Biochemistry, 1999. **38**(16): p. 4931-7.
38. Posner, B.A., A.G. Gilman, and B.A. Harris, *Regulators of G protein signaling 6 and 7. Purification of complexes with Gβ5 and assessment of their effects on G protein-mediated signaling pathways.* J Biol Chem, 1999. **274**(43): p. 31087-93.

39. Snow, B.E., et al., *A G protein gamma subunit-like domain shared between RGS11 and other RGS proteins specifies binding to Gβ5 subunits.* Proc Natl Acad Sci U S A, 1998. **95**(22): p. 13307-12.
40. Martemyanov, K.A. and V.Y. Arshavsky, *Kinetic approaches to study the function of RGS9 isoforms.* Methods Enzymol, 2004. **390**: p. 196-209.
41. Soundararajan, M., et al., *Structural diversity in the RGS domain and its interaction with heterotrimeric G protein α-subunits.* Proc Natl Acad Sci U S A, 2008. **105**(17): p. 6457-62.
42. Slep, K.C., et al., *Structural determinants for regulation of phosphodiesterase by a G protein at 2.0 A.* Nature, 2001. **409**(6823): p. 1071-7.
43. de Alba, E., et al., *Solution structure of human GAIP (Gα interacting protein): a regulator of G protein signaling.* J Mol Biol, 1999. **291**(4): p. 927-39.
44. Moy, F.J., et al., *NMR structure of free RGS4 reveals an induced conformational change upon binding Galpha.* Biochemistry, 2000. **39**(24): p. 7063-73.
45. Chen, Z., et al., *Structure of the RGS domain of p115RhoGEF.* Nat Struct Biol, 2001. **8**(9): p. 805-9.
46. Cabrera, J.L., et al., *Identification of the Gβ5-RGS7 protein complex in the retina.* Biochem Biophys Res Commun, 1998. **249**(3): p. 898-902.
47. Makino, E.R., et al., *The GTPase activating factor for transducin in rod photoreceptors is the complex between RGS9 and type 5 G protein β subunit.* Proc Natl Acad Sci U S A, 1999. **96**(5): p. 1947-52.
48. Cheever, M.L., et al., *Crystal structure of the multifunctional Gβ5-RGS9 complex.* Nat Struct Mol Biol, 2008. **15**(2): p. 155-62.
49. Ponting, C.P. and P. Bork, *Pleckstrin's repeat performance: a novel domain in G-protein signaling?* Trends Biochem Sci, 1996. **21**(7): p. 245-6.
50. Anderson, G.R., et al., *The membrane anchor R7BP controls the proteolytic stability of the striatal specific RGS protein, RGS9-2.* J Biol Chem, 2007. **282**(7): p. 4772-81.
51. Chatterjee, T.K., Z. Liu, and R.A. Fisher, *Human RGS6 gene structure, complex alternative splicing, and role of N terminus and G protein γ-subunit-like (GGL) domain in subcellular localization of RGS6 splice variants.* J Biol Chem, 2003. **278**(32): p. 30261-71.
52. Zhang, K., et al., *Structure, alternative splicing, and expression of the human RGS9 gene.* Gene, 1999. **240**(1): p. 23-34.
53. Rahman, Z., et al., *Cloning and characterization of RGS9-2: a striatal-enriched alternatively spliced product of the RGS9 gene.* J Neurosci, 1999. **19**(6): p. 2016-26.
54. Granneman, J.G., et al., *Molecular characterization of human and rat RGS 9L, a novel splice variant enriched in dopamine target regions, and chromosomal localization of the RGS 9 gene.* Mol Pharmacol, 1998. **54**(4): p. 687-94.
55. Giudice, A., et al., *Identification and characterization of alternatively spliced murine Rgs11 isoforms: genomic structure and gene analysis.* Cytogenet Cell Genet, 2001. **94**(3-4): p. 216-24.
56. Chatterjee, T.K. and R.A. Fisher, *Mild heat and proteotoxic stress promote unique subcellular trafficking and nucleolar accumulation of RGS6 and other*

RGS proteins. Role of the RGS domain in stress-induced trafficking of RGS proteins. J Biol Chem, 2003. **278**(32): p. 30272-82.
57. Thomas, E.A., P.E. Danielson, and J.G. Sutcliffe, *RGS9: a regulator of G-protein signalling with specific expression in rat and mouse striatum.* J Neurosci Res, 1998. **52**(1): p. 118-24.
58. Arshavsky, V.Y., et al., *Regulation of transducin GTPase activity in bovine rod outer segments.* J Biol Chem, 1994. **269**(31): p. 19882-7.
59. Angleson, J.K. and T.G. Wensel, *Enhancement of rod outer segment GTPase accelerating protein activity by the inhibitory subunit of cGMP phosphodiesterase.* J Biol Chem, 1994. **269**(23): p. 16290-6.
60. Otto-Bruc, A., B. Antonny, and T.M. Vuong, *Modulation of the GTPase activity of transducin. Kinetic studies of reconstituted systems.* Biochemistry, 1994. **33**(51): p. 15215-22.
61. Skiba, N.P., J.A. Hopp, and V.Y. Arshavsky, *The effector enzyme regulates the duration of G protein signaling in vertebrate photoreceptors by increasing the affinity between transducin and RGS protein.* J Biol Chem, 2000. **275**(42): p. 32716-20.
62. Martemyanov, K.A., J.A. Hopp, and V.Y. Arshavsky, *Specificity of G protein-RGS protein recognition is regulated by affinity adapters.* Neuron, 2003. **38**(6): p. 857-62.
63. Watson, A.J., A. Katz, and M.I. Simon, *A fifth member of the mammalian G-protein β-subunit family. Expression in brain and activation of the β2 isotype of phospholipase C.* J Biol Chem, 1994. **269**(35): p. 22150-6.
64. Zhang, J.H. and W.F. Simonds, *Copurification of brain G-protein β5 with RGS6 and RGS7.* J Neurosci, 2000. **20**(3): p. RC59.
65. Yoshikawa, D.M., M. Hatwar, and A.V. Smrcka, *G protein β5 subunit interactions with α subunits and effectors.* Biochemistry, 2000. **39**(37): p. 11340-7.
66. Lindorfer, M.A., et al., *Differential activity of the G protein β5γ2 subunit at receptors and effectors.* J Biol Chem, 1998. **273**(51): p. 34429-36.
67. Mirshahi, T., et al., *Distinct sites on G protein βγ subunits regulate different effector functions.* J Biol Chem, 2002. **277**(39): p. 36345-50.
68. Zhou, J.Y., D.P. Siderovski, and R.J. Miller, *Selective regulation of N-type Ca channels by different combinations of G-protein βγ subunits and RGS proteins.* J Neurosci, 2000. **20**(19): p. 7143-8.
69. Maier, U., et al., *Gβ5γ2 is a highly selective activator of phospholipid-dependent enzymes.* J Biol Chem, 2000. **275**(18): p. 13746-54.
70. Fletcher, J.E., et al., *The G protein β5 subunit interacts selectively with the Gq α subunit.* J Biol Chem, 1998. **273**(1): p. 636-44.
71. Watson, A.J., et al., *A novel form of the G protein β subunit Gβ5 is specifically expressed in the vertebrate retina.* J Biol Chem, 1996. **271**(45): p. 28154-60.
72. Jones, M.B. and J.C. Garrison, *Instability of the G-protein β5 subunit in detergent.* Anal Biochem, 1999. **268**(1): p. 126-33.

73. Sondek, J. and D.P. Siderovski, *Gγ-like (GGL) domains: new frontiers in G-protein signaling and β-propeller scaffolding.* Biochem Pharmacol, 2001. **61**(11): p. 1329-37.
74. Snow, B.E., et al., *Fidelity of G protein β-subunit association by the G protein γ-subunit-like domains of RGS6, RGS7, and RGS11.* Proc Natl Acad Sci U S A, 1999. **96**(11): p. 6489-94.
75. Yost, E.A., et al., *Live cell analysis of G protein β5 complex formation, function, and targeting.* Mol Pharmacol, 2007. **72**(4): p. 812-25.
76. Martemyanov, K.A., et al., *R7BP, a novel neuronal protein interacting with RGS proteins of the R7 family.* J Biol Chem, 2005. **280**(7): p. 5133-6.
77. Kovoor, A., et al., *Co-expression of Gβ5 enhances the function of two Gγ subunit-like domain-containing regulators of G protein signaling proteins.* J Biol Chem, 2000. **275**(5): p. 3397-402.
78. Chen, C.K., et al., *Instability of GGL domain-containing RGS proteins in mice lacking the G protein β-subunit Gβ5.* Proc Natl Acad Sci U S A, 2003. **100**(11): p. 6604-9.
79. Schwindinger, W.F., et al., *Mice with deficiency of G protein γ3 are lean and have seizures.* Mol Cell Biol, 2004. **24**(17): p. 7758-68.
80. Lobanova, E.S., et al., *Transducin gamma-subunit sets expression levels of α- and β-subunits and is crucial for rod viability.* J Neurosci, 2008. **28**(13): p. 3510-20.
81. Narayanan, V., et al., *Intramolecular interaction between the DEP domain of RGS7 and the Gβ5 subunit.* Biochemistry, 2007. **46**(23): p. 6859-70.
82. Xie, K., et al., *Gbeta5 recruits R7 RGS proteins to GIRK channels to regulate the timing of neuronal inhibitory signaling.* Nat Neurosci, 2010. **13**(6): p. 661-3.
83. Wickman, K.D., et al., *Recombinant G-protein βγ-subunits activate the muscarinic-gated atrial potassium channel.* Nature, 1994. **368**(6468): p. 255-7.
84. Levay, K., et al., *Gbeta5 prevents the RGS7-Gαo interaction through binding to a distinct Gγ-like domain found in RGS7 and other RGS proteins.* Proc Natl Acad Sci U S A, 1999. **96**(5): p. 2503-7.
85. Karan, S., et al., *A model for transport of membrane-associated phototransduction polypeptides in rod and cone photoreceptor inner segments.* Vision Res, 2008. **48**(3): p. 442-52.
86. Deretic, D., *A role for rhodopsin in a signal transduction cascade that regulates membrane trafficking and photoreceptor polarity.* Vision Res, 2006. **46**(27): p. 4427-33.
87. Calvert, P.D., et al., *Light-driven translocation of signaling proteins in vertebrate photoreceptors.* Trends Cell Biol, 2006. **16**(11): p. 560-8.
88. Arshavsky, V.Y., T.D. Lamb, and E.N. Pugh, Jr., *G proteins and phototransduction.* Annu Rev Physiol, 2002. **64**: p. 153-87.
89. He, W., C.W. Cowan, and T.G. Wensel, *RGS9, a GTPase accelerator for phototransduction.* Neuron, 1998. **20**(1): p. 95-102.
90. Martemyanov, K.A., et al., *The DEP domain determines subcellular targeting of the GTPase activating protein RGS9 in vivo.* J Neurosci, 2003. **23**(32): p. 10175-81.

91. Lishko, P.V., et al., *Specific binding of RGS9-Gβ5L to protein anchor in photoreceptor membranes greatly enhances its catalytic activity.* J Biol Chem, 2002. **277**(27): p. 24376-81.
92. Hu, G. and T.G. Wensel, *R9AP, a membrane anchor for the photoreceptor GTPase accelerating protein, RGS9-1.* Proc Natl Acad Sci U S A, 2002. **99**(15): p. 9755-60.
93. Anderson, G.R., et al., *Expression and localization of RGS9-2/Gβ5/R7BP complex in vivo is set by dynamic control of its constitutive degradation by cellular cysteine proteases.* J Neurosci, 2007. **27**(51): p. 14117-27.
94. Drenan, R.M., et al., *Palmitoylation regulates plasma membrane-nuclear shuttling of R7BP, a novel membrane anchor for the RGS7 family.* J Cell Biol, 2005. **169**(4): p. 623-33.
95. Keresztes, G., et al., *Expression patterns of the RGS9-1 anchoring protein R9AP in the chicken and mouse suggest multiple roles in the nervous system.* Mol Cell Neurosci, 2003. **24**(3): p. 687-95.
96. Harbury, P.A., *Springs and zippers: coiled coils in SNARE-mediated membrane fusion.* Structure, 1998. **6**(12): p. 1487-91.
97. Chen, Y.A. and R.H. Scheller, *SNARE-mediated membrane fusion.* Nat Rev Mol Cell Biol, 2001. **2**(2): p. 98-106.
98. Burchett, S.A., et al., *Regulation of stress response signaling by the N-terminal dishevelled/EGL-10/pleckstrin domain of Sst2, a regulator of G protein signaling in Saccharomyces cerevisiae.* J Biol Chem, 2002. **277**(25): p. 22156-67.
99. Song, J.H., J.J. Waataja, and K.A. Martemyanov, *Subcellular targeting of RGS9-2 is controlled by multiple molecular determinants on its membrane anchor, R7BP.* J Biol Chem, 2006. **281**(22): p. 15361-9.
100. Drenan, R.M., et al., *R7BP augments the function of RGS7•Gβ5 complexes by a plasma membrane-targeting mechanism.* J Biol Chem, 2006. **281**(38): p. 28222-31.
101. Jia, L., M.E. Linder, and K.J. Blumer, *Gi/o signaling and the palmitoyltransferase DHHC2 regulate palmitate cycling and shuttling of RGS7 family-binding protein.* J Biol Chem, 2011. **286**(15): p. 13695-703.
102. Grabowska, D., et al., *Postnatal induction and localization of R7BP, a membrane-anchoring protein for regulator of G protein signaling 7 family-Gβ5 complexes in brain.* Neuroscience, 2008. **151**(4): p. 969-82.
103. Bouhamdan, M., et al., *Brain-specific RGS9-2 is localized to the nucleus via its unique proline-rich domain.* Biochim Biophys Acta, 2004. **1691**(2-3): p. 141-50.
104. Zhang, J.H., et al., *Nuclear localization of G protein beta 5 and regulator of G protein signaling 7 in neurons and brain.* J Biol Chem, 2001. **276**(13): p. 10284-9.
105. Panicker, L.M., et al., *Nuclear localization of the G protein β 5/R7-regulator of G protein signaling protein complex is dependent on R7 binding protein.* J Neurochem, 2010. **113**(5): p. 1101-12.
106. Hu, G., Z. Zhang, and T.G. Wensel, *Activation of RGS9-1 GTPase acceleration by its membrane anchor, R9AP.* J Biol Chem, 2003. **278**(16): p. 14550-4.

107. Masuho, I., et al., *Membrane anchor R9AP potentiates GTPase-accelerating protein activity of RGS11•Gβ5 complex and accelerates inactivation of the mGluR6-G(o) signaling.* J Biol Chem, 2010. **285**(7): p. 4781-7.
108. Baker, S.A., et al., *Kinetic mechanism of RGS9-1 potentiation by R9AP.* Biochemistry, 2006. **45**(35): p. 10690-7.
109. Baker, S.A., et al., *The outer segment serves as a default destination for the trafficking of membrane proteins in photoreceptors.* J Cell Biol, 2008. **183**(3): p. 485-98.
110. Gospe, S.M., 3rd, et al., *Membrane attachment is key to protecting transducin GTPase-activating complex from intracellular proteolysis in photoreceptors.* J Neurosci, 2011. **31**(41): p. 14660-8.
111. Cao, Y., et al., *Membrane anchoring subunits specify selective regulation of RGS9•Gβ5 GAP complex in photoreceptor neurons.* J Neurosci, 2010. **30**(41): p. 13784-93.
112. Cao, Y., et al., *Targeting of RGS7/Gbeta5 to the dendritic tips of ON-bipolar cells is independent of its association with membrane anchor R7BP.* J Neurosci, 2008. **28**(41): p. 10443-9.
113. Orlandi, C., et al., *GPR158/179 regulate G protein signaling by controlling localization and activity of the RGS7 complexes.* J Cell Biol, 2012. **197**(6): p. 711-9.
114. Anderson, G.R., et al., *R7BP complexes with RGS9-2 and RGS7 in the striatum differentially control motor learning and locomotor responses to cocaine.* Neuropsychopharmacology, 2010. **35**(4): p. 1040-50.
115. Keresztes, G., et al., *Absence of the RGS9•Gβ5 GTPase-activating complex in photoreceptors of the R9AP knockout mouse.* J Biol Chem, 2004. **279**(3): p. 1581-4.
116. Anderson, G.R., R. Lujan, and K.A. Martemyanov, *Changes in striatal signaling induce remodeling of RGS complexes containing Gβ5 and R7BP subunits.* Mol Cell Biol, 2009. **29**(11): p. 3033-44.
117. Martemyanov, K.A., et al., *Functional comparison of RGS9 splice isoforms in a living cell.* Proc Natl Acad Sci U S A, 2008. **105**(52): p. 20988-93.
118. Psifogeorgou, K., et al., *RGS9-2 is a negative modulator of μ-opioid receptor function.* J Neurochem, 2007. **103**(2): p. 617-25.
119. Garzon, J., et al., *Activation of μ-opioid receptors transfers control of Gα subunits to the regulator of G-protein signaling RGS9-2: role in receptor desensitization.* J Biol Chem, 2005. **280**(10): p. 8951-60.
120. Sandiford, S.L. and V.Z. Slepak, *The Gβ5-RGS7 complex selectively inhibits muscarinic M3 receptor signaling via the interaction between the third intracellular loop of the receptor and the DEP domain of RGS7.* Biochemistry, 2009. **48**(10): p. 2282-9.
121. Cao, Y., et al., *Retina-specific GTPase accelerator RGS11•Gβ5S•R9AP is a constitutive heterotrimer selectively targeted to mGluR6 in ON-bipolar neurons.* J Neurosci, 2009. **29**(29): p. 9301-13.

122. Bouhamdan, M., et al., *Brain-specific regulator of G-protein signaling 9-2 selectively interacts with α-actinin-2 to regulate calcium-dependent inactivation of NMDA receptors.* J Neurosci, 2006. **26**(9): p. 2522-30.
123. Benzing, T., et al., *Interaction of 14-3-3 protein with regulator of G protein signaling 7 is dynamically regulated by tumor necrosis factor-α.* J Biol Chem, 2002. **277**(36): p. 32954-62.
124. Ibi, M., et al., *Involvement of NOX1/NADPH oxidase in morphine-induced analgesia and tolerance.* J Neurosci, 2011. **31**(49): p. 18094-103.
125. Liu, Z. and R.A. Fisher, *RGS6 interacts with DMAP1 and DNMT1 and inhibits DMAP1 transcriptional repressor activity.* J Biol Chem, 2004. **279**(14): p. 14120-8.
126. Liu, Z., T.K. Chatterjee, and R.A. Fisher, *RGS6 interacts with SCG10 and promotes neuronal differentiation. Role of the G γ subunit-like (GGL) domain of RGS6.* J Biol Chem, 2002. **277**(40): p. 37832-9.
127. Hunt, R.A., et al., *Snapin interacts with the N-terminus of regulator of G protein signaling 7.* Biochem Biophys Res Commun, 2003. **303**(2): p. 594-9.
128. Kim, E., et al., *Interaction between RGS7 and polycystin.* Proc Natl Acad Sci U S A, 1999. **96**(11): p. 6371-6.
129. Charlton, J.J., et al., *Multiple actions of spinophilin regulate μ opioid receptor function.* Neuron, 2008. **58**(2): p. 238-47.
130. Seno, K., et al., *A possible role of RGS9 in phototransduction. A bridge between the cGMP-phosphodiesterase system and the guanylyl cyclase system.* J Biol Chem, 1998. **273**(35): p. 22169-72.
131. Kovoor, A., et al., *D2 dopamine receptors colocalize regulator of G-protein signaling 9-2 (RGS9-2) via the RGS9 DEP domain, and RGS9 knock-out mice develop dyskinesias associated with dopamine pathways.* J Neurosci, 2005. **25**(8): p. 2157-65.
132. Ballon, D.R., et al., *DEP-domain-mediated regulation of GPCR signaling responses.* Cell, 2006. **126**(6): p. 1079-93.
133. Chen, J.G., et al., *A seven-transmembrane RGS protein that modulates plant cell proliferation.* Science, 2003. **301**(5640): p. 1728-31.
134. Rojkova, A.M., et al., *Gγ subunit-selective G protein β5 mutant defines regulators of G protein signaling protein binding requirement for nuclear localization.* J Biol Chem, 2003. **278**(14): p. 12507-12.
135. Luo, D.G., T. Xue, and K.W. Yau, *How vision begins: an odyssey.* Proc Natl Acad Sci U S A, 2008. **105**(29): p. 9855-62.
136. Pugh, E.N., Jr., *RGS expression level precisely regulates the duration of rod photoresponses.* Neuron, 2006. **51**(4): p. 391-3.
137. Lyubarsky, A.L., et al., *RGS9-1 is required for normal inactivation of mouse cone phototransduction.* Mol Vis, 2001. **7**: p. 71-8.
138. Krispel, C.M., et al., *Prolonged photoresponses and defective adaptation in rods of Gβ5-/- mice.* J Neurosci, 2003. **23**(18): p. 6965-71.
139. Nishiguchi, K.M., et al., *Defects in RGS9 or its anchor protein R9AP in patients with slow photoreceptor deactivation.* Nature, 2004. **427**(6969): p. 75-8.

140. Cheng, J.Y., et al., *Bradyopsia in an Asian man.* Arch Ophthalmol, 2007. **125**(8): p. 1138-40.
141. Hartong, D.T., J.W. Pott, and A.C. Kooijman, *Six patients with bradyopsia (slow vision): clinical features and course of the disease.* Ophthalmology, 2007. **114**(12): p. 2323-31.
142. Garzon, J., et al., *RGS9 proteins facilitate acute tolerance to mu-opioid effects.* Eur J Neurosci, 2001. **13**(4): p. 801-11.
143. Kim, K.J., et al., *Differential expression of the regulator of G protein signaling RGS9 protein in nociceptive pathways of different age rats.* Brain Res Dev Brain Res, 2005. **160**(1): p. 28-39.
144. Seeman, P., et al., *Consistent with dopamine supersensitivity, RGS9 expression is diminished in the amphetamine-treated animal model of schizophrenia and in postmortem schizophrenia brain.* Synapse, 2007. **61**(5): p. 303-9.
145. Blundell, J., et al., *Motor coordination deficits in mice lacking RGS9.* Brain Res, 2008. **1190**: p. 78-85.
146. Gold, S.J., et al., *RGS9-2 negatively modulates L-3,4-dihydroxyphenylalanine-induced dyskinesia in experimental Parkinson's disease.* J Neurosci, 2007. **27**(52): p. 14338-48.
147. Cabrera-Vera, T.M., et al., *RGS9-2 modulates D2 dopamine receptor-mediated Ca2+ channel inhibition in rat striatal cholinergic interneurons.* Proc Natl Acad Sci U S A, 2004. **101**(46): p. 16339-44.
148. Celver, J., M. Sharma, and A. Kovoor, *RGS9-2 mediates specific inhibition of agonist-induced internalization of D2-dopamine receptors.* J Neurochem, 2010. **114**(3): p. 739-49.
149. Tekumalla, P.K., et al., *Elevated levels of ΔFosB and RGS9 in striatum in Parkinson's disease.* Biol Psychiatry, 2001. **50**(10): p. 813-6.
150. Burchett, S.A., et al., *Regulators of G protein signaling: rapid changes in mRNA abundance in response to amphetamine.* J Neurochem, 1998. **70**(5): p. 2216-9.
151. Terzi, D., et al., *R7BP modulates opiate analgesia and tolerance but not withdrawal.* Neuropsychopharmacology, 2012. **37**(4): p. 1005-12.
152. Burns, M.E. and T.G. Wensel, *From molecules to behavior: new clues for RGS function in the striatum.* Neuron, 2003. **38**(6): p. 853-6.
153. Sanchez-Blazquez, P., et al., *The Gβ5 subunit that associates with the R7 subfamily of RGS proteins regulates μ-opioid effects.* Neuropharmacology, 2003. **45**(1): p. 82-95.
154. Jedema, H.P., et al., *Chronic cold exposure increases RGS7 expression and decreases α2-autoreceptor-mediated inhibition of noradrenergic locus coeruleus neurons.* Eur J Neurosci, 2008. **27**(9): p. 2433-43.
155. Singh, R.K., et al., *Olanzapine increases RGS7 protein expression via stimulation of the Janus tyrosine kinase-signal transducer and activator of transcription signaling cascade.* J Pharmacol Exp Ther, 2007. **322**(1): p. 133-40.
156. Shelat, P.B., et al., *Ischemia-induced increase in RGS7 mRNA expression in gerbil hippocampus.* Neurosci Lett, 2006. **403**(1-2): p. 157-61.

157. Lopez-Fando, A., et al., *Expression of neural RGS-R7 and Gβ5 Proteins in Response to Acute and Chronic Morphine.* Neuropsychopharmacology, 2005. **30**(1): p. 99-110.
158. Witherow, D.S., et al., *Gβ5•RGS7 inhibits Gα q-mediated signaling via a direct protein-protein interaction.* J Biol Chem, 2003. **278**(23): p. 21307-13.
159. Shuey, D.J., et al., *RGS7 attenuates signal transduction through the Gα q family of heterotrimeric G proteins in mammalian cells.* J Neurochem, 1998. **70**(5): p. 1964-72.
160. Maity, B., et al., *Regulator of G protein signaling 6 (RGS6) protein ensures coordination of motor movement by modulating GABAB receptor signaling.* J Biol Chem, 2012. **287**(7): p. 4972-81.
161. Rao, A., et al., *Gβ5 is required for normal light responses and morphology of retinal ON-bipolar cells.* J Neurosci, 2007. **27**(51): p. 14199-204.
162. Shim, H., et al., *Defective retinal depolarizing bipolar cells in regulators of G protein signaling (RGS) 7 and 11 double null mice.* J Biol Chem, 2012. **287**(18): p. 14873-9.
163. Zhang, J., et al., *RGS7 and -11 complexes accelerate the ON-bipolar cell light response.* Invest Ophthalmol Vis Sci, 2010. **51**(2): p. 1121-9.
164. Chen, F.S., et al., *Functional redundancy of R7 RGS proteins in ON-bipolar cell dendrites.* Invest Ophthalmol Vis Sci, 2010. **51**(2): p. 686-93.
165. Cao, Y., et al., *Regulators of G protein signaling RGS7 and RGS11 determine the onset of the light response in ON bipolar neurons.* Proc Natl Acad Sci U S A, 2012. **109**(20): p. 7905-10.
166. Mojumder, D.K., Y. Qian, and T.G. Wensel, *Two R7 regulator of G-protein signaling proteins shape retinal bipolar cell signaling.* J Neurosci, 2009. **29**(24): p. 7753-65.
167. Maguire, J.J. and A.P. Davenport, *Regulation of vascular reactivity by established and emerging GPCRs.* Trends Pharmacol Sci, 2005. **26**(9): p. 448-54.
168. Hercule, H.C., et al., *Regulator of G protein signalling 2 ameliorates angiotensin II-induced hypertension in mice.* Exp Physiol, 2007. **92**(6): p. 1014-22.
169. Heximer, S.P., et al., *Hypertension and prolonged vasoconstrictor signaling in RGS2-deficient mice.* J Clin Invest, 2003. **111**(4): p. 445-52.
170. Tang, K.M., et al., *Regulator of G-protein signaling-2 mediates vascular smooth muscle relaxation and blood pressure.* Nat Med, 2003. **9**(12): p. 1506-12.
171. Gross, V., et al., *Autonomic nervous system and blood pressure regulation in RGS2-deficient mice.* Am J Physiol Regul Integr Comp Physiol, 2005. **288**(5): p. R1134-42.
172. Calo, L.A., et al., *Increased expression of regulator of G protein signaling-2 (RGS-2) in Bartter's/Gitelman's syndrome. A role in the control of vascular tone and implication for hypertension.* J Clin Endocrinol Metab, 2004. **89**(8): p. 4153-7.
173. Semplicini, A., et al., *Reduced expression of regulator of G-protein signaling 2 (RGS2) in hypertensive patients increases calcium mobilization and ERK1/2 phosphorylation induced by angiotensin II.* J Hypertens, 2006. **24**(6): p. 1115-24.

174. Yang, J., et al., *Genetic variations of regulator of G-protein signaling 2 in hypertensive patients and in the general population.* J Hypertens, 2005. **23**(8): p. 1497-505.
175. Bondjers, C., et al., *Transcription profiling of platelet-derived growth factor-B-deficient mouse embryos identifies RGS5 as a novel marker for pericytes and vascular smooth muscle cells.* Am J Pathol, 2003. **162**(3): p. 721-9.
176. Cho, H., et al., *Pericyte-specific expression of Rgs5: implications for PDGF and EDG receptor signaling during vascular maturation.* FASEB J, 2003. **17**(3): p. 440-2.
177. Adams, L.D., et al., *A comparison of aorta and vena cava medial message expression by cDNA array analysis identifies a set of 68 consistently differentially expressed genes, all in aortic media.* Circ Res, 2000. **87**(7): p. 623-31.
178. Zhou, J., et al., *Characterization of RGS5 in regulation of G protein-coupled receptor signaling.* Life Sci, 2001. **68**(13): p. 1457-69.
179. Wang, Q., et al., *Receptor-selective effects of endogenous RGS3 and RGS5 to regulate mitogen-activated protein kinase activation in rat vascular smooth muscle cells.* J Biol Chem, 2002. **277**(28): p. 24949-58.
180. Nisancioglu, M.H., et al., *Generation and characterization of RGS5 mutant mice.* Mol Cell Biol, 2008. **28**(7): p. 2324-31.
181. Brodde, O.E. and M.C. Michel, *Adrenergic and muscarinic receptors in the human heart.* Pharmacol Rev, 1999. **51**(4): p. 651-90.
182. Wang, H., et al., *Expression of multiple subtypes of muscarinic receptors and cellular distribution in the human heart.* Mol Pharmacol, 2001. **59**(5): p. 1029-36.
183. Krejci, A. and S. Tucek, *Quantitation of mRNAs for M(1) to M(5) subtypes of muscarinic receptors in rat heart and brain cortex.* Mol Pharmacol, 2002. **61**(6): p. 1267-72.
184. Kitazawa, T., et al., *M3 muscarinic receptors mediate positive inotropic responses in mouse atria: a study with muscarinic receptor knockout mice.* J Pharmacol Exp Ther, 2009. **330**(2): p. 487-93.
185. Fu, Y., et al., *Endogenous RGS proteins and Gα subtypes differentially control muscarinic and adenosine-mediated chronotropic effects.* Circ Res, 2006. **98**(5): p. 659-66.
186. Zuberi, Z., L. Birnbaumer, and A. Tinker, *The role of inhibitory heterotrimeric G proteins in the control of in vivo heart rate dynamics.* Am J Physiol Regul Integr Comp Physiol, 2008. **295**(6): p. R1822-30.
187. Harvey, R.D., *Muscarinic receptor agonists and antagonists: effects on cardiovascular function.* Handb Exp Pharmacol, 2012(208): p. 299-316.
188. Dhein, S., C.J. van Koppen, and O.E. Brodde, *Muscarinic receptors in the mammalian heart.* Pharmacol Res, 2001. **44**(3): p. 161-82.
189. DiFrancesco, D. and P. Tortora, *Direct activation of cardiac pacemaker channels by intracellular cyclic AMP.* Nature, 1991. **351**(6322): p. 145-7.
190. DiFrancesco, D. and C. Tromba, *Inhibition of the hyperpolarization-activated current (I_f) induced by acetylcholine in rabbit sino-atrial node myocytes.* J Physiol, 1988. **405**: p. 477-91.

191. Yatani, A., et al., *Heart rate regulation by G proteins acting on the cardiac pacemaker channel.* Science, 1990. **249**(4973): p. 1163-6.
192. Wu, J., et al., *Morphological and membrane characteristics of spider and spindle cells isolated from rabbit sinus node.* Am J Physiol Heart Circ Physiol, 2001. **280**(3): p. H1232-40.
193. Kurachi, Y., *G protein regulation of cardiac muscarinic potassium channel.* Am J Physiol, 1995. **269**(4 Pt 1): p. C821-30.
194. Sakmann, B., A. Noma, and W. Trautwein, *Acetylcholine activation of single muscarinic K+ channels in isolated pacemaker cells of the mammalian heart.* Nature, 1983. **303**(5914): p. 250-3.
195. Wickman, K., et al., *Abnormal heart rate regulation in GIRK4 knockout mice.* Neuron, 1998. **20**(1): p. 103-14.
196. Doupnik, C.A., et al., *RGS proteins reconstitute the rapid gating kinetics of gbetagamma-activated inwardly rectifying K+ channels.* Proc Natl Acad Sci U S A, 1997. **94**(19): p. 10461-6.
197. Fu, Y., et al., *Endogenous RGS proteins modulate SA and AV nodal functions in isolated heart: implications for sick sinus syndrome and AV block.* Am J Physiol Heart Circ Physiol, 2007. **292**(5): p. H2532-9.
198. Zhang, Q., M.A. Pacheco, and C.A. Doupnik, *Gating properties of GIRK channels activated by Gα(o)- and Ga(i)-coupled muscarinic m2 receptors in Xenopus oocytes: the role of receptor precoupling in RGS modulation.* J Physiol, 2002. **545**(Pt 2): p. 355-73.
199. Keren-Raifman, T., et al., *Expression levels of RGS7 and RGS4 proteins determine the mode of regulation of the G protein-activated K(+) channel and control regulation of RGS7 by Gβ5.* FEBS Lett, 2001. **492**(1-2): p. 20-8.
200. Herlitze, S., J.P. Ruppersberg, and M.D. Mark, *New roles for RGS2, 5 and 8 on the ratio-dependent modulation of recombinant GIRK channels expressed in Xenopus oocytes.* J Physiol, 1999. **517 (Pt 2)**: p. 341-52.
201. Saitoh, O., et al., *RGS7 and RGS8 differentially accelerate G protein-mediated modulation of K+ currents.* J Biol Chem, 1999. **274**(14): p. 9899-904.
202. Jaen, C. and C.A. Doupnik, *Neuronal Kir3.1/Kir3.2a channels coupled to serotonin 1A and muscarinic m2 receptors are differentially modulated by the "short" RGS3 isoform.* Neuropharmacology, 2005. **49**(4): p. 465-76.
203. Krapivinsky, G., et al., *The G-protein-gated atrial K+ channel I_{KACh} is a heteromultimer of two inwardly rectifying K(+)-channel proteins.* Nature, 1995. **374**(6518): p. 135-41.
204. Jaen, C. and C.A. Doupnik, *RGS3 and RGS4 differentially associate with G protein-coupled receptor-Kir3 channel signaling complexes revealing two modes of RGS modulation. Precoupling and collision coupling.* J Biol Chem, 2006. **281**(45): p. 34549-60.
205. Zhang, P. and U. Mende, *Regulators of G-protein signaling in the heart and their potential as therapeutic targets.* Circ Res, 2011. **109**(3): p. 320-33.
206. Rogers, J.H., et al., *RGS4 causes increased mortality and reduced cardiac hypertrophy in response to pressure overload.* J Clin Invest, 1999. **104**(5): p. 567-76.

207. Tamirisa, P., K.J. Blumer, and A.J. Muslin, *RGS4 inhibits G-protein signaling in cardiomyocytes.* Circulation, 1999. **99**(3): p. 441-7.
208. Tokudome, T., et al., *Regulator of G-protein signaling subtype 4 mediates antihypertrophic effect of locally secreted natriuretic peptides in the heart.* Circulation, 2008. **117**(18): p. 2329-39.
209. Patten, M., et al., *Endotoxin induces desensitization of cardiac endothelin-1 receptor signaling by increased expression of RGS4 and RGS16.* Cardiovasc Res, 2002. **53**(1): p. 156-64.
210. Owen, V.J., et al., *Expression of RGS3, RGS4 and Gi alpha 2 in acutely failing donor hearts and end-stage heart failure.* Eur Heart J, 2001. **22**(12): p. 1015-20.
211. Fujita, S., et al., *A regulator of G protein signalling (RGS) protein confers agonist-dependent relaxation gating to a G protein-gated K+ channel.* J Physiol, 2000. **526 Pt 2**: p. 341-7.
212. Anderson, G.R., E. Posokhova, and K.A. Martemyanov, *The R7 RGS protein family: multi-subunit regulators of neuronal G protein signaling.* Cell Biochem Biophys, 2009. **54**(1-3): p. 33-46.
213. Martemyanov, K.A. and V.Y. Arshavsky, *Biology and functions of the RGS9 isoforms.* Prog Mol Biol Transl Sci, 2009. **86**: p. 205-27.
214. Traynor, J.R., et al., *RGS9-2: probing an intracellular modulator of behavior as a drug target.* Trends Pharmacol Sci, 2009. **30**(3): p. 105-11.
215. Burchett, S.A., M.J. Bannon, and J.G. Granneman, *RGS mRNA expression in rat striatum: modulation by dopamine receptors and effects of repeated amphetamine administration.* J Neurochem, 1999. **72**(4): p. 1529-33.
216. Shevchenko, A., et al., *In-gel digestion for mass spectrometric characterization of proteins and proteomes.* Nat Protoc, 2006. **1**(6): p. 2856-60.
217. Obradovic, Z., et al., *Exploiting heterogeneous sequence properties improves prediction of protein disorder.* Proteins, 2005. **61 Suppl 7**: p. 176-82.
218. Peng, K., et al., *Optimizing long intrinsic disorder predictors with protein evolutionary information.* J Bioinform Comput Biol, 2005. **3**(1): p. 35-60.
219. Zieske, L.R., *A perspective on the use of iTRAQ reagent technology for protein complex and profiling studies.* J Exp Bot, 2006. **57**(7): p. 1501-8.
220. Shilov, I.V., et al., *The Paragon Algorithm, a next generation search engine that uses sequence temperature values and feature probabilities to identify peptides from tandem mass spectra.* Mol Cell Proteomics, 2007. **6**(9): p. 1638-55.
221. Ow, S.Y., et al., *iTRAQ underestimation in simple and complex mixtures: "the good, the bad and the ugly".* J Proteome Res, 2009. **8**(11): p. 5347-55.
222. Dice, J.F., *Chaperone-mediated autophagy.* Autophagy, 2007. **3**(4): p. 295-9.
223. McDonough, H. and C. Patterson, *CHIP: a link between the chaperone and proteasome systems.* Cell Stress Chaperones, 2003. **8**(4): p. 303-8.
224. Massey, A.C., C. Zhang, and A.M. Cuervo, *Chaperone-mediated autophagy in aging and disease.* Curr Top Dev Biol, 2006. **73**: p. 205-35.
225. Radivojac, P., et al., *Intrinsic disorder and functional proteomics.* Biophys J, 2007. **92**(5): p. 1439-56.

226. Haag Breese, E., et al., *The disordered amino-terminus of SIMPL interacts with members of the 70-kDa heat-shock protein family.* DNA Cell Biol, 2006. **25**(12): p. 704-14.
227. Song, J., et al., *Intrinsically disordered gamma-subunit of cGMP phosphodiesterase encodes functionally relevant transient secondary and tertiary structure.* Proc Natl Acad Sci U S A, 2008. **105**(5): p. 1505-10.
228. Uversky, V.N., et al., *Effect of zinc and temperature on the conformation of the gamma subunit of retinal phosphodiesterase: a natively unfolded protein.* J Proteome Res, 2002. **1**(2): p. 149-59.
229. Rohde, M., et al., *Members of the heat-shock protein 70 family promote cancer cell growth by distinct mechanisms.* Genes Dev, 2005. **19**(5): p. 570-82.
230. Jeong, H., et al., *Lethality and centrality in protein networks.* Nature, 2001. **411**(6833): p. 41-2.
231. Han, J.D., et al., *Evidence for dynamically organized modularity in the yeast protein-protein interaction network.* Nature, 2004. **430**(6995): p. 88-93.
232. Cusick, M.E., et al., *Interactome: gateway into systems biology.* Hum Mol Genet, 2005. **14 Spec No. 2**: p. R171-81.
233. Devos, D. and R.B. Russell, *A more complete, complexed and structured interactome.* Curr Opin Struct Biol, 2007. **17**(3): p. 370-7.
234. Wilkins, M.R. and S.K. Kummerfeld, *Sticking together? Falling apart? Exploring the dynamics of the interactome.* Trends Biochem Sci, 2008. **33**(5): p. 195-200.
235. Liu, L., et al., *Proteomic characterization of the dynamic KSR-2 interactome, a signaling scaffold complex in MAPK pathway.* Biochim Biophys Acta, 2009. **1794**(10): p. 1485-95.
236. Iff, J., et al., *Differential proteomic analysis of STAT6 knockout mice reveals new regulatory function in liver lipid homeostasis.* J Proteome Res, 2009. **8**(10): p. 4511-24.
237. Paulo, J.A., W.J. Brucker, and E. Hawrot, *Proteomic analysis of an α7 nicotinic acetylcholine receptor interactome.* J Proteome Res, 2009. **8**(4): p. 1849-58.
238. Bai, Y., et al., *The in vivo brain interactome of the amyloid precursor protein.* Mol Cell Proteomics, 2008. **7**(1): p. 15-34.
239. Lindquist, S. and E.A. Craig, *The heat-shock proteins.* Annu Rev Genet, 1988. **22**: p. 631-77.
240. Daugaard, M., M. Rohde, and M. Jaattela, *The heat shock protein 70 family: Highly homologous proteins with overlapping and distinct functions.* FEBS Lett, 2007. **581**(19): p. 3702-10.
241. Qian, S.B., et al., *Characterization of rapidly degraded polypeptides in mammalian cells reveals a novel layer of nascent protein quality control.* J Biol Chem, 2006. **281**(1): p. 392-400.
242. Majeski, A.E. and J.F. Dice, *Mechanisms of chaperone-mediated autophagy.* Int J Biochem Cell Biol, 2004. **36**(12): p. 2435-44.
243. Yusupov, M.M., et al., *Crystal structure of the ribosome at 5.5 A resolution.* Science, 2001. **292**(5518): p. 883-96.

244. Kramer, G., et al., *The ribosome as a platform for co-translational processing, folding and targeting of newly synthesized proteins.* Nat Struct Mol Biol, 2009. **16**(6): p. 589-97.
245. Frydman, J., *Folding of newly translated proteins in vivo: the role of molecular chaperones.* Annu Rev Biochem, 2001. **70**: p. 603-47.
246. Bukau, B., *Ribosomes catch Hsp70s.* Nat Struct Mol Biol, 2005. **12**(6): p. 472-3.
247. Liang, P. and T.H. MacRae, *Molecular chaperones and the cytoskeleton.* J Cell Sci, 1997. **110 (Pt 13)**: p. 1431-40.
248. Hovland, R., J.E. Hesketh, and I.F. Pryme, *The compartmentalization of protein synthesis: importance of cytoskeleton and role in mRNA targeting.* Int J Biochem Cell Biol, 1996. **28**(10): p. 1089-105.
249. Li, D., H. Sun, and P. Levesque, *Antiarrhythmic drug therapy for atrial fibrillation: focus on atrial selectivity and safety.* Cardiovasc Hematol Agents Med Chem, 2009. **7**(1): p. 64-75.
250. Wickman, K., et al., *Structure, G protein activation, and functional relevance of the cardiac G protein-gated K+ channel, I_{KACh}.* Ann N Y Acad Sci, 1999. **868**: p. 386-98.
251. Mirshahi, T., T. Jin, and D.E. Logothetis, *G beta gamma and KACh: old story, new insights.* Sci STKE, 2003. **2003**(194): p. PE32.
252. Hollinger, S. and J.R. Hepler, *Cellular regulation of RGS proteins: modulators and integrators of G protein signaling.* Pharmacol Rev, 2002. **54**(3): p. 527-59.
253. Martemyanov, K.A. and V.Y. Arshavsky, *Noncatalytic domains of RGS9-1.Gβ5L play a decisive role in establishing its substrate specificity.* J Biol Chem, 2002. **277**(36): p. 32843-8.
254. Kennedy, M.E., J. Nemec, and D.E. Clapham, *Localization and interaction of epitope-tagged GIRK1 and CIR inward rectifier K+ channel subunits.* Neuropharmacology, 1996. **35**(7): p. 831-9.
255. Bettahi, I., et al., *Contribution of the Kir3.1 subunit to the muscarinic-gated atrial potassium channel I_{KACh}.* J Biol Chem, 2002. **277**(50): p. 48282-8.
256. Koyrakh, L., et al., *The heart rate decrease caused by acute FTY720 administration is mediated by the G protein-gated potassium channel I.* Am J Transplant, 2005. **5**(3): p. 529-36.
257. McGrath, M.F. and A.J. de Bold, *Transcriptional analysis of the mammalian heart with special reference to its endocrine function.* BMC Genomics, 2009. **10**: p. 254.
258. Doupnik, C.A., T. Xu, and J.M. Shinaman, *Profile of RGS expression in single rat atrial myocytes.* Biochim Biophys Acta, 2001. **1522**(2): p. 97-107.